



**ADDIS ABABA UNIVERSITY
SCHOOL OF EARTH SCIENCES**

**HYDROGEOLOGICAL ASSESSMENT ON UPPER
MILLE RIVER CATCHMENT**

By:

Eden Dessalegn

Advisor: Tilahun Azagegn (Ph.D.)

Co-advisor: Asfawossen Asrat

September, 2020

Addis Ababa

**ADDIS ABABA UNIVERSITY
COLLEGE OF NATURAL SCIENCE
SCHOOL OF EARTH SCIENCE**

**HYDROGEOLOGICAL ASSESSMENT ON UPPER MILLE
RIVER CATCHMENT**

**A THESIS SUBMITTED TO SCHOOL OF EARTH SCIENCE,
ADDIS ABABA UNIVERSITY IN PARTIAL FULFILMENT OF
THE REQUIREMENTS FOR DEGREE OF MASTER OF
SCIENCE IN HYDROGEOLOGY**

BY:

EDEN DESSALEGN

ADVISOR: TILAHUN AZAGEGN (PH.D.)

CO-ADVISOR: PROFESSOR ASFAWOSSEN ASRAT

SEPTEMBER, 2020

ADDIS ABABA

Addis Ababa University
College of Natural science
School of Earth Science

This is to certify that the Thesis Prepared by Eden Desslegn, entitled: Groundwater Resource Evaluation in Gelana and Mille River Catchments submitted in the partial fulfilment for the requirements for the Degree of Master of Science in Hydrogeology complies with the regulations of the University and meets the accepted standard with respect to originality and quality.

Approved by Board of Examiners: Signed by the Examining Committee

<u>Dr. Tilahun Azagegn</u>	_____	_____
Advisor	Signature	Date
 Dr.Dessie Nadew	_____	_____
Examiner	Signature	Date
 Prof.Tenalem Ayenew	_____	_____
Examiner	Signature	Date
 Dr.Balemual Atnafu	_____	_____
Chairman of School or graduate	Signature	Date

AUTHOR STATEMENT

By my signature below, I declare and confirm that this thesis is my own work. I have followed all ethical and technical principles of research in preparation, data analysis and compilation of this thesis work. Any scholarly matter that is included in the thesis has been given recognition in citation.

Eden Desslegn

Signature: _____

TABLE OF CONTENTS

Contents	Pages
TABLE OF CONTENTS	i
LIST OF FIGURES.....	v
LIST OF TABLES	vii
ACRONYMS.....	viii
ACKNOWLEDGMENT	x
ABSTRACT	xi
CHAPTER ONE	1
1. INTRODUCTION.....	1
1.1 Background	1
1.2 Problem Statement	2
1.3 Objective	2
1.3.1 General Objective.....	2
1.3.2 Specific objectives.....	2
1.4 Procedures for the proposed activities	2
1.5 Methodology.....	3
1.6 Significance of the research	4
1.7 Literature Review	4
CHAPTER TWO	8
2. DESCRIPTION OF THE STUDY AREA	8
2.1 Location.....	8
2.2 Physiography and Drainage.....	8
2.3 Climate	10

CHAPTER THREE.....	12
3. GEOLOGY	12
3.1 Regional Geologic setting	12
3.2 Geology of the study area.....	14
3.2.1 Lower Basalt (Ashangi Basalt) (Tv1).....	14
3.2.2 Aiba Formation (Tv2).....	15
3.2.3 Tarmaber basalt (Tv4)	16
3.2.4 Kemise Formation (Tk)	16
3.2.5 Quaternary Sediments.....	17
3.3 Geological Structures.....	19
3.3.1 Dikes	20
3.3.2 Joints.....	20
CHAPTER FOUR.....	21
4. HYDROMETEOROLOGY	21
4.1 Meteorological stations and data	21
4.2 Meteorological parameters	21
4.3 Temperature.....	24
4.4 Relative humidity, sunshine hours and wind speed.....	24
4.5 Determination of aerial depth of precipitation	25
4.6 Thiessen polygon method	25
CHAPTER FIVE.....	27
5.0 Recharge Estimation	27
5.1 Base flow separation methods.....	27
5.2 Chloride mass-balance method.....	29
5.3 SWAT (soil and water assessment tool)	29
5.3.1 Swat model water balance	30

5.3.2 Surface Runoff lags	31
5.3.3 Potential Evapotranspiration	32
5.3.4 Model Setup	33
5.4 Result and Discussion	42
5.4.1 Sensitivity analysis	43
5.4.2 Calibrations	45
5.4.3 Validation of model.....	46
5.4.4 Water balance components of the study area watershed	48
5.4.5 Modelling performance	49
CHAPTER SIX.....	50
6. AQUIFER CHARACTERIZATIONS	50
6.1 Introduction	50
6.2 Aquifer Characteristics	50
6.2.1 Intergranular Aquifer with High Productivity	51
6.2.2 Intergranular Aquifer with Medium Productivity	52
6.2.3 Weathered and fractured aquifer with Medium Productivity	56
6.2.4 Low productive aquifers (Aquitard).....	59
6.3 Groundwater Flow Direction.....	60
6.4 Groundwater Recharge-Discharge Mechanism.....	61
6.5 Hydraulic Characteristics of Aquifers	64
6.5.1 Types of Aquifer	64
6.5.2 Transmissivity (TD or T).....	66
6.5.3 Hydraulic Conductivity (K)	68
6.5.4 Groundwater reserve estimation in study area	69

CHAPTER SEVEN.....	70
7 HYDROGEOCHEMISTRY.....	70
7.2 Evaluation of Hydro chemical Parameters and Ions.....	72
7.2.1 Physiochemical Parameters	72
7.3 Major ions	77
7.3.1 Sodium and Potassium.....	77
7.3.2 Magnesium and Calcium	77
7.3.3 Carbonates.....	78
7.3.4 Major Ions and their relationship with TDS map.....	78
7.3.5 Sulphates and Nitrates	79
7.3.6 Chloride	80
7.4 Water Types	81
7.5 Water Quality	83
7.5.1 Water Quality for Irrigation Purposes	84
CHAPTER EIGHT.....	86
8. CONCLUSION AND RECOMMENDATION.....	86
8.1 Conclusion	86
8.2 Recommendation.....	88
References	89
Annex	94

LIST OF FIGURES

Figure 1 Location of the study area.....	8
Figure 2. Physiography of the study area.	10
Figure 3. Geological map of the Northern Ethiopian plateau.....	14
Figure 4. A) Alaji formation (Wuchale); B) Contact between the Alaji rhyolite and Tarmaber Basalt.....	15
Figure 5. Highly fractured and weathered rhyolite in Kolbo area.	16
Figure 6. Swampy areas between Hayk and Ardibo.	18
Figure 7. Geological map of the area	19
Figure 8. A) Columnar joints in Wurgessa Study area B Dikes near a ridge in Sulula	20
Figure 9. Distribution of Metrological and River gauge Stations in the study area and close surrounding.....	22
Figure 10. A) Seasonal and spatial distribution of rainfall and B) elevation vs precipitation relationship.....	23
Figure 11. Mean annual rainfall distribution	24
Figure 12. Thiessen polygon of stations in the study area	26
Figure 13. baseflow of Pasomile River	28
Figure 14. Base flow of Megenagna River.....	28
Figure 15. The reclassified land use map of the study area.....	38
Figure 16. Soil type map of the study area	40
Figure 17. Slope map of the study area.....	42
Figure 18. Graphical representation of sensitivity analysis with t-test and p-value ...	45
Figure 19. Simulated and observed average monthly flows.....	46
Figure 20. Scatter plot of the simulated vs. observed average monthly flows during calibration.....	46

Figure 21. Simulated and observed average monthly flows generated during validation.....	47
Figure 22. Scatter plot of the simulated vs. observed average monthly flows	48
Figure 23 Vertical distribution of aquifer from well log at Mersa Darimo	53
Figure 24 Vertical distribution of aquifer from well log at Mehal Amba	56
Figure 25 Vertical distribution of aquifer from well log at Tisabalima	54
Figure 26 springs, at Robit (Hayk) (A) and Kent Aba Mersa (B)	57
Figure 27 Vertical distribution of aquifer from well log at Seglen located.....	58
Figure 28 Hydrogeological map of the catchment.....	59
Figure 29 west to east hydrogeological cross section	60
Figure 30 Groundwater level contour map show interpreted groundwater flow directions.....	61
Figure 31 Simple hydrogeological cross-sections of Hayk and Ardibo lakes.....	63
Figure 32 Specialized plots	66
Figure 33 Spatial distribution of Transmissivity value map	67
Figure 34 Spatial distribution of Hydraulic conductivity value map.....	69
Figure 35 Error distributions Graph.....	71
Figure 36 sample distribution of Hydrochemical data.....	72
Figure 37 TDS distribution Map.....	74
Figure 38 Hardness map of the area.....	76
Figure 39 TDS Vs Na ⁺⁺ K ⁺ and TDS Vs Ca ⁺² + Mg ⁺² relationships	79
Figure 40 Chloride map.....	80
Figure 41 Piper plot of Hydrochemical samples in study area.	82
Figure 42 Irrigation water classification on samples collected from the study area...	85

LIST OF TABLES

Table 1. metrological data together with their location on the basis to determine the water balance of the catchment.....	21
Table 2. Thiessen polygon calculation for the study area	26
Table 3. General performance rating for recommended statistics for monthly time steps.....	36
Table 4. Land use name with SWAT land use code with their area coverage	37
Table 5. Soil name and percent of coverage in the study area	39
Table 6. Soil type with their description in the study area.	39
Table 7. slope class with description and area coverage.....	41
Table 8. Hydrological parameter selected for both flow calibration and validation ..	43
Table 9. Result of the sensitivity analysis parameters for flow calibration.....	44
Table 10. water balanced component of the study area.	48
Table 11. Stream flow calibration and validation results on monthly basis.....	49
Table 12. range of hardness with its description	75
Table 13. Summery statistics of the groundwater sample result	81
Table 14 Comparison with water quality standards for drinking water	83
Table 15 General classification of water sodium hazard based on SAR values.....	84

ACRONYMS

ADSWE	Amhara Design and Supervision Works Enterprises
ALPHA_BF	Base flow alpha factor
BFI	Base Flow Index
BFS	Base Flow Separation
CH2_CN2	Manning's "n" value for the main channel
CMB	Chloride Mass Balance
EC	Electrical conductivity
ESCO	Soil evaporation compensation factor
ET	Evapotranspiration
GSE	Geological survey of Ethiopia
GW_DELAY	Groundwater delay
GW_REVAP	Groundwater revap coefficient
GWL	Ground water Level
GWQMN	Threshold water depth in the Shallow aquifer for flow
HRU	Hydrological Response Unit
ITCZ	Inter-Tropical Convergence Zone
m.a.s.l	Meter above Sea Level
MCM	Million Cubic Meter per Month
MCE	Metaferia Consulting Engineers
NMS	National Meteorological Service
MOWIE	Ministry of Water, Irrigation and Energy
NSE	Nash - Sutcliffe efficiency
PET	Potential evaporation
R .F	Rainfall
R2	Coefficient of Determination

RECHARGE_DP	Groundwater recharge to deep aquifer
REVAMP	Threshold depth of water in the shallow
RSR	Root mean square error observation standard deviation ratio
SAR	Sodium Absorption Ratio
SOL_BD	Soil bulk density
SOL_K	Saturated hydraulic conductivity
SURLAG	Surface runoff lags time
SWAT	Soil and Water Assessment Tool
SWL	Static Water Level
TDS	Total Dissolved Solute
TEJ	Easterly Jet
UTM	Universal Transverse Mercator
VES	Vertical Electric Sounding
WB	Water Balance
WXGEN	Weather Generator

ACKNOWLEDGMENT

Above all I am honoured to the King of Heaven and Earth Lord Jesus Christ who is the ultimate means of my success.

I owe debt to Dr Tilahun A. for his priceless guidance, and equipping me with knowledge of Earth science and Hydrogeology which is important to bring this work up to the standard.

I extend my thanks to my co-advisor professor Asfawossen Asrat for his valuable comments.

I am also very for thankful for my friends Sadam Ebrahim ,Zekarias Ashine as well as Samrawit yimam who have helped in the Field work along with my paper and for the encouragement you have given me to do better

ABSTRACT

The study aims to elaborate and give some detailed picture of the Hydrogeological features of the study area. Mainly by characterization the aquifer, recharge mechanism, groundwater flow conditions and hydrochemistry of the groundwater. The basin is part of the western escarpment of Afar rift and measures about 1367 km². The mean annual precipitation as calculated by Thiessen polygon method is found to be 1157.6mm. The amount of recharge that is contributed to the subsurface as calculated by using Base flow separation, chloride mass balance and SWAT modelling gives a value of 135.9 mm, 115.66 mm and 140.48 mm (after calibration) and 138.5 (after validation) respectively. To describe the aquifer system of the area pumping test data, well completion reports, well logs and geology of the area were analysed. The study area is characterized by deep groundwater systems on average 214 m (depth of the wells) and groundwater reserve of the graben is estimated 3670.24 MCM. Hydraulic characteristics are spatially variable, in the area transmissivity of the valley ranges from 2.4–1580 m²/d. Its hydraulic conductivity ranges from 0.06 –18.1m/d. The Quaternary unconsolidated sediments are the main aquifer units in the area. The general trend for groundwater flow from piezometric heads is generally from west to east. Piper plots were used to classify the water chemistry of the area. Groundwater type of the area generally evolved from Ca-Mg-HCO₃ or Mg-Ca-HCO₃ water type in the area closer to western escarpment to Na-Ca-HCO₃ water type in the eastern part of the area. The water is also suitable for drinking purpose based on the standards.

Keyword: groundwater, resource, recharges estimation, hydrochemistry, and aquifer characterization

CHAPTER ONE

1. INTRODUCTION

1.1 Background

Groundwater is the safest and most reliable water source, used in domestic, irrigation, industries and for various municipal purposes. Groundwater development for water supply purposes from low discharge springs and dug wells, is not that preferable because these are found to be of inadequate yield and no longer resistant to scanty rain years, while most of them might completely dry out and never easily recover after the prolonged drought time.

The occurrence, origin, movement and chemical constituents of groundwater are dependent on geology/ lithology, geomorphology /landforms, drainage density, rainfall, geological structures/lineaments, slope, land use/land cover and the soil profile of the groundwater regime Tesfaye Tessema (2015).

Meanwhile the availability, quantity and the quality of groundwater resource must be studied to ensure the supply for the current demands and possible increased demand with population increases and change of life styles (Getachew, 2004).

Even though Ethiopia is called “the water tower of Africa” but the potential of the country is not known in a clear manner as well as utilization of the existing water resources and management are poor in the country.

In order to increase and sustain the development of the country, proper utilization and management of groundwater makes hydrogeological assessment very essential.

The upper Mile River Catchment aquifer systems, provides water supply for different cities like, Hayek town, Wichale town, Mesrsa town and other towns found in the catchment. Besides, it also provides water supply for rural communities found in the catchment.

Therefore, groundwater that is being extracted from this catchment for different purposes supports a large number of population and infrastructures and hence, it is very important to know and assess the available resource quantitatively and qualitatively.

1.2 Problem Statement

The consumption of the groundwater is not based on understanding of the groundwater resource and groundwater management. Especially in Hayk and Mersa towns as well as other towns where the population, industrial and agriculture activities are growing at an alarming rate the abstraction rate of the groundwater is increasing from time to time not knowing how over-abstraction affects the groundwater table.

Having a knowledge of hydrogeology in general have great economic and development implication as groundwater is being used extensively for domestic, agricultural & industrial purposes.

1.3 Objective

1.3.1 General Objective

The ultimate objective of this research is to assess the hydrogeology of the upper Mille River catchment

1.3.2 Specific objectives

The specific objectives of the research will be to

- Estimate the groundwater recharge
- Analyse and interpret water quality both in situ and in the laboratory
- Identify the recharge and discharge zones
- Classify hydrogeological units based on its productivity

1.4 Procedures for the proposed activities

Procedure 1: Review of Existing Literatures, Reports and Maps include:-

Technical reports and maps prepared by governmental agencies, Technical publications in scientific journals ,Books, Reviewing of existing water wells drilling logs and reports. Thesis and research papers conducted in the area and elsewhere on relevant topics.

Procedure 2: Field work have been done to fill the data gaps in this stage those include:-

- confirmation of all the collected data in the pre-field work
- measurement parameters are (PH, EC, T)
- water sampling for determination of the water quality and hydrochemistry
- geomorphological, lithological, structural hydrogeological, etc. studies to construct maps
- collection of secondary data from different sources borehole logs, pumping test data, hydrogeochemical data, geophysical data and hydrogeology feasibility report and well completion report will be collected

1.5 Methodology

In order to achieve the objectives of the research certain methodologies have been applied. Hydrogeological work has been carried out by collecting hydrogeological and hydrological data of the study area. It was obtained from Amhara design and supervision works enterprise (ADSWE), water work design and supervision Enterprises (WWDSE), Geological survey of Ethiopia (GSE) and Zonal Water Bureaus.

Field investigation was carried out from January 10- January 25. It was concentrated on differentiating the rock units of groundwater significance and in collecting hydrogeological information.

During field activity a total of 21 water samples has been collected on systematically selected site in bore holes' hand dug wells and springs. In addition, Hydrochemical parameters (pH, EC and T) have been measured in the field using digital pH meter and conductivity meter. Representative water samples were analysed to examine the suitability of the groundwater for such applications as drinking and agricultural use.

During post field activity 30m resolution of soil and land use/land cover map of the study area has been prepared from dataset obtained from the Ministry of Water Irrigation and Energy.

Land cover, soil map, Hydrometeorological elements and environmental tracer (Cl) data have been used to evaluate the groundwater recharge in the study area with the required format. Recharge rate has been estimated using the baseflow separation approach, chloride mass balance method and SWAT (soil and water assessment tool).

Groundwater discharge and recharge area are identified using piezometric contour, topography and chemical parameters by using water levels from springs and wells. All the required analysis has been manipulated using the appropriate software's and the results are presented in maps and tables.

1.6 Significance of the research

The output of this research is to bring attention to the importance of understanding and improving groundwater governance and management. Moreover, it is to bring attention to this invisible water resource before pollution or depletion of the resource cause severe economic, environmental and social dislocations. Mainly it will provide a very useful tool for future studies over the area and in areas with similar hydrographic conditions.

1.7 Literature Review

Molla Demlle (2000) studied the geology, hydrology, and hydrogeology of Hayk-Ardibo catchment. The main objectives of the study were to understand and map the different lithologic units and characterize them in to hydrostratigraphic units in order to analyse the water balance of the catchment including Lake Hayk and Lake Ardibo. Two major hydrostratigraphic units were mapped the Quaternary unconsolidated sediments and the fractured volcanic rocks, both had good permeability meanwhile The results showed that the water balance of the area was estimated to be 162.3 mcm and the analysed water hydrochemistry indicate that surface water was magnesium bicarbonate type, while the groundwater was calcium bicarbonate type and it was safe to use for drinking and agriculture. .

Meanwhile Getachew Asmare (2005) conducted model based groundwater system analysis for Hayk-Ardibo catchment to understand the interaction between the surface and groundwater of the Hayk-Ardibo Catchment. The values obtained from steady-state model suggests The volumetric budget terms for groundwater flow components for the Hayk-Ardibo catchments simulated to be as follows: Groundwater inflow is $6.5393855E+04$ m³/d and Groundwater outflow 65389 m³/d. which means that substantial amount of groundwater leaves catchment.

Furthermore Jemal Ibrahim (2011) conducted landslide assessment and hazard zonation in Mersa and Wurgessa by identifying the various causative and triggering slope instability factors and by preparing landslide hazard zonation map of the study area. It was found that the slope material which has experienced failures of varied forms was mainly; residual soils, poorly graded colluvial and alluvial material. Most of the slope failures were associated with; high relative relief, steep slopes, adverse groundwater flowing conditions, kinematic structural discontinuities, bare or sparsely vegetated lands and stream bank and toe erosion.

In the proximity of the study area evaluation of groundwater resource potential in Borkena river catchment, Awash basin was studied by Getachew Tsigie(2015)was done main aim of the study was to understand the groundwater potential of Borkena river catchment for domestic and agricultural use by using groundwater flow modelling and hydrochemistry .

The PMWIN model was calibrated for steady state condition by matching simulated and observed hydraulic head for different periods. The calibration were accepted small error of simulated heads and the overall root mean square errors for simulated hydraulic heads were found to be 3.96m.the the hydrochemistry of the area showed the groundwater were suitable both for domestic and agricultural use.

Meanwhile Groundwater Potential evaluation and flow dynamics of Hormat-Golina River catchment, Kobo Valley was conducted by Afework Desalegn (2011) using runoff coefficient methods as well as Chloride mass balance (CMB) method, Darcy and conventional water balance approaches were used to estimate recharge, to characterize the aquifer system of the area pumping test data, well completion reports, well logs and geology of the area were analysed. The Quaternary unconsolidated sediments are the main aquifer units in the area and from the analysed water in the laboratory was found that the water contained low sodium and can therefore be used for irrigation and domestic water use.

In addition in the same area the geology, hydrology, hydrogeology and hydrochemistry of the Borkena catchment was studied based on conventional geologic and hydrogeological mapping, water sample analysis and assessment and interpretation of hydrometeorological data by Mesfin Sahele (2001). The main

objective of the work was to understand the different lithologic unit and to characterize and group them into hydrostratigraphic unit and map them as well as analyse the water balance and the water quality of the area and seven rock units and three set of faults were identified Among the rock units, scoriaceous and basaltic lava flow and alluvial deposits cover more than 70 percent of the catchment and colluvial and river channel deposits were the promising units as well as the water bodies were found to be low total dissolved solids (TDS) and low electrical conductivity (EC) values as a result they were classified as freshwater.

Furthermore groundwater resources evaluation of Walga river basin in central Ethiopia was conducted by Kassahun Beyene (2005) the basin is part of the western central Ethiopian plateau. Using methods like Hydrometeorological, geological, hydrogeological, Hydrochemical investigation and conventional methods were used for groundwater resource potential evaluation of Walga Basin three litho-stratigraphic succession were identified in the area, which include Precambrian basement, Mesozoic sedimentary rocks and Cenozoic volcanics Based on analysis made both quantitatively and qualitatively of aquifer characteristics, the area was categorized in to three aquifer systems which were low, medium & high productivity aquifers. The scoriaceous basaltic aquifer around Woliso area had the highest potential with high well yield also the analysed water for quality both in the field and laboratory gave low TDS fresh waters of the area and it had concentrations below permissible limit for water supply, irrigation & industrial uses and High fluoride concentration was observed in some thermal spring waters.

Furthermore Kobo Chefa groundwater resource evaluation, assessment and test wells drilling were done by Federal Democratic Republic of Ethiopia Ministry of Water, Irrigation and Energy (2018) methodologies used in the report include integration of the data and detail geological mapping of the whole area which included the study area. Surface geophysical surveys (VES and Magnetic) were also conducted. From the estimated annual dynamic recharge and static groundwater storage, it can be concluded that about 87 MCM, 78 MCM, 31 MCM and 27MCM per year can be exploited from the alluvial aquifers respectively of Mersa-Girana, Robit-Tisabalima and Woldia. Intermountain valleys marginal grabens which were the highest potential of the lithology's found in the area.

On the other hand integrated geophysical investigation using Vertical Electrical Sounding (VES) and Magnetic methods were conducted to investigate groundwater potential zones and geological structures at Woldia University and Mechare Meda, North Wollo Zone, Getachew Belay (2018) which includes some part of the study area. The main objective of the study was to assess and evaluate groundwater potential zones of Woldia University and Mechare Meda and the interpretation showed that the area was composed of two aquifers, the first was the Upper Basalt aquifer, which is slightly confined between alluvial deposits, and moderately fractured Basalt and Trachytes and the second is Lower Basalt aquifer which is confined by the moderately fractured Basalt. The depth of the upper aquifer is ranging from 20 to 60m while the depth of the lower aquifer is greater than 180m. The geological fractures found in the area had orientation of NW–SE, and NE–SW.

Characterizing groundwater dynamics using major ion hydro geochemistry and environmental isotope tools were employed to tributary streams of Muger River Catchment in the north and Holota River Catchments in the south were done by Kidist Hailu (2016). Hydrogeochemical study reveals that water types vary from CaHCO_3 type to, NaHCO_3 type and low TDS to high value as well as Radon concentration has indicated that also high value in the main River and low in tributary streams meanwhile The stable isotopes signature of the deep aquifer indicted that groundwater was enriched and was recharged through long subsurface path relative to the deep aquifers found in Tributary streams which were depleted and groundwater level map and isotopic signature showed that groundwater divide shifts from surface water divide.

CHAPTER TWO

2. DESCRIPTION OF THE STUDY AREA

2.1 Location

The study area is located in the western margin of the Afar rift on the escarpment. On the Northwestern and western part of the escarpment. Geographically the region is bounded within 550000-600000E and 1240000-1300000N .The total area of the catchment is 1367 km² and it is crossed by the main road from Addis Ababa to via Dessie

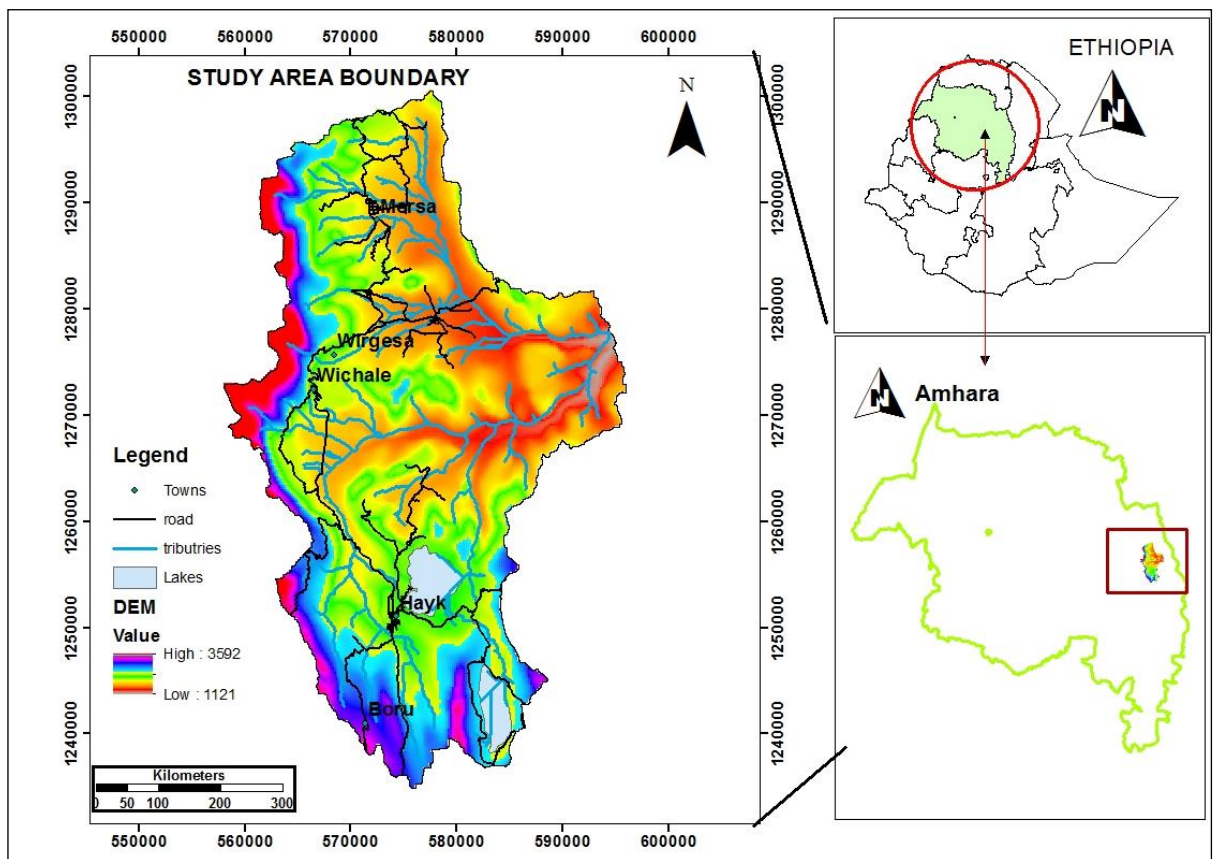


Figure 1 Location of the study area

2.2 Physiography and Drainage

Erosional process and volcano-tectonic activities make up the physiography of the study area (Molla 2000). It is part of the western escarpment and northern western boundaries of the Afar margin.

Based on the map developed from DEM (Digital Elevation Model) the area has an overall elevation difference within the steep fault escarpment have an elevation up to 3592 with minimum elevation 1121 m a.s.l that comes from the Graben which is bounded by faults which comprise of lakes, peats, swamps and agricultural lands.

The drainage network of the study area is dendritic they are structurally controlled streams and they are dominant in the study area. The major Rivers in the area are the Nile and Gelana in which Mille River starts from the southwestern part of the study area and drains into the major Mille River and Gelana River starts from north western part of the area drains into the major Mille River to the east in the rift. There also are streams drain towards the nearby lakes locally in the area namely Lake Ardibo outflows to Lake Hayk seasonally through local graben.

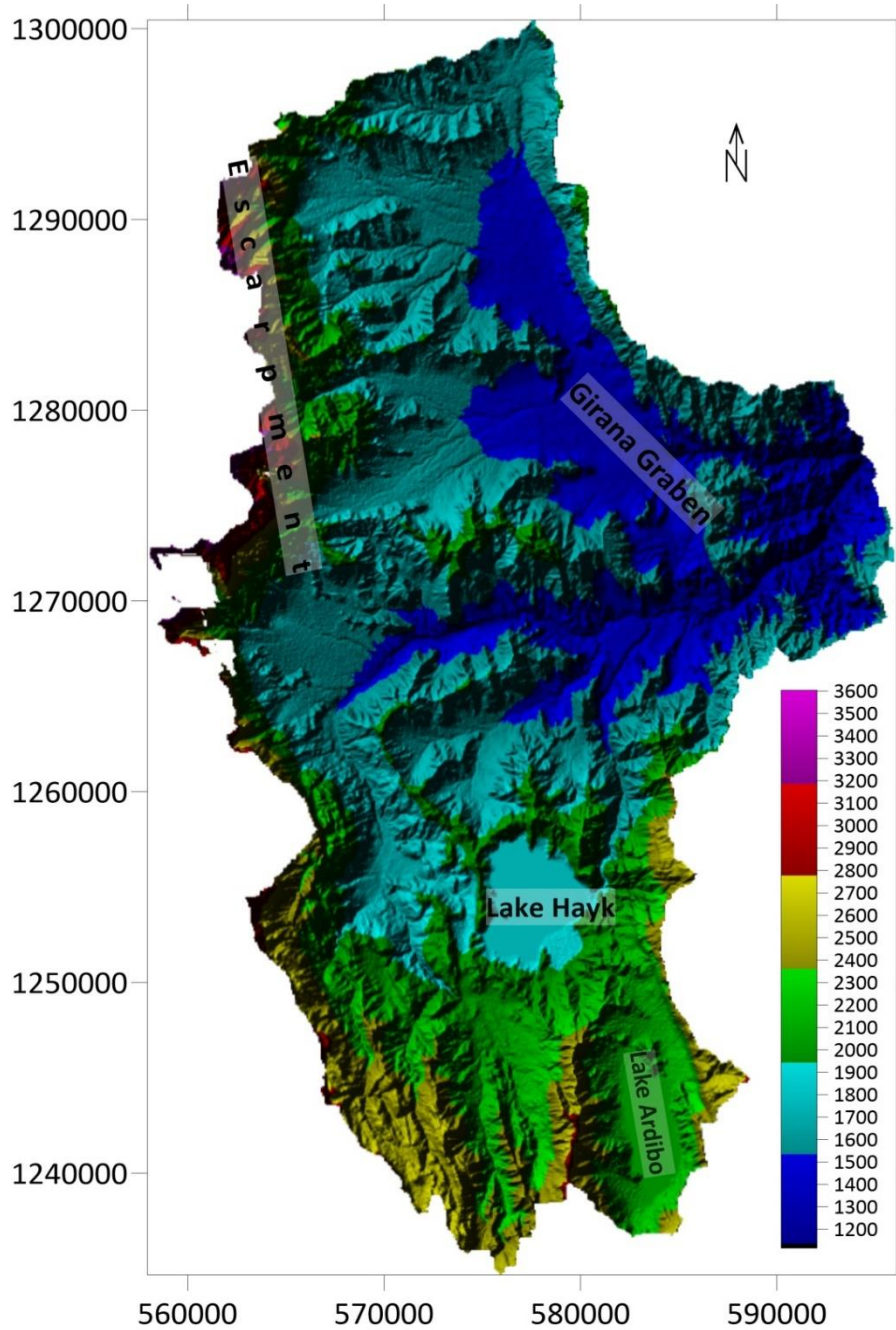


Figure 2. Physiography of the study area.

2.3 Climate

The seasonally changing position of the sun heats differently the land and the ocean in, which brings latitudinal pressure gradients brings asymmetry with movements of pressure systems, causing a north-south propagating global tropical rain belt (ITCZ). The wind systems also play a big part (Tropical Easterly Jet (TEJ), East African Low Level Jet (EALLJ), El Niño-Southern Oscillation (ENSO)

(Endalew, 2007) as well as the development of the Indian monsoon. The climate system and the circulation in the tropics are controlled by the development of the Indian monsoon (Gadgil et al. 2007).

The ITCZ (global pressure systems with the allied wind system, in other words the dry northeasterly winds meet the wet wind southeasterly winds then condenses) and the difference in topography brings different climate and season determines the distribution and pattern of Ethiopia's climate (Block and Rajagopalsn, 2007). The ITCZ is controlled by the difference in the surface temperature of the Indian Ocean, which relates to the variability of the ElNiño Southern Oscillation (Haile, 1990).

The seasonal migration of the ITCZ controls the climate of the study area which is conditioned by the convergence of the trade winds of the northern and southern hemispheres and the associated atmospheric circulation. The rainy season in the area extends from March to May and from June to September; indicating a bimodal rainfall pattern (Otterbach L., 1995).

CHAPTER THREE

3 GEOLOGY

3.1 Regional Geologic setting

The Ethiopian flood basalts are associated with felsic pyroclastic rocks (Ethiopian Trap Basalts) are the result of continental volcanic rocks that erupted before the onset of continental rifting and sea-floor spreading in the Afar, which is alleged to be associated with the Afar plume activity (Sileshi, 2015). The majority of these volcanics erupted mainly around 30 Ma ago during a relatively short, <5 Myr period of time (Berhe et al., 1987; Hofmann et al., 1997; Kieffer et al., 2004).

Following this peak of fissural activity, large shield volcanoes formed on the surface of the volcanic plateau. In many instances the shield volcanism was comagmatic with the flood volcanism that formed the main volcanic plateau (Kieffer et al., 2004). The entire plateau volcanic sequence is sub-divided into the following formations: Ashangi basalts, Aiba basalts, Alaji basalts/ rhyolites and Tarmaber basalts, from the oldest to the youngest. Based on a number of previous studies, e.g. Zanettin et al. (1974), Mengesha Tefera et al (1996) and Tesfaye Chernet (1993), these formations have the following characteristics.

Ashange Basalt Formation

The unit constitutes the lower sequence unconformably lying on the Mesozoic marine sediments. It is recognized by thin lava flows, (< 10 m) developing relatively less steep topography. The Ashangi basalt sequence, on the western half of the northern Ethiopian plateau (e.g. Lima Limo section), is flat-lying and undeformed. Contrariwise, there is observational indication for minor faulting and tilting within the Ashangi basaltic pile north of the Wereta-Woldia road and east of upper Tekeze River signifying that deformation of the flood basalts happened during their emplacement. This formation is basically made up of a series of extensive basalt flows, and at places with minor interbeds of acidic layers (rhyolitic pyroclastics).

The units are usually aphyric and strongly weathered with intercalations of tuff and paleosols. The total thickness of Ashangi basalts is estimated to be 200 to 1200 m (Tesfaye Chernet, 1993). Sequence of the unit is commonly injected by dolerite sills

and dykes. The Ashangi basalt cycle is different from those of Aiba, Alaji and Tarmaber. The stratigraphic reconstruction of the terrains is usually difficult by the bad phase of conservation of the rocks themselves. On the other hand lack of evident unconformities, the difference between Ashangi basalts and Aiba basalts is based on the point that the former is more intensively weathered and at places faulted and tilted, while the latter can be found in clearly fresh, compact, continuous and unbroken flows (Zanettin et al., 1974).

Aiba Basalt Formation

Aiba Formation constitutes second round of fissural basalt volcanism. The unit is composed of thicker basalt flows (10-50 m) that normally form steep topographic cliffs. This sequence at times comprises minor amounts of felsic yields with variable thicknesses. The basalts flows are extensive, flat-lying, layered and generally aphyric. The overall thickness of this sequence on average is 200m and the maximum is 600m (Tesfaye Chernet, 1993). Aiba basalts unconformably lay on top of the tilted Ashangi basalts in the eastern portion of the north-eastern plateau.

Tarmaber Basalt Formation

The unit is overlaid on the Alaji rhyolitic pyroclastics and flood lavas, locally thick sequences of basalt flows have been flows out during mid-Miocene, from low-angled shield volcanoes that have constructed prominent land features such as the Simien, Meghezez and Choke-Menghistu and Guna volcanic massifs. The shield volcanic formation contains sequences of alternating basalts, rhyolitic and trachytic lava flows, tuff and ignimbrite, particularly near the summits (Keffer et al, 2004). The basalt is usually cut by a network of mafic and felsic dyke swarms. Tarmaber basalt flows are thinner and less continuous than the underlying Ashanghi and Aiba flood basalts. Tarmaber basalts are heterogeneous but characteristically more porphyritic, containing abundant and often large phenocrysts of plagioclase, pyroxene and olivine. After shield volcanic activity, subsequent volcanism was largely confined to regions of rifting (Keffer et al, 2004).

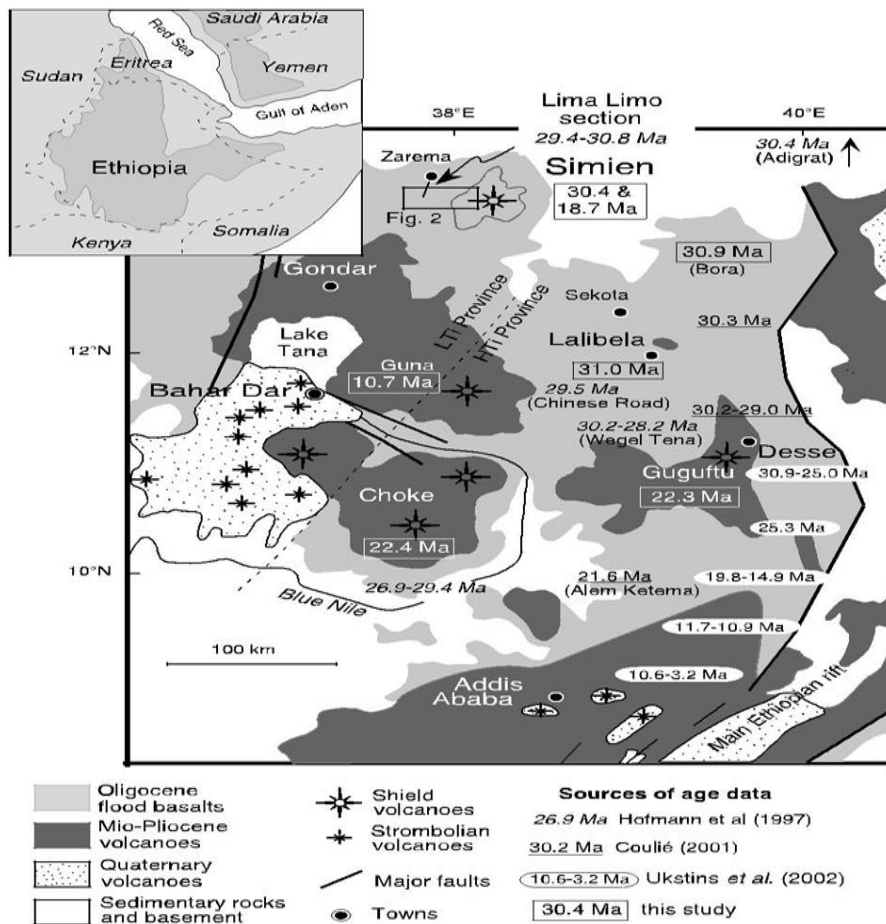


Figure 3. Geological map of the Northern Ethiopian plateau (Keiffer et al., 2004)

3.2 Geology of the study area

3.2.1 Lower Basalt (Ashangi Basalt) (Tv1)

The Eocene-Oligocene Ashangi basalts cover most part of the study area and it is found at lower elevation of the North western, south western, central and south eastern parts. The basalt represents the lowermost parts of volcanic successions. Because of their weak strength, they do not form steep cliffs, but they are continuous and small non-continuous outcrops exposed in road cuts, stream beds and steep slope of chains of mountains. It is a dark colour and texturally it varies from the medium to coarse grained.

The unit is weathered, altered and it is friable by hand with a single blow of geological hammer. It is also characterized by the vein material that fills the fractures and pore spaces in some places. The material filling is mostly calcite. In the

meantime, because it is highly affected by tectonic disturbances it may enhance the hydraulic properties of the rock.

It is also characterized by the vein material that fills the fractures and pore spaces in some places. The material filling is mostly calcite. In the meantime, because it is highly affected by tectonic disturbances it may enhance the hydraulic properties of the rock. Meanwhile the contact between underlying rock units in the study area cannot be seen. There is also reddish paleosoil exposed along Dessie-Hayk road.

3.2.2 Aiba Formation (Tv2)

The Oligocene Aiba basalt covers a small part of the area with a lateral thickness about 100km². This rock unit is found at higher elevation than the Ashangi formation. It is characterized by dark gray to greenish colour and fine to medium grained texture. It is comprised of alternating layers of basal scoria vascular Oliven pyroxen phyri, agglomerates, rhyolitic Tuff, rhyolitic obsidian basalt and aphanatic basalt horizontally stratified according GSE (1998).

Lava flows, dikes and sills are a mode of occurrences of this unit. Meanwhile columnar joints are exposed at Golo River and in the southwestern part of the Wurgessa area (Jemal 2011) there are also dike intrusions in high elevated ridges of Mersa, Sulula and Pasomile area. In the meantime the formation forms a steep cliff than the Ashangi basalts and shows less alteration and weathering relatively. The total vertical thickness varies from 200 to 1000.

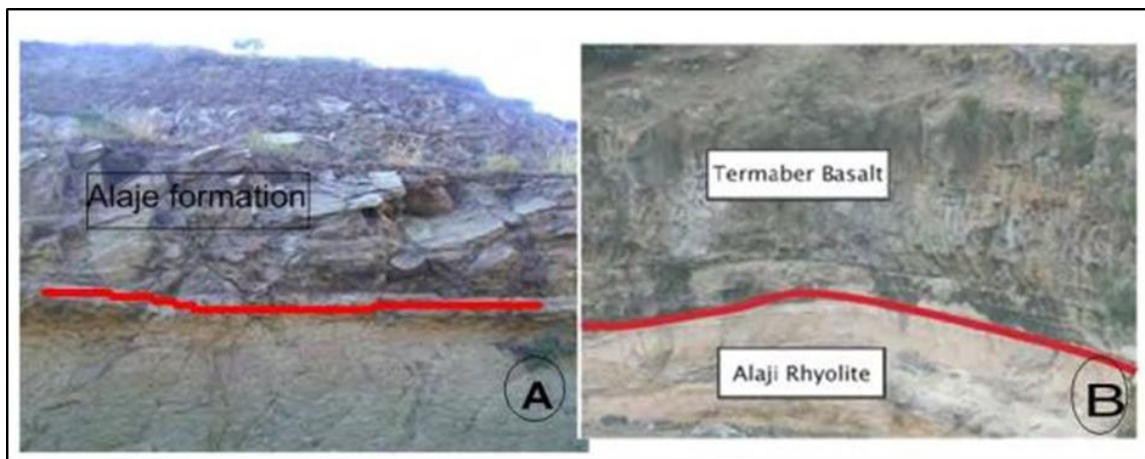


Figure 4. A) Alaji formation (Wuchale); B) Contact between the Alaji rhyolite and Tarmaber Basalt; (Source: Tesfaye Kidane, 2010).

3.2.3 Tarmaber basalt (Tv4)

The Oligo-Miocene Tarmaber Basalt covers a small portion of the area with a lateral thickness 10 km². It's the youngest from the other basalt units in the study area. It is a fine grained dark coloured basaltic unit characterized by columnar jointing. In some outcrops, this unit is associated with rare tuffaceous and volcanic ash units and it is exposed in road cuts and River beds. The name is adopted from (Zanettin et al 1974; Tefera et al., 1996). It forms an elevated area with (> 3000 m a. s. l.) and forms ridges. The total vertical thickness varies from 100 to 1000 m.

3.2.4 Kemise Formation (Tk)

The Late Miocene Kemise Formation is mainly exposed in the east of the study area around Kobe. It is also exposed at southeast of the Lake Hayk area. It covers up to 144km² of the study area and it consists of Rhyolite, ignimbrite, Tuff and ash. The outcrop is found usually as discontinuous tectonic blocks bounded by normal slip faults (GSE 2011). It is light gray, pink and brownish fine to coarse grained in texture it is slightly weathered at places it forms ridge.

It has tectonic contact with the underlying Ashenge basalt. In the meantime the Kemise formation comprises of pink and greenish gray rhyolitic ignimbrite with medium to coarse grained size grains with vesicles at some places and they are sometimes filled with secondary calcite.



Figure 5. Highly fractured and weathered rhyolite in Kolbo area.

3.2.5 Quaternary Sediments

3.2.5.1 Alluvial Sediments

The alluvial sediments are one of the youngest units in the area they are found in the northeast and southwest part. They are deposited in the low-lying areas within very gentle slopy areas. It is classified into fine to coarse grained size according to the energy of the river and depositional basin width and depth. It is characterized by black cotton, fine to coarse grained clay, silt, and clay, sand and silt deposits. A very thick alluvial deposit found in Mersa area in both sides of Birbissa River and in Paso Mille area. This soil is mostly covered with extensive farming.

3.2.5.2 Colluvial and alluvio-colluvial Sediments

This formation results from gravitational force assisted by runoff and wind. It is exposed mainly at Northeastern and central part of the study area. They are loose, unconsolidated, composed of highly fragmented rocks. They are deposited in the slopy part of the mountains. The size of the deposit varies from gravel size to very large blocks. Residual soils and colourful material with thickness less than 5m are deposited in Wurgessa and Tisabalima area.

3.2.5.3 Inter-mountain Alluvial sediments

This formation covers a small part of the study area. It is largely found in shallow areas. They are characterized by mostly fine clay and silt. It is found in the marginal greens as well as alluvial-lacustrine deposits along river valleys and old channels on the alluvial and colluvial deposits.

3.2.5.4 Peat bogs, swamps and wetland deposits

Peat deposits cover large areas of the world's landmass and are formed by the accumulation of partially decomposed and disintegrated plant material (such as mosses, sedges, and grasses). In wetland areas where unfavorable conditions, including lack of oxygen supply, inhibit complete decay an area that is periodically or continuously inundated by shallow water or has saturated soils. plant growth and other biological activities are adapted to the wet conditions (Hobbs, 1986; O'Kelly and Pichan, 2013). The deposit is found in wetter (seasonal swamps) parts of the Graben.

It is found mainly between Lake Hayk and Lake Ardibo. It is characterized by Black cotton soil mainly clay and fine silt.



Figure 6. Swampy areas between Hayk and Ardibo.

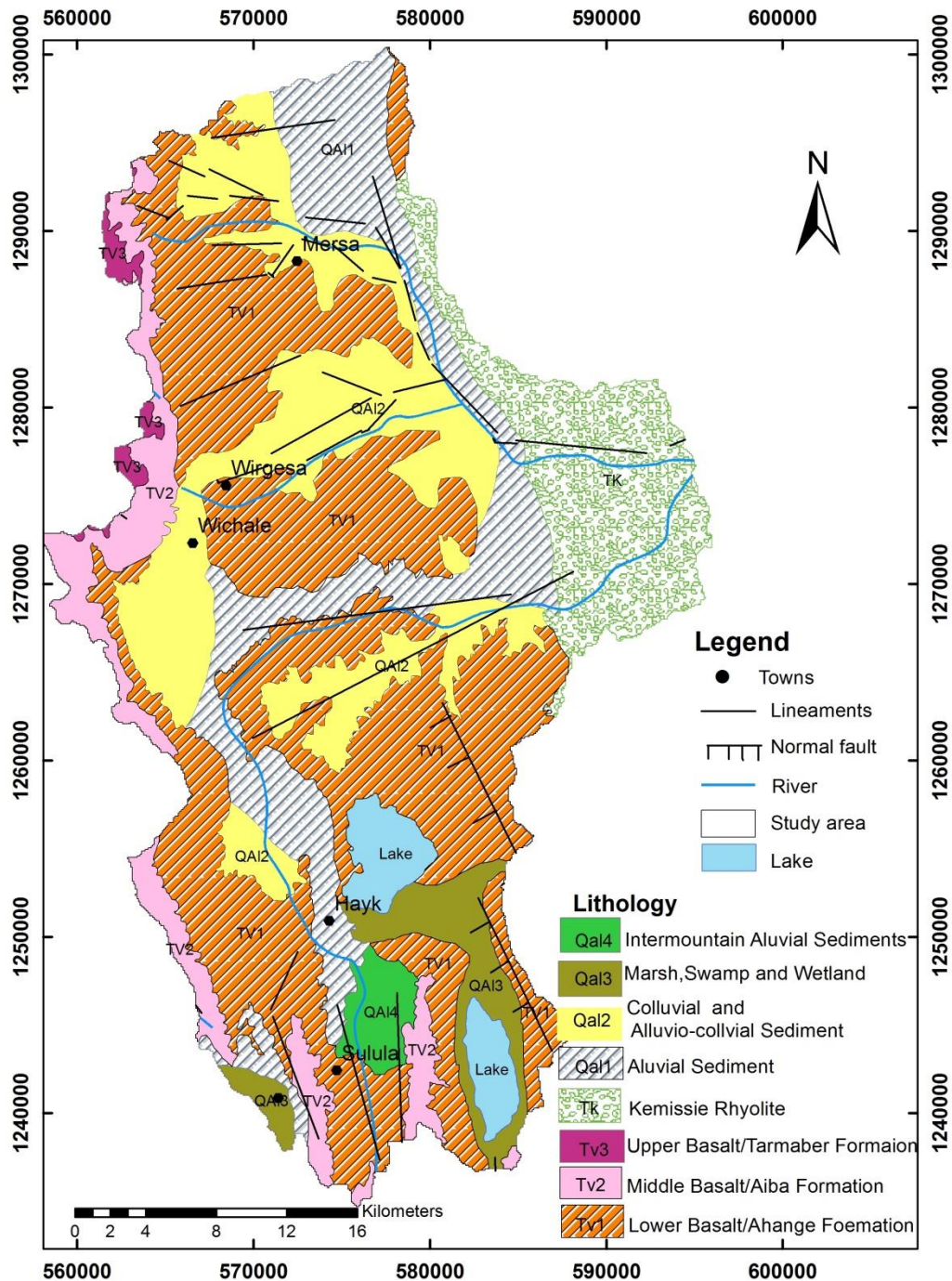


Figure 7. Geological map of the area

3.3 Geological Structures

The study area is highly affected by rift tectonics features since it is located at the Western of Afar margin. It is highly affected by normal faults, joints and basaltic dikes.

The study area marks the outer tectonic boundary of the Afar so it is basically characterized by NNW-SSE structures and with rare E-W structures (Molla, 2000).

3.3.1 Dikes

Basaltic dikes with the strike orientation of NW-SE exposed near sable ridge and at the crossing of Birbissa streams of Mersa area (Jemal, 2011). It is also exposed near the Tekelehayimanot church in Sulula area. These dikes are aphanitic basalt with width up to 1 to 2 meter figure 3.4. These weak zones may act as a barrier or may be conduits for the passage of water.

3.3.2 Joints

Joints are geological structures which are formed as a result of expansion due to cooling, or relief of pressure as overlying rocks are removed by erosion (Jemal, 2011). It push out in various directions, usually vertically. It usually occur as sets, with each set made up of joints that are parallel to each other figure 8. Some of the joints and fractures and bedding planes are parallel to the slope in the study area and they may serve as a conduit for water flow. Joints are exposed near Gatira Giorgis at Wurgessa.



Figure 8. A) Columnar joints in Wurgessa (575505 E, 1278293 N) study area; B Dikes near a ridge in Sulula (574382E, 1241174N).

CHAPTER FOUR

4 HYDROMETEOROLOGY

4.1 Meteorological stations and data

All the data needed were collected from the National Meteorological Service (NMS) and Ministry of Water, Irrigation and Energy (MOWIE), such as rainfall, temperature, starting from 1987's to present for few stations, but the range of record history differs among different station so for that reason from 1999-2013 data were used for SWAT model.

A set of daily available meteorological data was collected from 9 stations from the National Meteorological Agency (NMA).

The rainfall, temperature, and evapotranspiration affect the resource availability of the surface and groundwater than other climatic parameters. The study gives more emphasis to those parameters in order to characterize the hydro-meteorology of the study area.

4.2 Meteorological parameters

There are nine meteorological stations within and around the study area. The overall meteorological parameters available in the study area are; rainfall, temperature, relative humidity, wind speed, and sunshine hours.

Table 1. metrological data together with their location on the basis to determine the water balance of the catchment

Station	UTM Easting	UTM Northing	ANNUAL rain fall (mm)	Elevation (m)
Hayk	574140	1249618	1196.1	1985
Wurgessa	567429	1275878	1293.2	2000
Mersa	572503	1289258	1076.5	1578
Bati	610764	1237709	958.9	1660
Kombolcha	578284	1225144	1029.7	1857
Sirinka	566840	1298886	1030.9	1861
Werebabo	581754	1250892	1161.9	2118
Bokeksa	595971	1264978	1063.1	1712
Wuchale	565965	1273075	1192.3	1948

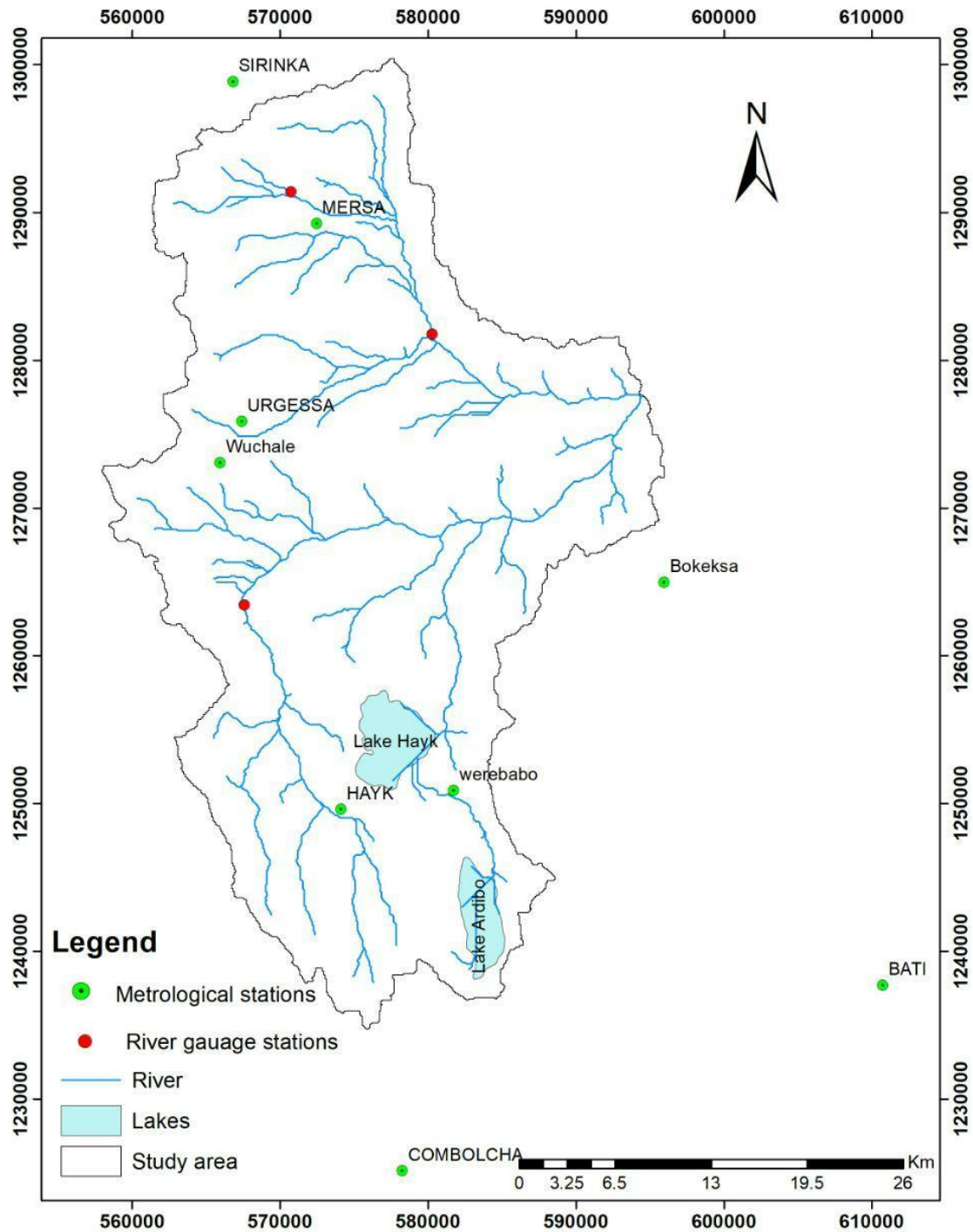


Figure 9. Distribution of Metrological and River gauge Stations in the study area and close surrounding.

The study area is represented by 9 stations. Accordingly, as shown in Figure (10) below, the basin has bimodal rainfall "small rain" or "Belg" lasting from March to May and the "Big Rain" or "Kirermit" lasting from July to September and when we

see the Annual rainfall vs elevation (in Figure 9): shows that there is a small tendency of an increasing rainfall amount with elevation.

Which means the amount of rainfall is moderately related to elevation and it is affected somehow by topography. Generally high amount rainfall, relatively occurs at the high elevation areas than in the low area, but this doesn't mean that elevation is the only factor that controls the amount of rainfall, it is also related to different factors, so this mean we cannot totally depend on altitude rather it's better to use different methods to calculate rainfall depth of the study area.

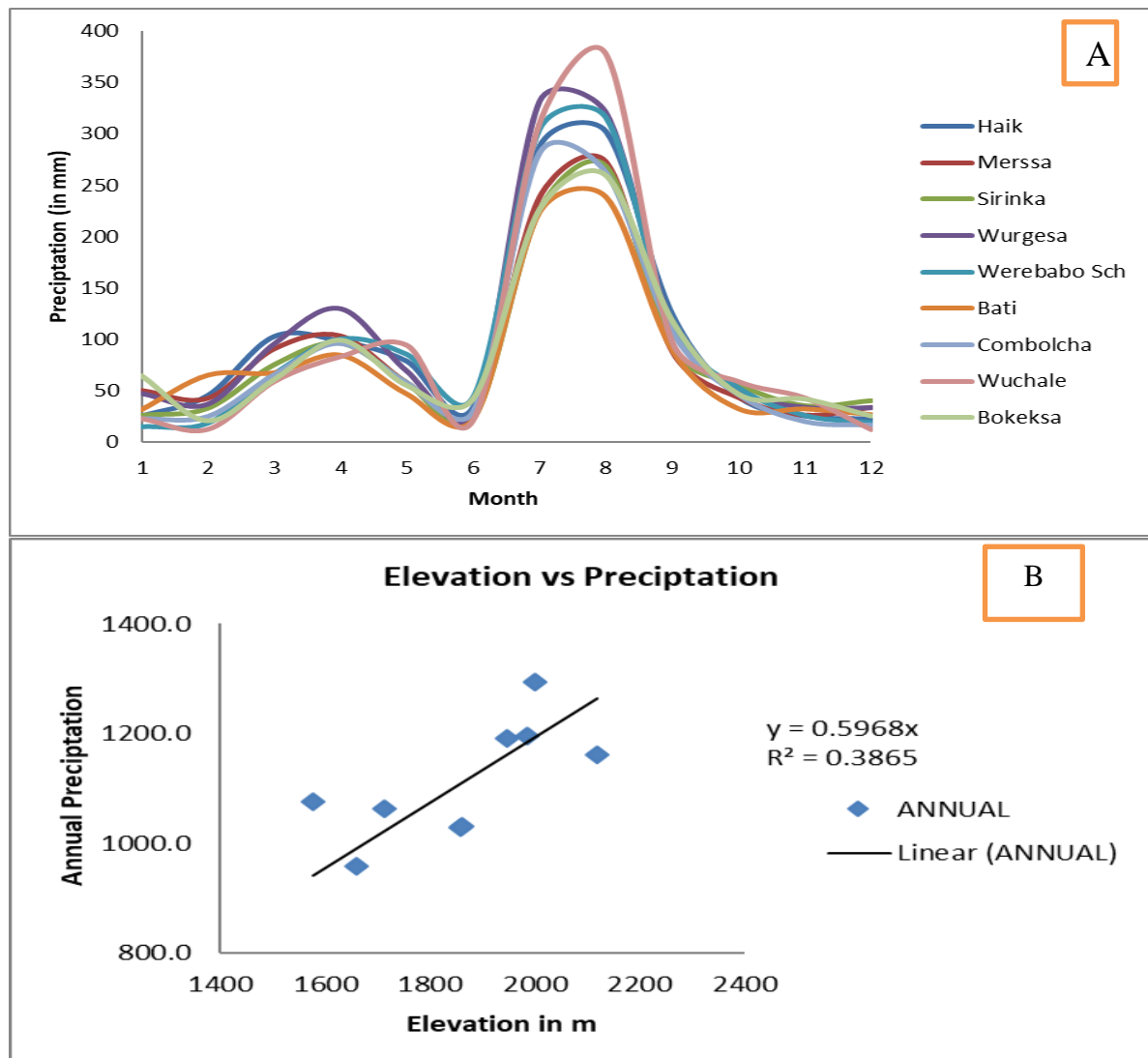


Figure 10. A) Seasonal and spatial distribution of rainfall and B) elevation vs precipitation relationship (source National Meteorological Agency)

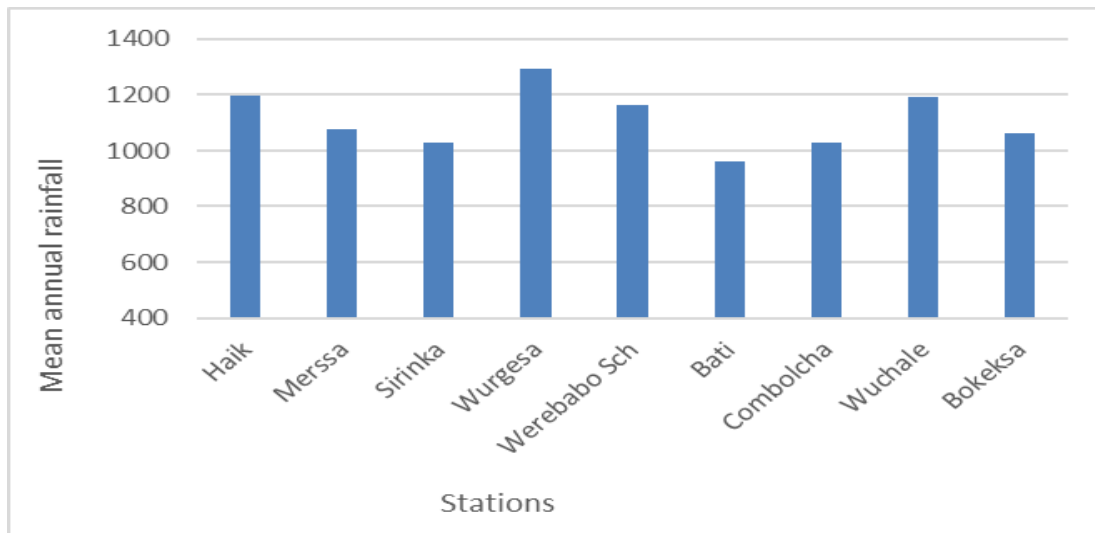


Figure 11. Mean annual rainfall distribution

While, the minimum annual rainfall occurs over pairs of stations in Bati, sirinka and the maximum rainfall occurs at Wurgessa and Hayk. Overall, for all available stations in the study area, the mean largest and smallest annual rainfalls recorded were 1293.2 mm and 958.9 mm, respectively, showing a difference of about 343.3 mm in the above figure 11.

4.3 Temperature

Monthly maximum and minimum temperature data (1987-2016) have been obtained for six stations within and near the study area. The mean monthly temperatures have been calculated for each station. From mean monthly temperature data Kombolcha, Bati, Sirinka, Werebabo, Mersa and Hayk or Haik they do not show a strict relationship with altitude. The mean annual temperature for these stations vary from the minimum average 17.43 °C for Hayk station to the maximum of 20.87 f °C for Bati and Mersa. (Annex 4)

4.4 Relative humidity, sunshine hours and wind speed

Even though there are no stations that measure humidity, wind and sunshine hour in the study area, but there are stations proximate to the study area that can measure the parameters. Relative humidity is measured 5 times a day, 06:00, 09:00, 12:00, 15:00, 18:00 hours 'mean annual humidity is found to be a higher Sirinka station (74.5 %) and lower for (42.8 %) at Kombolcha station.

Further, when it comes to daily sunshine hours during the wet season are low and during the dry season it is high in all stations and the highest mean annual daily sunshine hours is recorded in Kombolcha (9.1 hours) the lowest sunshine hours is recorded (5.1hours) in sirinka, annex 4.

On the meantime Wind speed is measured at 2 m above the ground surface. The highest mean wind speed (131.7km/h) is seen in the sirinka station while the lowest (33.8 km/h) is seen from Kombolcha station. Wind speed is generally high during summer season in all stations.

4.5 Determination of aerial depth of precipitation

There are lots of ways for computing areal rainfall from point data, including arithmetic, isohyets, and Thiessen polygon. Those data are as point data in the rain gauge stations and rainfall is highly affected by physiography of the area.

4.6 Thiessen polygon method

The arithmetic method gives reliable result only when there is even distribution of point measurements in the area and more or less flat topography (Dagnachew, 2018). since, it is not enough to use it for representation of the annual average rainfall instead Thiession polygon method was used as conventional approaches to calculate the annual average rainfall in the figure 12.

$$P_t = \frac{P_1A_1 + P_2A_2 + P_3A_3 + \dots + P_nA_n}{A_1 + A_2 + A_3 + \dots + A_n}$$

Where, P_t is the areal mean total annual rainfall, $P_1, P_2, P_3, \dots, P_n$: the rainfall at each station and, A_1, A_2, A_3, A_i : the area of influence by the individual station (i) determined based on Thiessen polygon method in table 2 and figure 11. This method gives rainfall values to which areas of observation station represent.

Table 2. Thiessen polygon calculation for the study area

Station	X	Y	Annual.r.f	Elevation(M)	Area(km2)	weight	Annual.r.f *weight
Hayk	574140	1249618	1196.1	1985	281.865	0.21	251.2
Urgessa	567429	1275878	1293.2	2000	193.3412	0.14	181.1
Mersa	572503	1289258	1076.5	1578	257.6371	0.19	204.5
Sirinka	566840	1298886	1030.9	1861	47.29874	0.03	30.9
werebabo	581754	1250892	1161.9	2118	204.9966	0.15	174.3
Bokeksa	595971	1264978	1063.1	1712	187.0734	0.14	148.8
Wuchale	565965	1273075	1191.1	1948	194.6873	0.14	166.8
			1144.7				1157.6

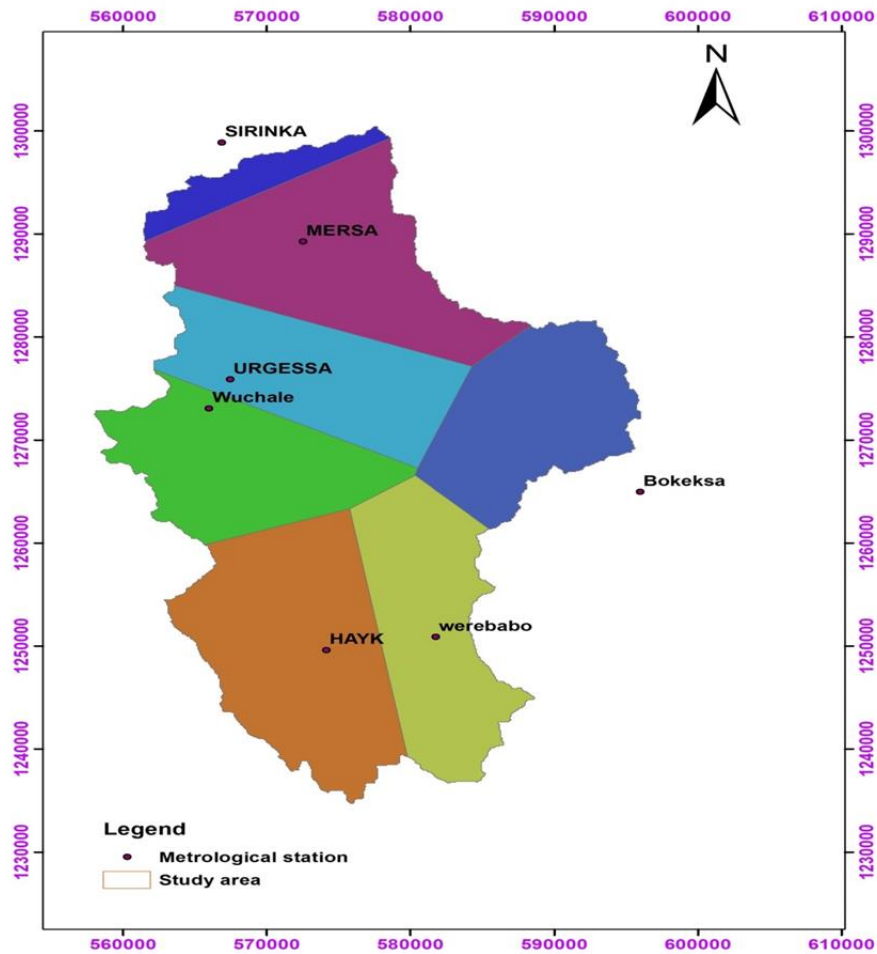


Figure 12. Thiessen polygon of stations in the study area

CHAPTER FIVE

5.0 Recharge Estimation

Recharge is the primary method through which water enters an aquifer there can be several sources of recharge to a groundwater system. These include precipitation, river, inter-aquifer flows and irrigation losses. It is very important to know the amount of groundwater recharge in order to manage resource. There are several methods for estimating groundwater recharge on this research to compare the results between those methods and to obtain an average value of recharge. Chloride mass balance and Base flow separation as well as SWAT were used.

5.1 Base flow separation methods

Base flow is the portion of the stream flow that flows between precipitation events. It is the portion of stream flow, delayed shallow subsurface flow. BFS method uses a river discharge time-series to separate the base flow and surface runoff of the river. Using two methods, graphical and spreadsheet software and among several base flow methods on this paper Base flow index (BFI) was used.

Graphical base flow Separation Method

This method is used to plot base flow of plot the base flow of a flood hydrograph in which the base flow intersects the falling limb. In which the Stream flow following to this point is assumed to be entirely base flow, up until the next rainfall event start of the hydrographic. Approaches of the graphical method in dividing base flow are very complex and those include constant discharge method, constant slope method and concave method.

The Time-plot base flow separation method

The software was developed by Gabriel Parodi; it uses daily flow values and an attenuation coefficient which is controlled by the slope, land-use land cover conditions within range of 0.9-0.995. A small difference between the resulting values has been observed and mean values are adapted for further computations. The conventional graphic base flow separation methods result May either underestimate or overestimate the component of the river discharge. Because of this, the result

obtained from the spread sheet program (Time plot) which considers the topographic characteristics of the basin and then estimates the base flow is used in this paper.

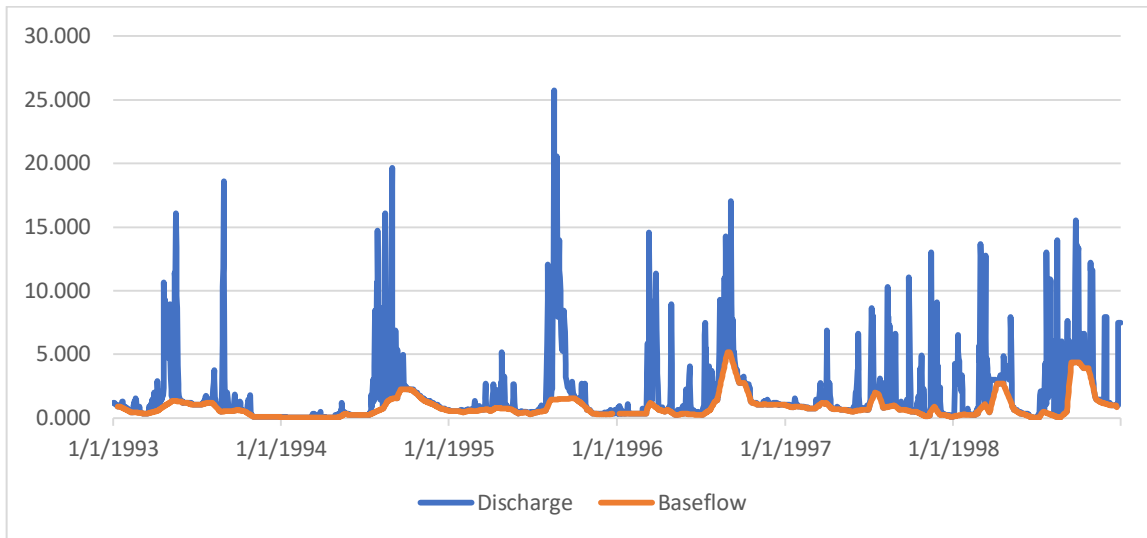


Figure 13. baseflow of Pasomile River

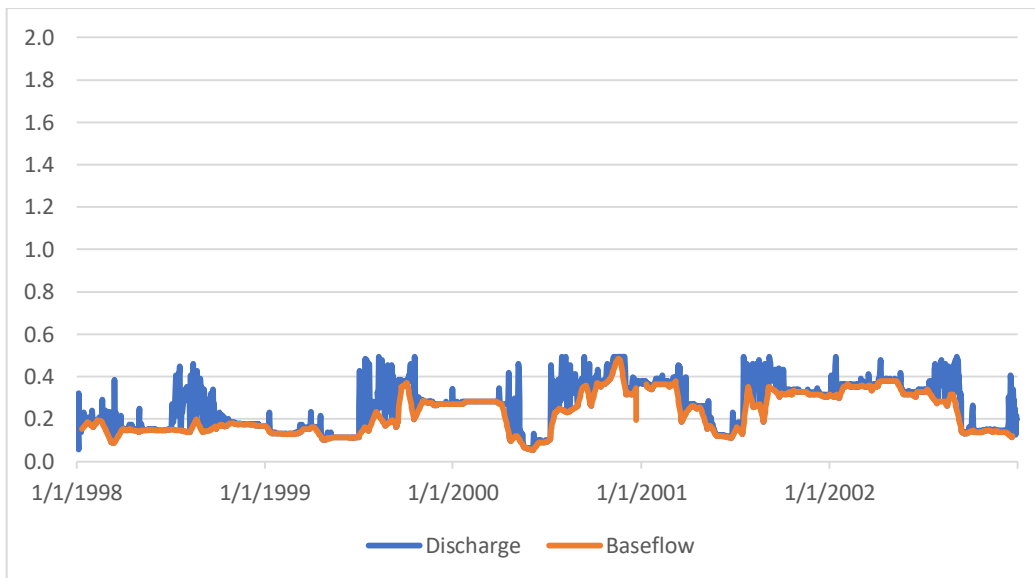


Figure 14. Base flow of Megenagna River

Results of an assessment of data from Pasomile River gauge in Hayk shows a mean river flow of $1.295\text{m}^3/\text{s}$, which represent a total flow of 204.19 mcm. On the other hand, the mean flow of Megenagna River at Mersa has become $0.275\text{ m}^3 / \text{s}$ which represent 173.4 MCM of the annual flow.

The recharge at the Megenagna River as calculated using Base flow separation is 142.5805 mm/year of 13% of an Average precipitation on the catchment. While it is 129.4 mm/year for Pasomile which represents 9% of total precipitation. The long term annual average recharge of the two Rivers is 135.9 mm/year.

5.2 Chloride mass-balance method

Chloride is regarded as a suitable environmental tracer since it is highly soluble, conservative and not substantially absorbed by vegetation. The chloride mass-balance method is convenient and inexpensive because of its simple data requirements. Recharge can be estimated by

$$R = P \times \frac{Cl_P}{Cl_{gw}}$$

Where R is recharge (mm/year); P is rainfall (mm/year); Cl_P is weighted average chloride concentration in rainfall (mg/L); and Cl_{gw} is (Marie , et al. 2010) average chloride concentration in groundwater (mg/L).

Precipitation samples from Dessie, has been used because there are no precipitation data within the study area. Chloride data were used from the laboratory analysed samples the mean concentration of chloride for rainfall is 0.98 mg/l. An average chloride in groundwater in the study area is 9.49 mg/l.

Calculated recharge has become 115.66 mm/year for the catchment. The recharge seems realistic and it matches with values estimated in other approaches. This calculation is based on the assumption that all recharge water from the plateau and escarpment flows and stored within the graben/valleys floor.

5.3 SWAT (soil and water assessment tool)

SWAT it's efficient model that functions on a daily time step at basin scale (Arnold, et al., 1998) SWAT model can be applied for different type of catchment areas starting from 0.015 km² to as large as 491,700 km² and its accuracy increases as the catchment area is small (Arnold, et al., 2000).

SWAT uses a two-level break-down of scheme; initially sub basin identification is carried out based on topographic standards, followed by further discretization using land use and soil type considerations. In Areas with the same soil type and land use form a Hydrologic Response Unit (HRU), a basic algorithmic unit assumed to be homogeneous in hydrologic response to land cover variation.

The watershed needs first to be separated into sub-basins, each having a main channel and a specific combination of land use, soil type and management practices, which will allow the specification of hydrological response units (HRU). Water balance computations are performed at this level of spatial discretization, and contributions of each HRU are then averaged out to represent water yield to the main channel. Water is then routed to the outlet of the watershed.

A major drawback of the large area hydrologic modelling of SWAT is the spatial detail

required to precisely simulate environmental processes. For example, it is difficult to capture the spatial inconsistency associated with precipitation within a watershed. Another limitation is data files can be difficult to manipulate and can contain several missing records. The model simulations can only be as accurate as the input data. The third limitation is that, the SWAT model does not simulate detailed event-based flood and sediment routing (Geremewu, 2013).

5.3.1 Swat model water balance

$$SW_t = SW_o + \sum_{t=1}^t (R_{day} - Q_{surf} - E_a - W_{seep} - Q_{gw}) \text{-----} 3$$

Where; SW_t is the final water content (mm H₂O), SW_o is the initial soil water content on day i (mm H₂O), t is time, days, R_{day} is the amount of precipitation on day i (mm H₂O), Q_{surf} is the amount of surface runoff on day i (mm H₂O), E_a is the actual evapotranspiration on day i (mm H₂O), W_{seep} is the amount of water entering the vadose (unsaturated) zone from the Soil profile on day i (mm H₂O), Q_{gw} is the amount of return flow on day i (mm H₂O).

The model reflects variances in evapotranspiration for different land use and soil type in the part of watersheds. The runoff was forecasted and separated from each HRU

and routed to obtain the total amount for the watershed. Hence, increase in the correctness gives an improved physical explanation of water balance.

5.3.2 Surface Runoff lags

In lag sub basin with a time concentration greater than 1 day, only a portion of the surface runoff will reach the main channel on the day it is generated. Swat incorporates a surface runoff storage feature to large part of the surface runoff release to the main channel .once surface runoff is calculated, the amount of surface runoff release to the main channel is calculated as;-

$$Q_{surf} = (Q'_{surf} + Q_{surf,i-1}) * (1 - \exp[-\frac{surlag}{t_{conc}}]) \text{-----(15)}$$

Where: Q_{surf} is the amount of surface runoff discharged to the main channel in a day (mm), $Q_{surf, i-1}$ is the surface runoff stored or lagged from the previous day (mm). $Surlag$ is the surface runoff lag coefficient, and t_{coc} is the time of concentration for the subbasins (hrs).

To simulate the ground water, SWAT divides groundwater into two aquifer systems: a shallow, unconfined aquifer, which gives return flow to streams within the watershed and a deep, confined aquifer which gives return flow to streams outside the watershed.

In SWAT the water balance for a shallow aquifer is calculated as:

$$aqsh,I = aqsh_{i-1} + W_{rchg} - Q_{gw} - W_{revap} - W_{deep} - W_{pump,sh} \text{----- (17)}$$

Where, $aqsh, i$ is the amount of water stored in the shallow aquifer on day i (mm), $aqsh, i-1$ is the amount of water stored in the shallow aquifer on day $i-1$ (mm), W_{rchg} is the amount of recharge entering the aquifer on day i (mm), Q_{gw} is the ground water flow, or base flow, or return flow, into the main channel on day i (mm), W_{revap} is the amount of water moving in to the soil zone in response to water deficiencies on day i (mm), W_{deep} is the amount of water percolating from the shallow aquifer in to the deep aquifer on day i (mm), and $W_{pump,sh}$ is the amount of water removed from the shallow aquifer by pumping on day i (mm).

$$\Delta V_{\text{stored}} = V_{\text{in}} - V_{\text{out}} \text{-----} \quad (18)$$

Where: ΔV_{stored} is the change in volume of storage during the time step (m³ water), V is the volume of inflow during the time step (m³ water), and V_{out} is the volume of outflow during the time step (m³ water).

The calculation can be further specified as:

$$V_{\text{stored}, 2} - V_{\text{stored}, 1} = \frac{\Delta t}{2} \{ [q_{\text{in}, 1} - q_{\text{in}, 2}] - [q_{\text{out}, 1} + q_{\text{out}, 2}] \} \text{-----} \quad (19)$$

Where; $q_{\text{in}, 1}$ is the inflow rate at the beginning of time step (m³/s), $q_{\text{in}, 2}$ is inflow rate at the end of time step (m³/s), $q_{\text{out}, 1}$ is the outflow rate at the beginning of time step (m³/s), $q_{\text{out}, 2}$ is the outflow rate at the end of time step (m³/s), Δt is the length of the time step (s), $V_{\text{stored}, 2}$ is the storage volume at the end of time step (m³H₂O), $V_{\text{stored}, 1}$ is the storage volume at the beginning of time step (m³H₂O).

The volume of water in the channel was divided by the outflow rate to compute the travel time.

$$TT = \frac{V_{\text{stored}}}{q_{\text{out}}} = \frac{V_{\text{stored}, 1}}{q_{\text{out}, 1}} = \frac{V_{\text{stored}, 2}}{q_{\text{out}, 2}} \text{-----} \quad (20)$$

5.3.3 Potential Evapotranspiration

There are several methods that are advanced to estimate potential evapotranspiration (PET). SWAT calculates potential evapotranspiration (PET) using three methods; the Priestley Taylor method (Priestley and Taylor, 1972), the Hargreaves method (Hargreaves, 2003) and the Penman-Monteith method (Monteith, 1965) cited in (Setegn S. G., 2010) and The approaches have several data needs of climate variables. Penman- Monteith (1965) method needs solar radiation, air temperature, relative humidity and wind speed; Priestley-Taylor method (1972) needs solar radiation, air temperature and relative humidity; but Hargreaves (2003) method requires an air temperature only. For this study Penman-Monteith was adopted to estimate potential evapotranspiration.

$$E_{to} = \frac{0.408(R_n - G) + Y \frac{900}{(T + 273)} U (e_s - e_a)}{\Delta + Y (1 + 0.34U)} \quad (16)$$

Where:

E_{to} = daily reference crop evapotranspiration [mm day⁻¹]

R_n = net radiations flux [MJm⁻² day⁻¹]

G = heat flux density in the soil, it is very small and can be neglected [MJ m⁻² day⁻¹]

T = mean daily air temperature [°C]

Y = psychometric constant [KPa °C⁻¹]

U = wind speed measured at 2 m height [ms⁻¹]

e_s = saturation vapor pressure $e_a = e_s \times RH$ [KPa]

RH = relative humidity [%]

$e_s - e_a$ = saturation vapor pressure deficit [KPa]

Δ = slope of the saturation vapor pressure curve [KPa°C⁻¹]

5.3.4 Model Setup

Watershed Delineation

The watershed and sub watershed delineation were performed using 30 m by 30 m resolution DEM data. The delineation was done using Arc SWAT in predefined streams and watershed delineated by ArcGIS. First, the SWAT project set up should create. Delineation of the watershed process includes six major steps of pre-defined streams and watersheds. This includes DEM setup, Dem projection setup, streams defined (predefined streams), and predefined watershed data set, create streams and outlet, and calculation of sub basin parameters. The watershed was discrete into 25 sub basins based on the 33 % threshold

Hydrologic Response Units Analysis

The sub watersheds divide into HRUs by allocating the threshold values of land use and land cover, soil and slope percentage. The SWAT user's manual suggests that a 20 % land use threshold, 10 % soil threshold and 20 % slope threshold are acceptable for most modelling applications. Therefore, for this study, HRU definition were done by accounting 20% land use, 10% soil and 20% slope threshold combination were

used. Based on the threshold combination the watershed classified into 355 hydrological responses unites (HRU) which have the same runoff producing unites, In general the threshold level used to eliminate the minor land use and land covers in sub basin, minor soil within a land use and land cover area and minor slope classes within a soil with specific land use and land cover area

Weather Data Definition

The WXGEN weather generator model included in SWAT were used to fill in gaps in measured records. The model was developed to generate precipitation using Markov chain-skewed or Markov Chain-exponential model (Williams, 1995). First order Markov – chain in which it was used to determine whether a day was dry or wet. Exponential or skewed distribution is used to generate Precipitation amount whenever a wet day occurs (Neitsch et al., 2005). The parameters needed for the weather generator are Hayk, Mersa, Bati Kombolcha Sirinka station were used. The WXGEN model was provided using average method .These values were calculated from the meteorological data available in the study area and outside the area. The Other meteorological data were prepared with their corresponding location table according to the SWAT format and integrated into the model using the weather data input wizard.

Sensitivity Analysis

Calibration is necessary to improve the values of the model parameters which can help to decrease the uncertainty in the model outputs. The model has a multiple parameter, the hard task is to choose which parameters are to be calibrated in which most of the values of these parameters are not exactly known. (Holvoet, et al., 2004). Sensitivity analysis is a process of testing and identifying model parameters that affects most the output from the model when changed. In other words, sensitivity analysis is the process of determining the rate of change in model output with respect to changes in model inputs (parameters) (Abbaspour, 2013). A parameter sensitivity analysis provides insights on which parameters contribute most to the output variance due to input variability (Holvoet *et al.*, 2005). Therefore, a parameter is considered sensitive when the change in that parameter causes large change on model output.

Model Performance Evaluation

To check the model simulation outputs in relative to the observed data, model performance evaluation is necessary. There are various methods to evaluate the model performance during the calibration and validation periods. For this study, three methods were used: coefficient of determination (R²), Nash-Sutcliffe efficiency (NSE) and Root mean square error observation standard deviation ratio (RSR)

Coefficient of determination (R²)

The R² is a measure of the part of the total variance of observed data explained by predictive data, a perfect fit also being one with a lower limit of zero and the upper limit of infinity. It tells us whether the model is over predicting (a value under one) or under predicting (a value over one).

$$R^2 = \left[\frac{\sum_{i=1}^n (O_i - O_{avg})(P_i - P_{avg})}{\left[\sum_{i=1}^n (O_i - O_{avg})^2 \sum_{i=1}^n (P_i - P_{avg})^2 \right]^{0.5}} \right]^2 \quad (22)$$

Nash - Sutcliffe efficiency (NSE)

The NSE tells us how well the model is performing in predication, a value of one indicates a perfect one to one relationship and any negative value tells us that the model is worse at predicting observed data than when using the mean of observed values to predict the data.

$$NSE = 1 - \frac{\sum_{i=1}^n (O_i - P_i)^2}{\sum_{i=1}^n (O_i - P_{avg})^2} \quad (23)$$

RMSE-observations standard deviation ratio (RSR)

RSR varies from the optimal of 0, which indicates zero RMSE or residual variation and therefore perfect model simulation, to a large positive value. The lower RSR value indicates the lower the RMSE and the better the model simulation performance. RSR can be calculated by dividing the root mean square error with a standard deviation of the observed flow (STD_{obs}).

$$RSR = \frac{RMSE}{STD_{Obs}} \quad (26)$$

Table 3. General performance rating for recommended statistics for monthly time steps (Moriiasi, 2007).

Performance	R ²	NSE	RSR	PBIAS (%)
Very good	0.75<R ² <1	0.75<R ² <1	0<RSR<0.50	PBIAS<±10
Good	0.65<R ² <0.75	0.65<R ² <0.75	0.50<RSR<0.6	±10<
Satisfactory	0.50<R ² <0.65	0.50<R ² <0.65	0.6<RSR<0.70	PBIAS±15 ±15<
Unsatisfactory	R ² <0.50	R ² <0.50	RSR <0.5	PBIAS±25 PBIAS > ±25

5.3.4.1 Land Use and Land Cover

The land use is one of the factors that affect runoff, evapotranspiration and surface erosion in a catchment (Yimer, 2015). The land use shows the spatial range and classification of the various land uses/ cover classes in the study area. The land use/cover data combined with the soil cover data creates the hydrologic characteristics of the basin or the study area, which in turn determines the surplus precipitation, recharge to the ground water system and the storage in the soil layers. Figure 15 shows reclassified land use map of the area.

Approximately 32% of the total catchment is a cropland whereas 22% is covered with sparse forest and the remaining are 46% are of consisted of open shrub land ,closed and open shrub land , water, open grassland, closed grassland, bare land, settlement and woodland based on table 4.

Table 4. Land use name with SWAT land use code with their area coverage

Object ID	Land use Name	LUSWAT code	Percent	Area (km ²)
1	Settlement	URLD	0.5%	6.81
2	Annual cropland	AGRR	32.3%	438.80
3	open shrubland	ORCD	25.0%	339.84
4	closed shrubland	ORCD	4.4%	59.32
5	closed grassland	PAST	0.1%	1.17
6	open grassland	PAST	2.8%	37.94
7	Waterland	WATR	2.4%	33.16
8	Barren	BARR	0.1%	1.08
9	Sparse forest	FRST	22.0%	298.67
10	Modern forest	FRSE	0.4%	5.66
11	Woodland	FRSD	0.1%	7.76

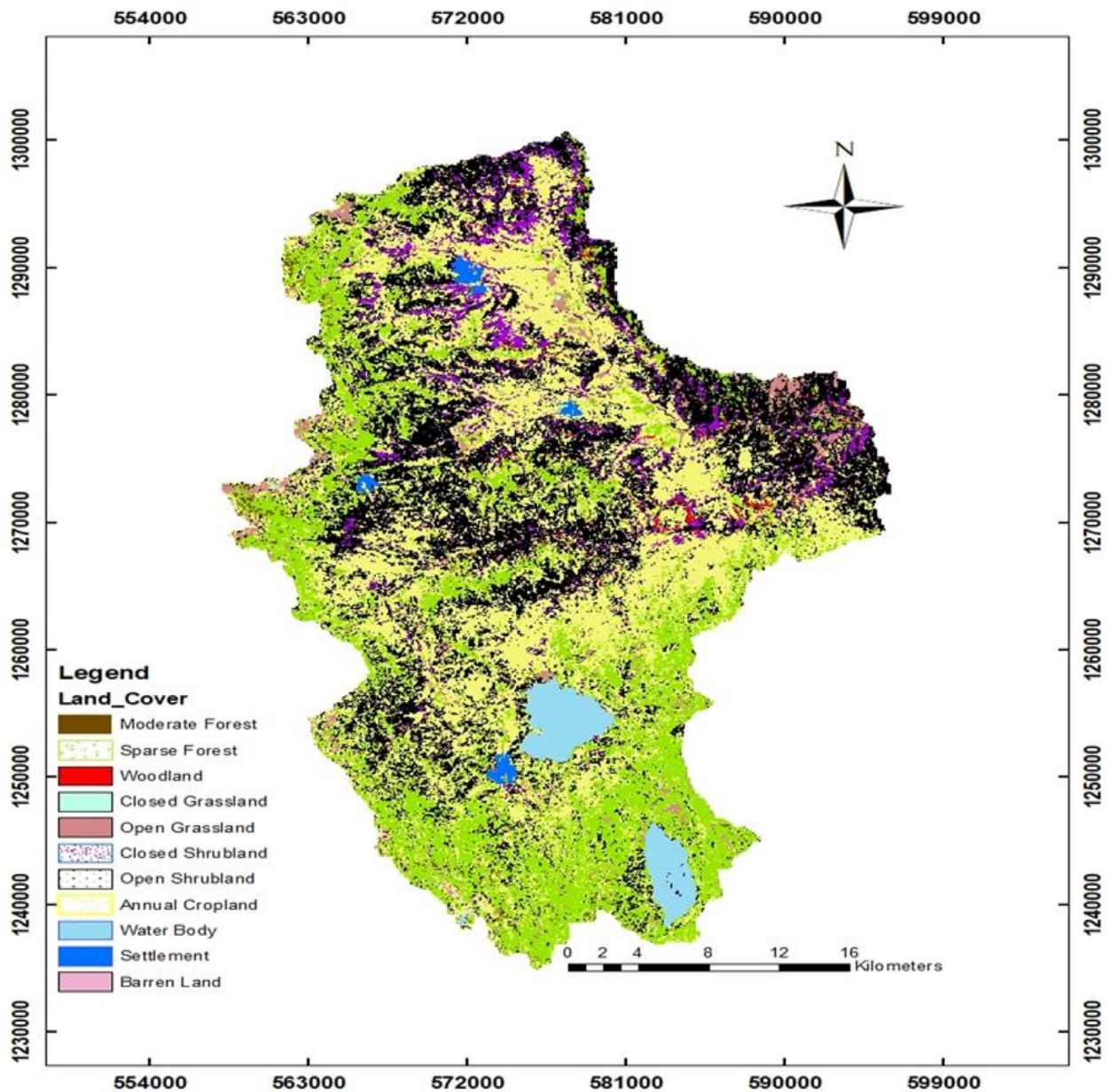


Figure 15. The reclassified land use map of the study area (source Ministry of Water Irrigation and Energy)

5.3.4.2 Soil

Soils are formed on account of the climate, physiography, geology and other factors responsible for soil formation and development (Afework, 2011). Soil maps and database of soil were used from Ministry of agriculture for the project. Different properties of soil such as soil texture, available water content, hydraulic conductivity & bulk density of different layers of each soil type were acquired.

In addition, physical properties (percentage sand, clay, and silt; soil texture class; soil texture class, and profile thickness), derived soil properties (hydraulic conductivity, bulk density, available water capacity, and soil organic matter content) and the basic properties of each profile of the four different soils in the watershed were obtained .

The datas mentioned above are helpful for a good understanding of the soils in the study area and built up a valuable database. Mainly four soil types differentiated: Leptosols, Euleptosols, Euvertisols and Eucambisols in figure 16.

Soils classified as Ltleptosols and Euleptosols covers more than 80 % of the total area and they are characterized by shallow to very shallow depth respectively and the rest of the area is consisted of Euvertisols and Eucambisols given in Table 5 with a description of soil table 6 (based on Yimer,2015).

Table 5. Soil name and percent of coverage in the study area

Objected ID	Soil Name	percent	Area(km ²)
1	Leptosols	68.0	925
2	Euleptosols	13.5	177
3	Euvertisols	10.9	148
4	Water	2.3	31
5	Eucambisols	6.0	80

Table 6. Soil type with their description in the study area.

Soil type	Label	Descriptions (depth in cm)
Leptosols	A	Very shallow (10-100 cm)
Euleptosols	A	Shallow to very shallow (30-300 cm)
Euvertisols	D	Moderately deep (100-1000 cm)
Eucambisols	D	Deep to very deep (300-1000 cm) stony phase, clay

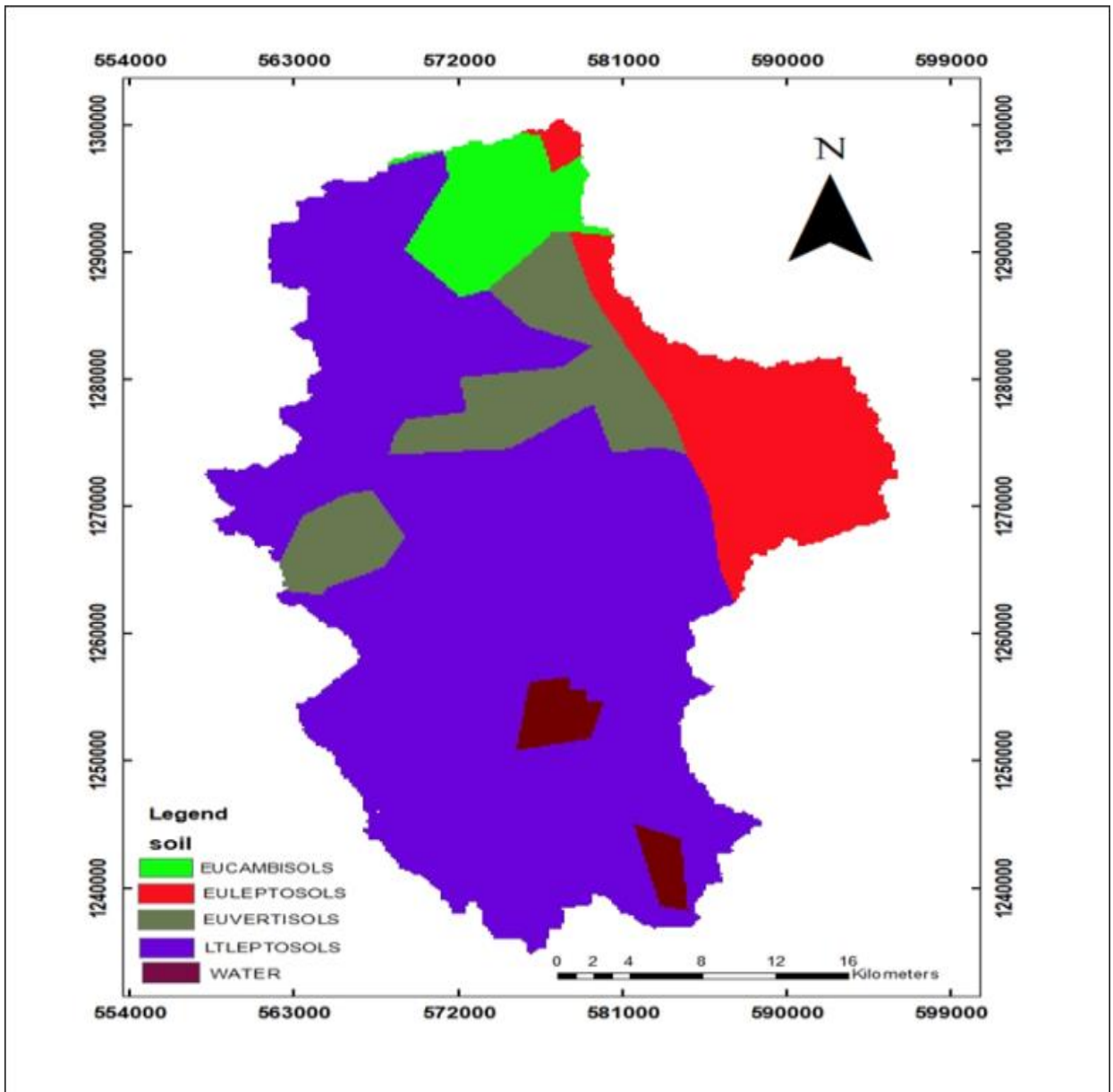


Figure 16. Soil type map of the study area (source Ministry of Water Irrigation and Energy)

5.3.4.3 Slope

The topography of the catchment has been prepared from the Shuttle Rader Topography Mission (SRTM) of 30m resolution dataset. The slope of the area ranges from 0° to 66° in figure 17 and table 7. Gentle slopes are observed within the plateau and covers 38% of the study area along with slightly steeper slopes with 31% coverage, in combined both covers large part large part of the region. On the other hand steep slopes are observed following the river gorges with covering 31% of the study area in figure 5 based on Tesfa Yimer.

Table 7. slope class with description and area coverage

Slope class			
[%]	Description	Area(km ²)	Coverage (%)
0-4	Gentle slope	565.11	38%
4– 9	Slightly steep	459.63	31%
9-15	Moderately steep	290.124	20%
15– 25	Steep	132.183	9%
25-66	Very steep	22.473	2%

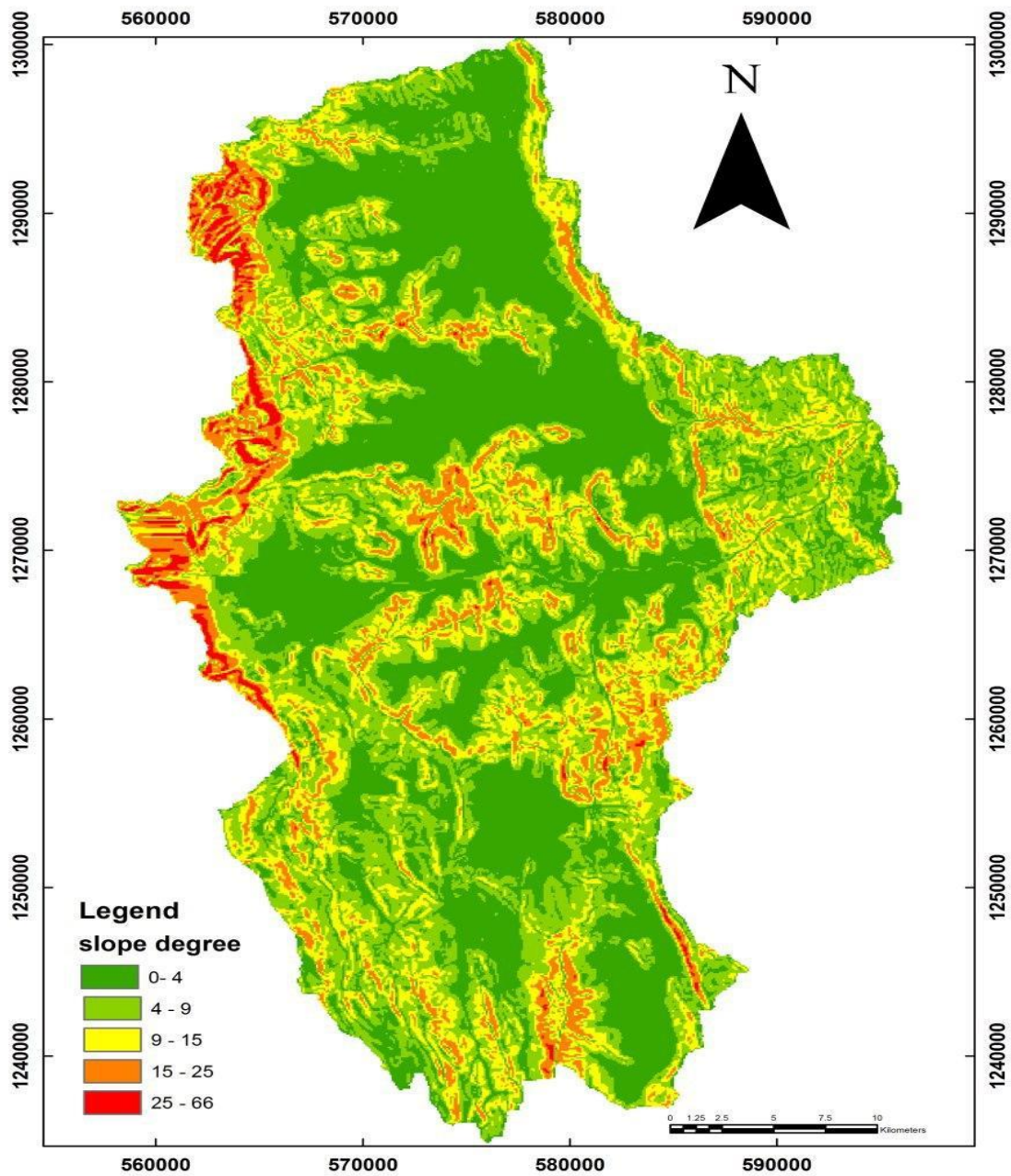


Figure 17. Slope map of the study area

5.4 Result and Discussion

The main result include three components: (i) flow parameter sensitivity analysis, (ii) SWAT-WB model calibration and validation for flow at the Pasomile River uses manual calibration methods (iii) Recharge of the area

5.4.1 Sensitivity analysis

Sensitivity analysis was done using flow parameters of SWAT based on monthly steps with observed data of the Pasomile River gauging station. For this analysis all SWAT parameters were considered and only 11 parameters were identified for calibration where they have substantial influence in monitoring the stream flow in the watershed. The most sensitive parameters for SWAT-WB were listed below and these sensitive parameters were considered for SWAT-WB model calibration. Table 8 indicates that parameters that resulting greater relative means to the sensitivity value of stream flow.

Table 8. Hydrological parameter selected for both flow calibration and validation

S/No	Parameter	Description of Parameters	Range Val
1	Revamp	Threshold depth of water in the shallow	0-500
2	ALPHA_BF	Base flow alpha factor	0-1
3	ESCO	Soil evaporation compensation factor	0-1
4	CH_N2	Manning's "n" value for the main channel	-0.01-0.3
5	SURLAG	Surface runoff lag time	0.05-24
6	GW_DELAEY	Groundwater delay	0-500
7	GW_REVAP	Groundwater revap coefficient	0.02-0.2
8	SOL_K	Saturated hydraulic conductivity(mm/hr)	0-2000
9	RCHRG_DP	Groundwater recharge to deep aquifer	0-1
10	SOL_BD	Soil bulk density	0-0.25
11	GWQMN	Threshold water depth in the Shallow aquifer for flow	0-5000

Table 9. Result of the sensitivity analysis parameters for flow calibration

N0	Parameter	Description	t- stat	P-Value	Rank
1	GW_DELAY	Groundwater delay	2.2343	0.0559	1
2	GW_REVAP	Groundwater revap coefficient	-1.8854	0.0961	2
3	SOL_K	Saturated hydraulic conductivity	-1.3917	0.2014	3
4	CH2_CN2	Manning's "n" value for the main channel	-1.2209	0.2568	4
5	RECHARGE_DP	Groundwater recharge to deep aquifer	1.1185	0.2958	5
6	GWQMN	Threshold water depth in the Shallow aquifer for flow	-0.9431	0.3732	6
7	ALPHA_BF	Base flow alpha factor	-0.7296	0.4864	7
8	REVAMP	Threshold depth of water in the shallow	0.6017	0.5641	8
9	SURLAG	Surface runoff lag time	0.3904	0.7046	9
10	SOL_BD	Soil bulk density	-0.3826	0.7119	10
11	ESCO	Soil evaporation compensation factor	0.3276	0.7516	11

The t-value measures the size of the difference relative to the variation in the sample data and P-value is the probability of observing a test statistic at least as large as the one calculated assuming the null hypothesis is true.

Ranking of sensitivity of parameters was determined by the absolute values of t-stat and P-value. The parameter having the highest absolute value of t-stat and the minimum P-value, would take the first rank of sensitivity in table 9 Which indicate any value change on this parameter would be most significantly affecting the dynamics of flow compared with other parameters. Based on the sensitivity analysis done for this watershed the most sensitive parameter found was groundwater delay in figure 18.

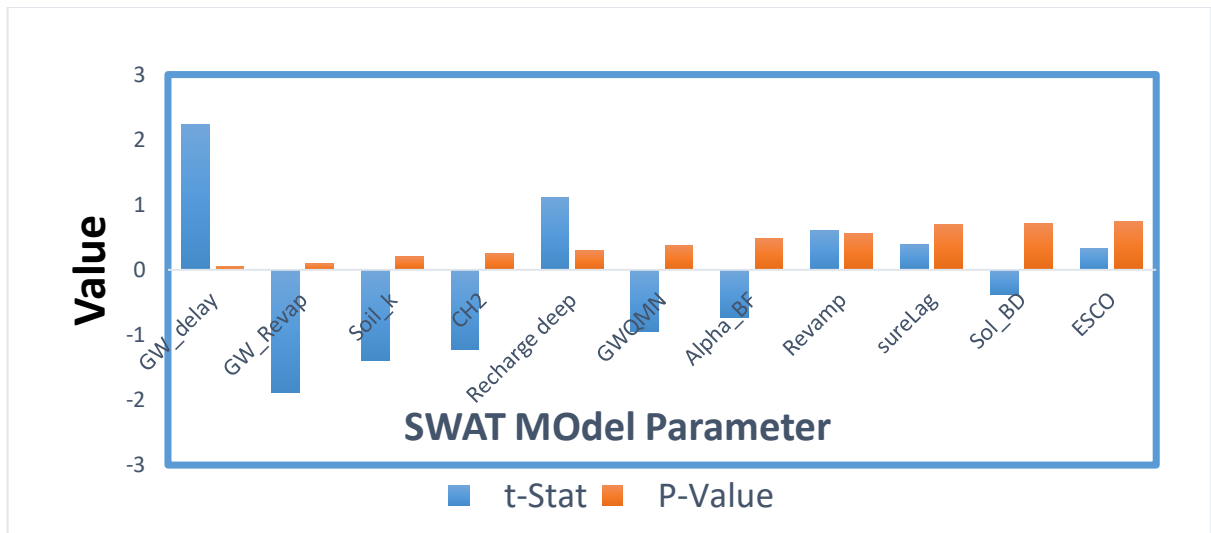


Figure 18. Graphical representation of sensitivity analysis with t-test and p-value

5.4.2 Calibrations

Model Calibration is the iterative process of comparing the model with real system, revising the model system if necessary until a model is accepted (Tesfa, 2015). It was carried from 2001 – 2010 at Pasomile River. Resulting statistics for the monthly simulations was shown in the figure 19 and 20. The flow was calibrated by the observed flow at the outlet of Pasomile River. The manual calibration has been done by changing the parameters iteratively until the model efficiency falls in the acceptable ranges with the optimum parameter value.

The model result between the observed and simulated stream flow indicated a good agreement between the observed and simulated discharge which were verified values of coefficient of determination (R^2), Nash Sutcliffe efficiency (NSE) and Root mean square error observation standard deviation ratio. The simulated flow resulted in NSE values of 0.7 and R^2 value of 0.87 and RSR value is 0.13 with observed data for the calibration period. The adequacy of the model is further indicated by its clear response to extreme rainfall events resulting in high runoff (2006) volume while low in low rainfall events resulting in low runoff (2001,2002&2004).

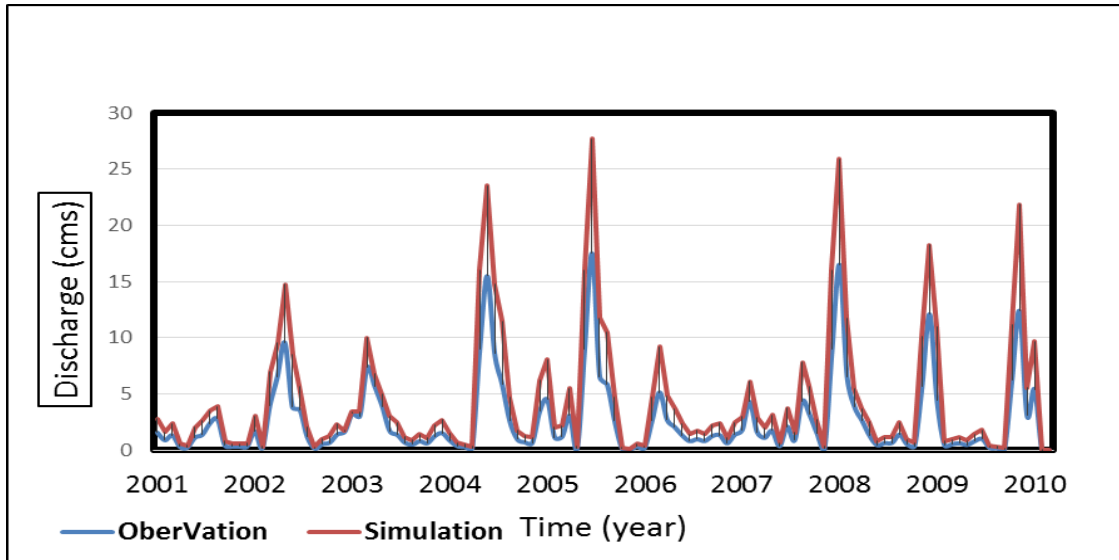


Figure 19. Simulated and observed average monthly flows

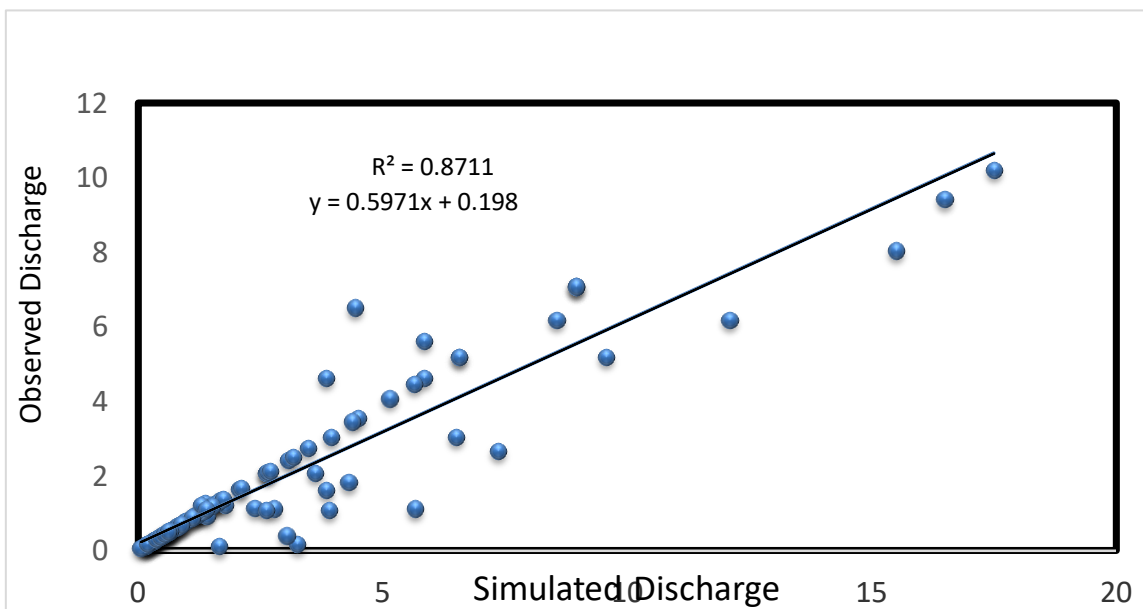


Figure 20. Scatter plot of the simulated vs. observed average monthly flows during calibration

5.4.3 Validation of model

Validation is the process of comparing the model and its behaviour to the real system and its behaviour (Tesfa, 2015). The model performance was done using independent dataset (2011-2013). The performance rating obtained was good and the

model is applicable to assess the hydrogeology of the area on the stream flow of Pasomile.

The model efficiency in validation process had also been determined by R^2 , NSE and RSR with values of 0.82, 0.73 and 0.2 respectively. Thus, based on the result the model had been showing its consistency with those optimized values of parameters in the study area. Those parameter values are representative for the study area. The agreement of simulated against the observed flow of the catchment is illustrated by the line graph in (figure 21&22). The adequacy of the model is also indicated by its clear response to extreme rainfall events resulting in high runoff (2013) volume while low in low rainfall events resulting in low runoff (2011&2012).

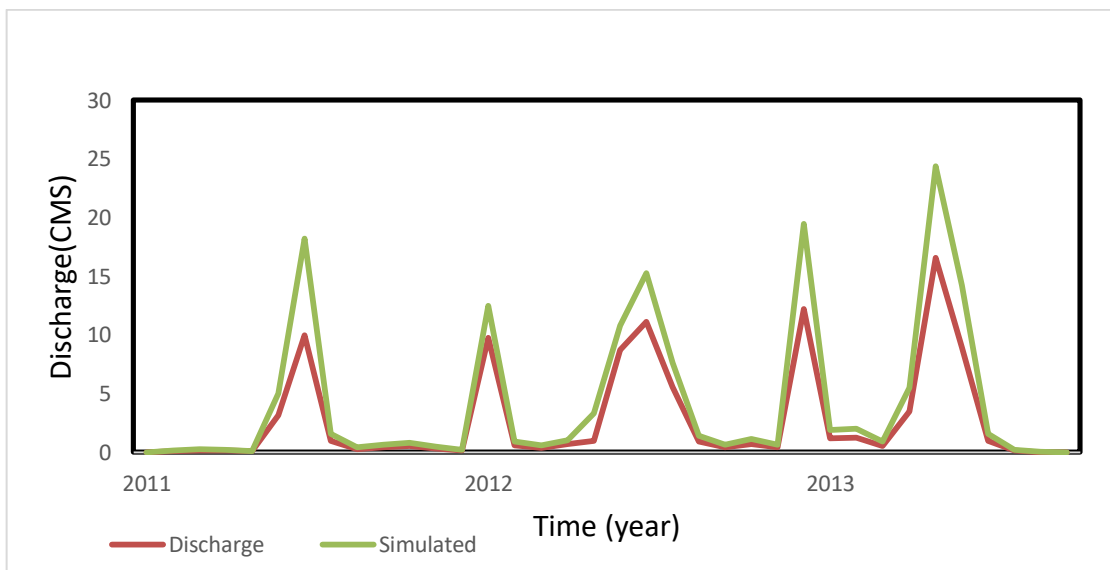


Figure 21. Simulated and observed average monthly flows generated during validation

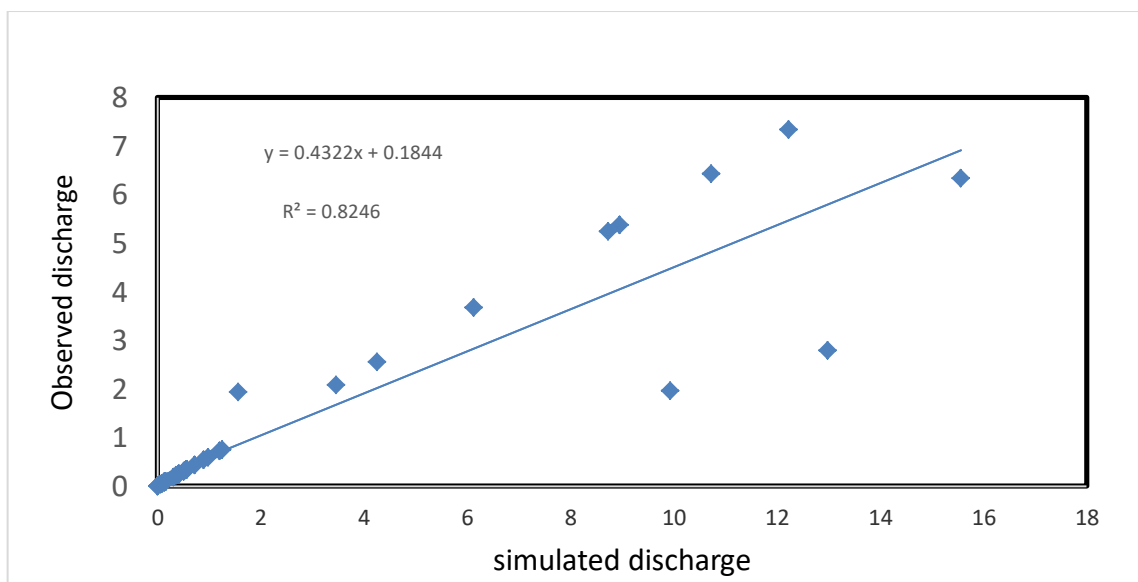


Figure 22. Scatter plot of the simulated vs. observed average monthly flows

5.4.4 Water balance components of the study area watershed

Hydrological parts of SWAT comprise surface runoff, infiltration, evapotranspiration (due to relatively low temperature and moderate vegetation coverage show low Et values in the water balance), lateral flow, tile drainage, percolation/deep seepage, consumptive use through pumping (if any), shallow aquifer contribution to stream flow for a nearby stream (base flow) and recharge by seepage from surface water bodies.

Table 10. water balanced component of the study area.

SWAT water Balanced				
WB_component	calibration		Validation	
	MM	%	MM	%
Precipitation	1105.2	100.0000	1102.0	100
surface Run off	143.71	13.0031	140.7	12.8
Lateral Q	528.75	47.8420	518.4	47.0
Ground water(Shallow AQ)Q	49.01	4.4336	40.0	3.6
Ground Water(Deep AQ) Q	14	1.2667	13.0	1.2
Revap(shal AQ Soil/plant	12.41	1.1229	11.0	1.0
Deep AQ Recharge	14.05	1.2713	13.5	1.2
Total Aquifer Recharge	140.48	12.7108	138.5	12.6
Total water yield	735.56	66.5545	700.0	63.5
percolation out of soil	138.64	12.5443	130.3	11.8
ET	280.7	25.3981	265.6	24.1
PET	647.2	58.5595	620.6	56.3

5.4.5 Modelling performance

For calibration it was done from 2001 to 2010 on monthly time series by changing the above parameters until reasonable values for R2 (Correlation Coefficient), NSE (Nash Sutcliff) and Root mean square error observation standard deviation ratio (RSR) were obtained. Validation was also done from the year 2011-2013 for NSE, RSR and R2 as listed in the table 11. Shows that the timing of runoff events is well predicted by the model.

Table 11. Stream flow calibration and validation results on monthly basis

Model Performance evaluation measurement	Model efficiency	
	Calibration(2001-2010)	Validation(2010-2013)
R2	0.87	0.82
NS	0.7	0.73
RSR	0.13	0.2

CHAPTER SIX

6 AQUIFER CHARACTERIZATIONS

6.1 Introduction

Groundwater is replenished by precipitation and depends on the local climate and geology, which leads to unevenly distribution in both quantity and quality. When it rains, some of the water runs off into streams, some evaporates, and some recharges aquifers (Moore et al., 1995).

An aquifer may be a layer of gravel or sand, sandstone, limestone, lava flow, or fractured granite. The location and yield of aquifers are dependent on geologic conditions, such as the size and sorting of grains in unconsolidated deposits and faulting, solution openings and fracturing in consolidated rocks.

Two properties of aquifers that affect the storage and flow of groundwater are porosity and hydraulic conductivity (Freeze and Cherry, 1979). Quaternary sediments and volcanic rocks cover much of the study area.

Quaternary sediments in the research area are composed of gravel, sands, silt and clay size ranges and its porosity depends on sorting, shape, orientation and packing which determine primary porosity of the rock. On the other hand, volcanic rocks, water occurrence is controlled by secondary porosity which in turn related to the rocks' mode of formation and modification by fractures.

Different hydrogeological unit's data have been used in this study (geological and geophysical information, meteorological, bore hole and remote sensing data, etc) were used to interpret and classify into different hydrogeological units.

6.2 Aquifer Characteristics

The nature and distribution of aquifers and aquicludes in a geologic system are controlled by the lithology, stratigraphy and structures of the geological deposits and formations (Freeze & Cherry, 1979). The aquifer and aquitard in the study area can be classified broadly as the unconsolidated sediment aquifers and volcanic aquifers.

The unconsolidated sediment aquifers mainly occupied the valley floor whereas the volcanic aquifers mainly constitute the escarpments and plateau part. Classification

was done from the information of surface geology, borehole lithologic log data, and pump test data. Based on these information major units are described below.

- Intergranular aquifer with High Productivity (50 to 80 l/s yield and $T > 400 \text{ m}^2/\text{d}$)
- Weathered and fractured aquifer with Medium Productivity (20 to 50 l/s yields and $100 < T < 400 \text{ m}^2/\text{d}$)
- Intergranular, aquifer with Medium Productivity (10 to 30 l/s yield and $50 > T < 200 \text{ m}^2/\text{d}$)
- Weathered and fractured aquifer with Low Productivity (2 to 10 l/s and $5 \text{ m}^2/\text{d} < T < 50 \text{ m}^2/\text{d}$)
- Weathered and fractured aquifer with very Low Productivity ($< 2 \text{ l/s}$ yields and $T < 5 \text{ m}^2/\text{d}$)

6.2.1 Intergranular Aquifer with High Productivity

The Quaternary colluvial and alluvial deposits are grouped in this category. These Quaternary sediments occupy an area of 452 sq.km of the study area.

It occurs by forming the flat topography with decreasing slope generally from west toward the east meanwhile it is filled with quaternary deposits that came largely from volcanic mountain. which are standing on the shoulders of the valley this deposit has a characteristic loose, incoherent and coarse to fine-grained deposits gathering on slopes by gravity and those with coarse grain size have better permeability and productivity.

Whereas those with very fine grain size have low permeability and productivity. Geological logs of the borehole and the geophysical surveying results values from the thickness of the sediments of the basins vary, but can reach about 280 m in the borehole drilled in Tisabalima. Generally western part of the valley is characterized by relatively coarse sediments while the deposit becomes finer towards east. With an average transmissivity values 789 sq.m/d and yield 50-86 l/.Figure 23, 24, 25 shows vertical distribution of the units.

6.2.2 Intergranular Aquifer with Medium Productivity

6.2.2.1 Inter-mountain Alluvial sediments

They are characterized by mostly by fine clay and silt formation they are found in the marginal grabens as well as alluvio-lauustrine deposits along river valleys. Furthermore the old channel on the Alluvial and colluvial deposits covers most part of the valley floor. This deposit has low to medium productivity based on the abundance of clay material. Meanwhile its hydraulic conductivity is dependent on the position within the geologic formation.

6.2.2.2 Peat bogs, swamps and wetland deposits

It is black cotton soil mainly clay and fine silt at the marginal grabens of seasonal swamps covered. It's found between the lakes and southwestern part of the valley fill. The hydrogeological zone is classified as a medium productivity zone. With transmissivity values 2.41 sq.m/d and yield 4 l/s at Bistima as well as at Boru-Selassie 744 sq.m/d with safe yield 6. 8l/s.

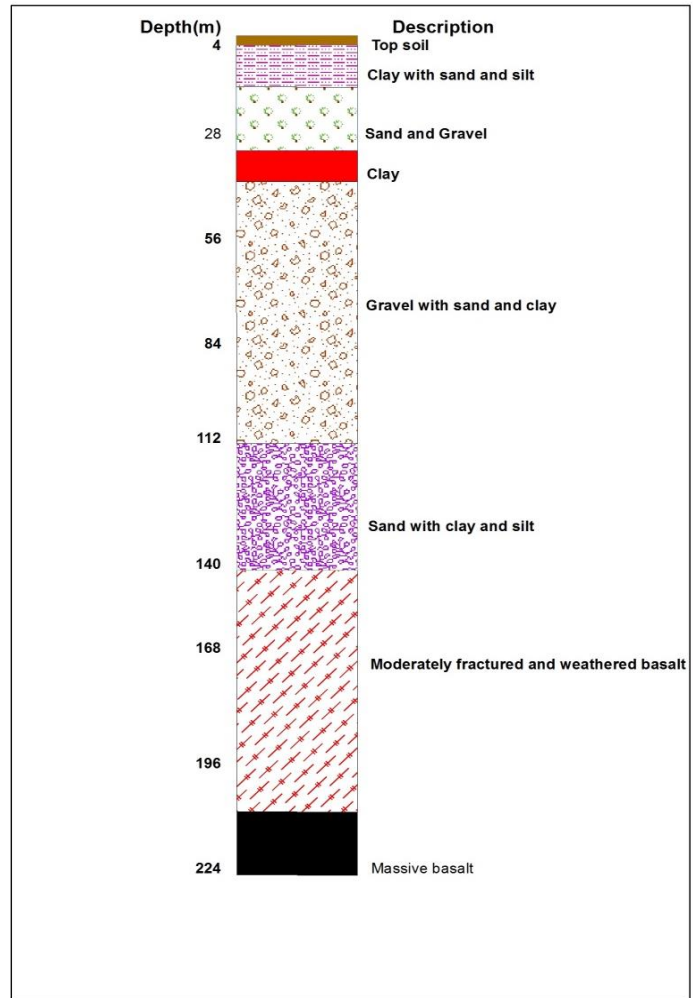


Figure 23 Vertical distribution of aquifer from well log at Mersa Darimo located on the Northeastern side of the valley (Quaternary colluvial and alluvial deposit), with the transmissivity values of $211\text{m}^2/\text{d}$, hydraulic conductivity of $19.3\text{m}/\text{d}$ and give yield of $72\text{ l}/\text{sec}$ (Modified from Amhara design and supervision works enterprise 2018)

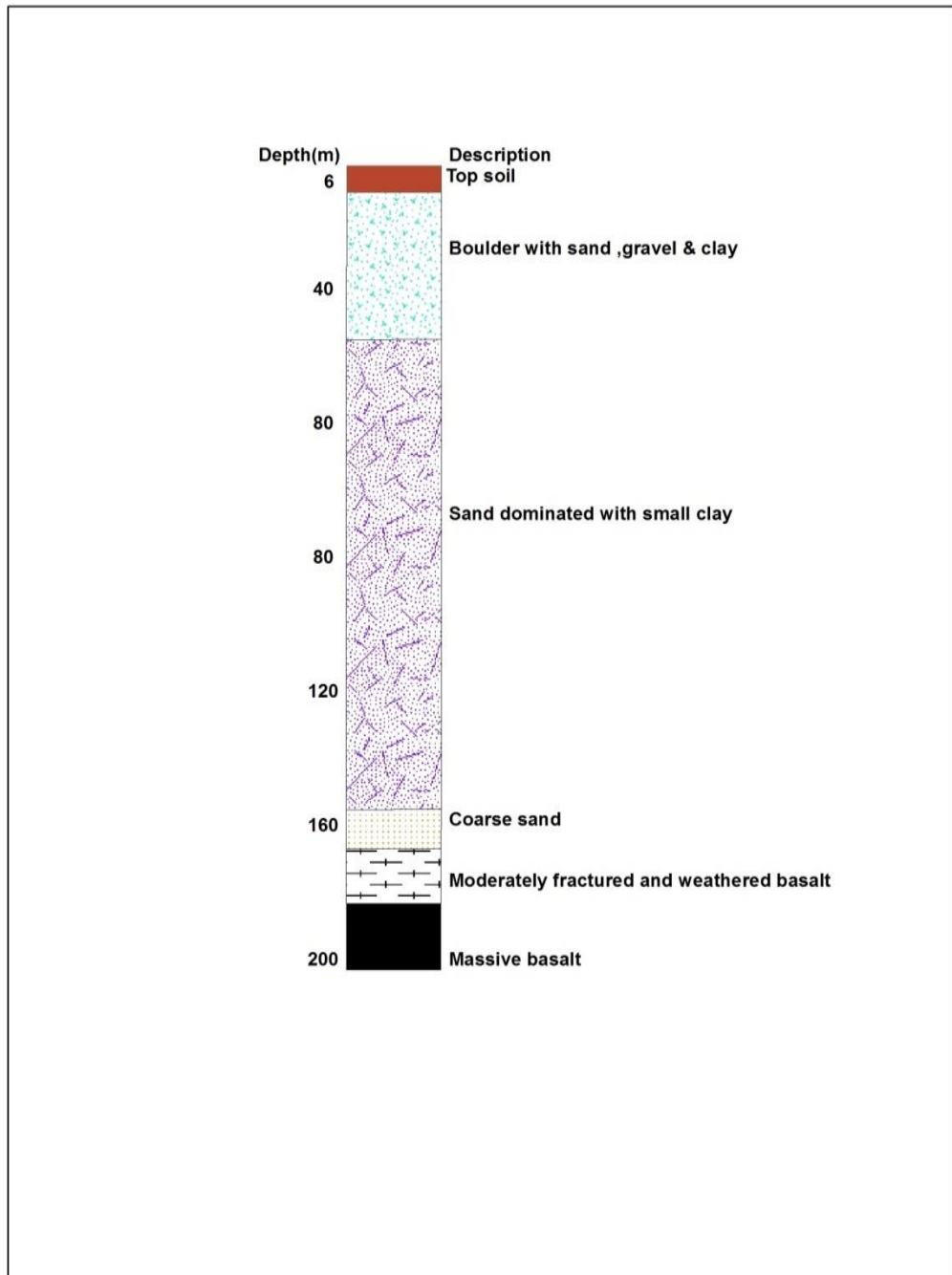


Figure 24 Vertical distribution of aquifer from well log at Mehal Amba located on the central part of the study area (Quaternary colluvial and alluvial deposit), with the transmissivity values of $333\text{m}^2/\text{d}$, hydraulic conductivity of $4.6.3\text{ m/d}$ and give yield of 72l/sec (Modified from Amhara design and supervision works enterprise 2016).

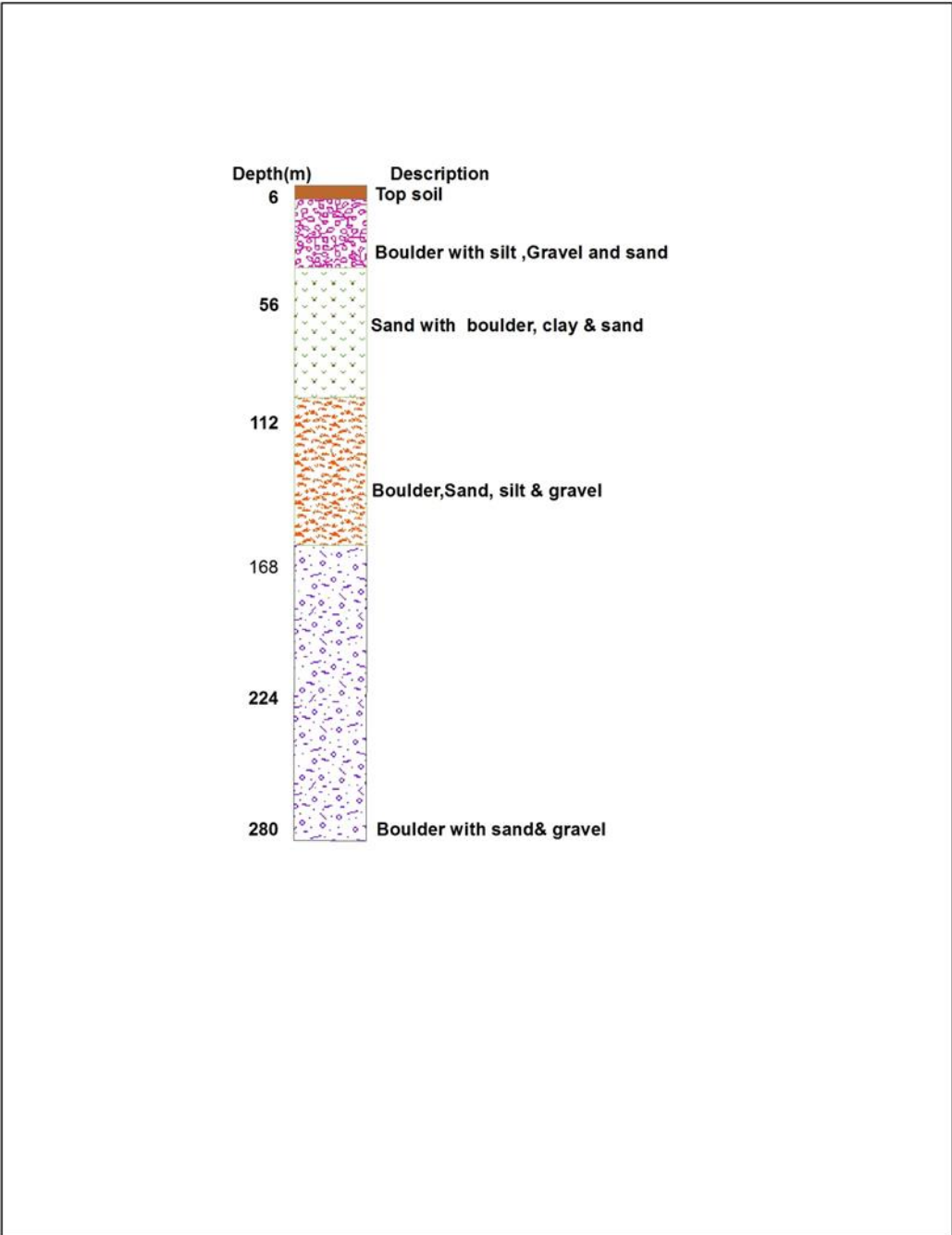


Figure 25 Vertical distribution of aquifer from well log at Tisabalima located on the western side of the valley (Quaternary colluvial and alluvial deposit), with the transmissivity values of $189\text{m}^2/\text{d}$, hydraulic conductivity of $1.85\text{m}/\text{d}$ and give yield of $58\text{ l}/\text{sec}$ (Modified from Amhara design and supervision works enterprise 2017).

6.2.3 Weathered and fractured aquifer with Medium Productivity

6.2.3.1 Volcanic rocks

Storage and transmission of groundwater in the volcanic rocks mostly depend on the kind of porosity and permeability formed during and after the rock formation. Different lithological units belong to this unit, but from the hydrogeological standpoint, they are grouped together as the volcanic aquifers which are mainly basalt and rhyolite.

Due to the previous tectonic events in the earlier, this formation is moderately to highly fracture, but in order to have a good permeability there should be an integrated combination of primary and secondary structures. In the meantime the fractured zones and the weathered mantle called the regolith are the storage for the groundwater.

In the study area there are many shallow source springs that came out through the regolith surfaces of volcanic rocks and serve as the main water supply for small communities, especially in the highland areas and its permeability is influenced by the intensity, degree, depth and extent of fractures and joints. Nonetheless, in some cases the presence of secondary infilling material decreases the permeability of such structures.

6.2.3.2 Tarmaber Basalt

This unit is found in the northern part of the study area with small coverage in the area. It's found at the very highland terrains (>3000m) for that reason it's mainly a recharge area. Its steepness topographic setup tends to limit the infiltration of water through the aquifer, which increases runoff to the rivers. Even though it possesses good fractured surfaces that results in good hydraulic properties. In general this unit is classified as moderate productive aquifer.

6.2.3.3 Aiba Basalt

The permeability in this aquifer is highly dependent on the degree, intensity and depth of fractures and joints, however variation in fracture system and topography in the study area leads to difference in potential to yield throughout its outcrop.

The cooling joints are improved by mechanical weathering and fracturing which will increase the vertical permeability; it allows the availability of springs at the escarpment and hillsides (GSE, 2013).

A spring at Mededo with a discharge of 50 l/s is an example of such condition. The latter occurred spring at the foot of the mountains (where there is a topographic discontinuity, Fault escarpments and dipressional areas) which includes Robit, Kent Aba, Gatira, and mecha, Bereko, Chereti, Girana and Hadiya, with a discharge of 1-50 l/s. It is mainly controlled by a fault which creates a conduit for groundwater flow (GSE, 2013).

Meanwhile ,somewhat dipper groundwater level tends to be shallow at the down through of the fault and allow the artesian groundwater and the existence of more than two springs in the area (GSE, 2013) figure 26 show two the springs in the area. In general this rock is categorized moderate productive aquifer.



Figure 26 springs, at Robit (Hayk) (A) and Kent Aba Mersa (B)

6.2.3.4 Ashenge Basalt

The unit is thick, deeply weathered and fractured. Hence it increases the porosity and sometimes the permeability of the rock as well as the groundwater flow and occurrence. In some cases the groundwater flows through those fractures tend to reduce the size of the open spaces due to the deposition of secondary infillings.

In general this unit is classified as medium productive aquifer. Depending on the depth and topographic setup. Among the high yield boreholes are those drilled around Girana and Mersa with transmissivity of 868.5 sq.m/d and 152 sq.m/d respectively and their safe yield is 78 l/s, and 80 l/s. The aquifer for those borehole is not only the Ashenge formation, but also the overlaying thick undifferentiated thick

sediment. Figure 27 shows the vertical distribution of the sediments and the Ashange basalt.

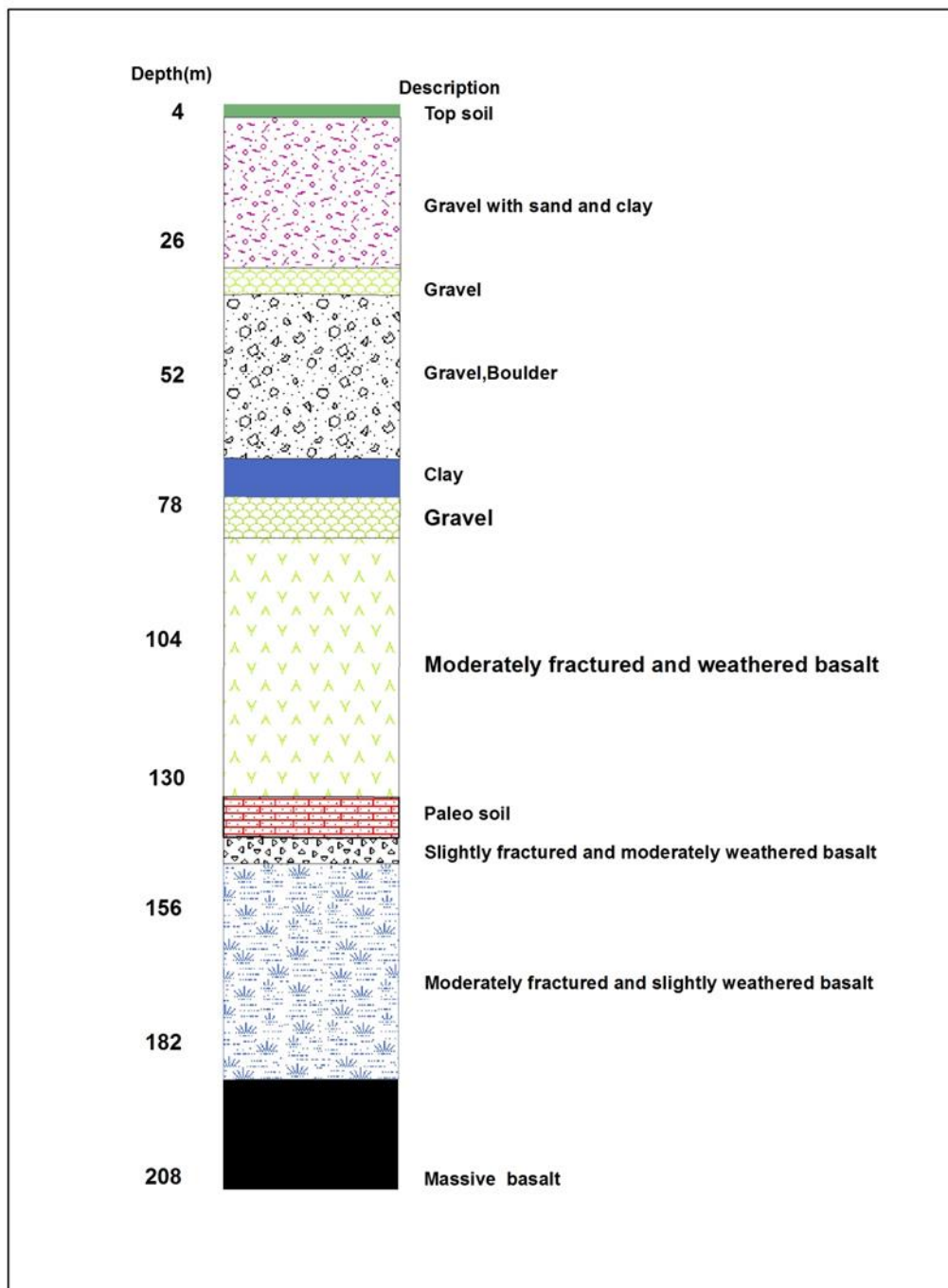


Figure 27 Vertical distribution of aquifer from well log at Seglen located on the south east of the valley (colluvial and alluvial deposit), with the transmissivity values of $>151\text{m}^2/\text{d}$, hydraulic conductivity of $1.75\text{m}/\text{d}$ and give yield of $60\text{l}/\text{sec}$ (Modified from Amhara design and supervision works enterprise 2019).

6.2.4 Low productive aquifers (Aquitard)

6.2.4.1 Kemise rhyolite

This hydrogeological unit is exposed in the eastern part of the study area. It consists of Rhyolite, Ignimbrite, Tuff and Ash by forming NW-SE trending chains of ridges on the foot and margins of Western Afar rift (GSE, 2013).

The permeability and transmissivity of this unit is highly reliant on the secondary fracturing, nevertheless the pore spaces are not well developed and are not good enough to transmit and store the groundwater (GSE, 2013).

No boreholes were drilled in the area, but nearby the study area borehole drilled in Arabati have a transmissivity values of 114 m²/d hydraulic conductivity of 1.52 m/d safe yield of the well is 19 l/s but the aquifer it's not only the Rhyolite but also the Alluvial deposit. Furthermore, due to its topographic setup and very low recharge the productivity of this unit is low in figure 28.

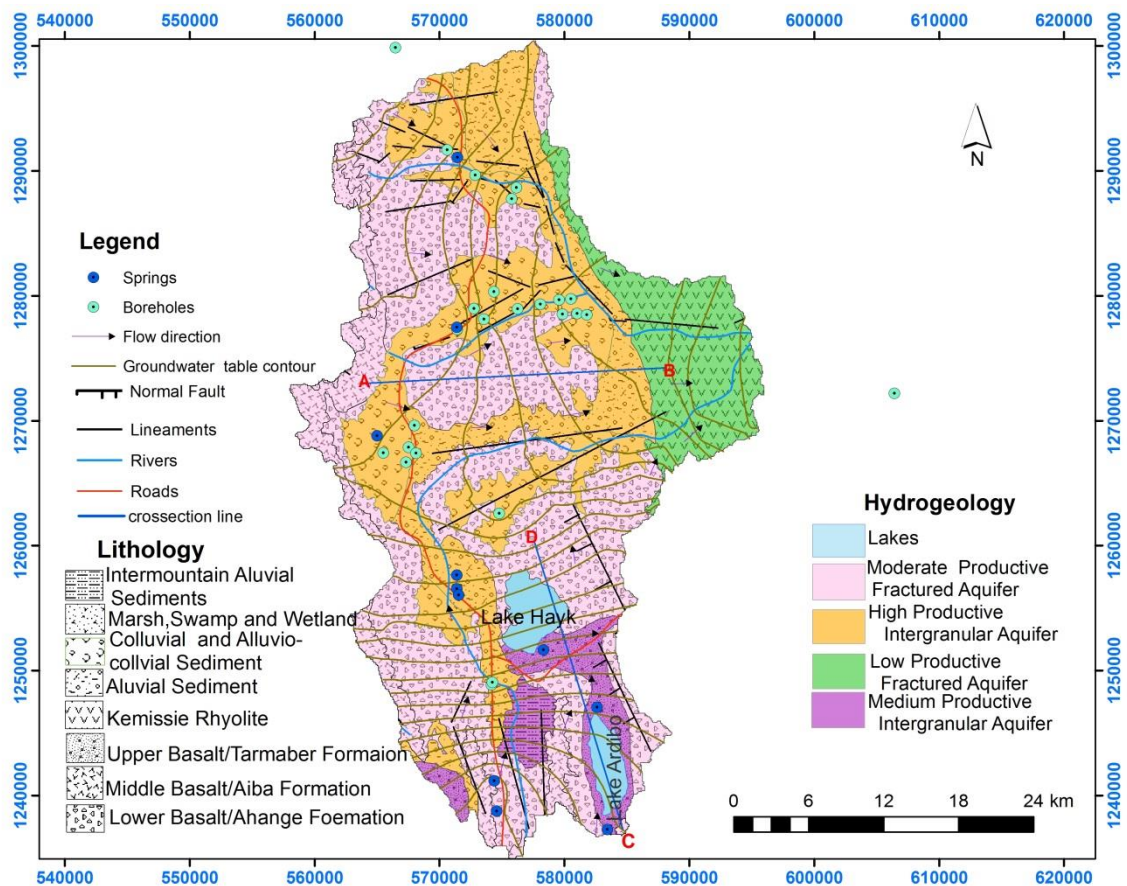


Figure 28 Hydrogeological map of the catchment

6.3 Groundwater Flow Direction

Maps of the water table are 2D illustration of 3D surfaces. Potentiometric surface is a surface of equal hydraulic heads or potentials, typically depicted by a map of equipotential such as a map of water-table elevations (Afework, 2011).

Nonetheless the data that used to make water-table and potentiometric-surface map where water level elevations from wells and springs. If the water table or potentiometric surface has a shallow gradient, the groundwater contours will be spaced well apart.

If the gradient is steep the groundwater contour will be closer together.

Groundwater will flow in the general direction that the water table or potentiometric surface is sloping (Fetter, 2001). The groundwater contour map in figure 30 was done using the field inventory data and secondary data. The movement of the groundwater in the area is controlled by discontinuity with the general orientation of the NNE-SSW and locally NNE-SSW and few E-W trending fractures.

At the mean time the weathered and fractured basalt allows the water to inter vertically and the E-W trending faults allows the water to move laterally in figure 29. The general groundwater flow direction is west (from Ambasal mountains) to the east except that there are localized flows observed in the locality of elevated hills.

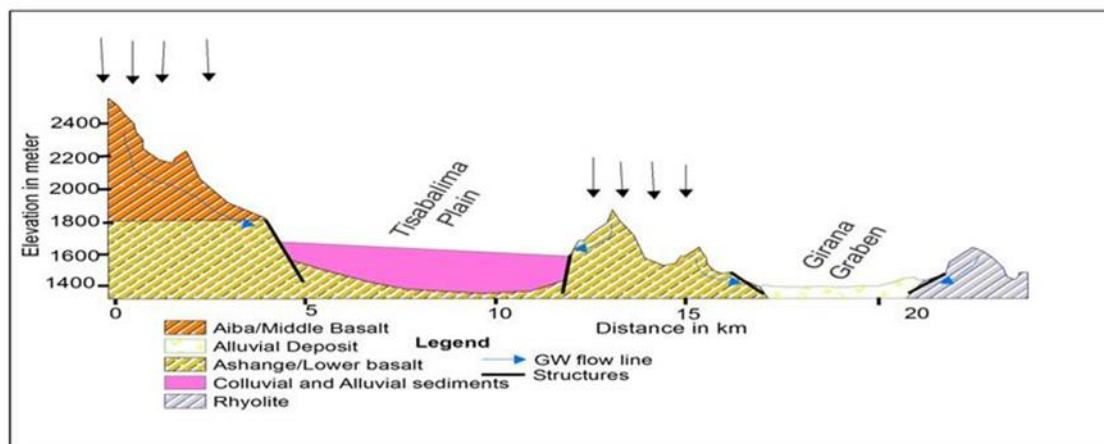


Figure 29 west to east hydrogeological cross section

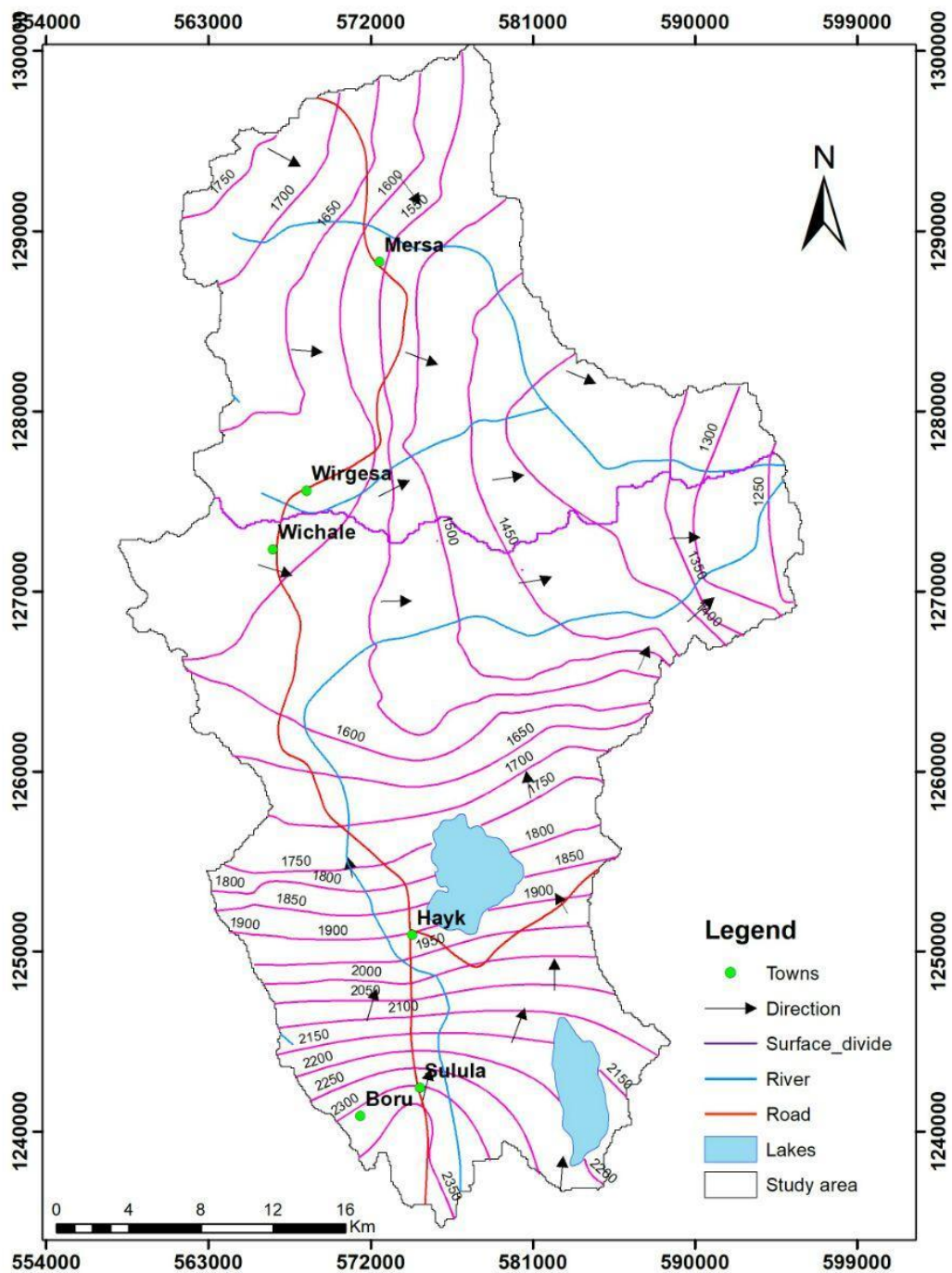


Figure 30 Groundwater level contour map show interpreted groundwater flow directions.

6.4 Groundwater Recharge-Discharge Mechanism

The recharge and discharge conditions of an area are controlled by numerous factors those include, climate, topography, drainage, geological framework, Hydrochemical

trend, land use/land cover and Pieziometric patterns are equally important in the classification of the area into recharge and discharge zones.

From the above-mentioned methods topography is the easiest way to indicate the flow direction and to describe discharge areas as topographic lows and recharge areas are topographic highs. Meanwhile recharge areas in the catchment have also been explained based on lithology, topography and structures in the area.

A topographic high area of the catchment is generally in the west along the Ambasal highlands is considered as recharge area of the catchment while the east is a discharge area. Similarly, careful observation and mapping of springs and seepages in the field have also helped to indicate the discharge and recharge zones.

The other technique to indicate the recharge-discharge area of the catchment is observing Geochemical and isotope data which support the short flow paths of recharge water through the aquifers and low salinity groundwater dominated by Ca-Mg-HCO₃.

The deeper regional flow systems in the catchment have longer flow paths which led to hydrolysis of minerals in the basaltic aquifers and in some locations enrichment by CO₂ from underlying rocks, resulting in groundwater with higher salinity dominated by Na-HCO₃ waters (Kebede et.al, 2005).

Further the TDS values of water from the wells are generally greater than for the springs. The general trend of TDS shows an increase towards the east direction implies that the water had travelled for a long distance and had longer periods of contact with the rocks in other word the groundwater evolves as it moves along its path (Freeze, 1979).

6.4.1. Groundwater and Surface Water Interactions

According to Molla Demlle et.al (2007), based on field observations of geomorphology, geology and spring events supported by water balance estimation and hydrochemistry, Lake Ardibo acquires a large amount of groundwater from the west through E–W running faults and from the south. It also loses groundwater to the north towards Lake Hayk (relatively lower topographic position).

The existence of N–S running faults allows the seepage of groundwater out of Lake Ardibo. But, there is also groundwater outflow from Lake Hayk to the west.

Meanwhile from the collected data mainly hydrogeology, hydrochemistry and with any isotope data revealed that the groundwater flow in the fractured and weathered zones in the highlands is the driving force in the hydrology of the catchment.

Nonetheless the limited isotope data result revealed that the two lakes are highly evaporated. Lake Hayk is more enriched and evaporated than Ardibo.

From their studies, it is definite that lakes leak substantial groundwater in which groundwater also feeds the lakes from the shallow flushed system rather from deep older waters with high residence time and ionic concentration.

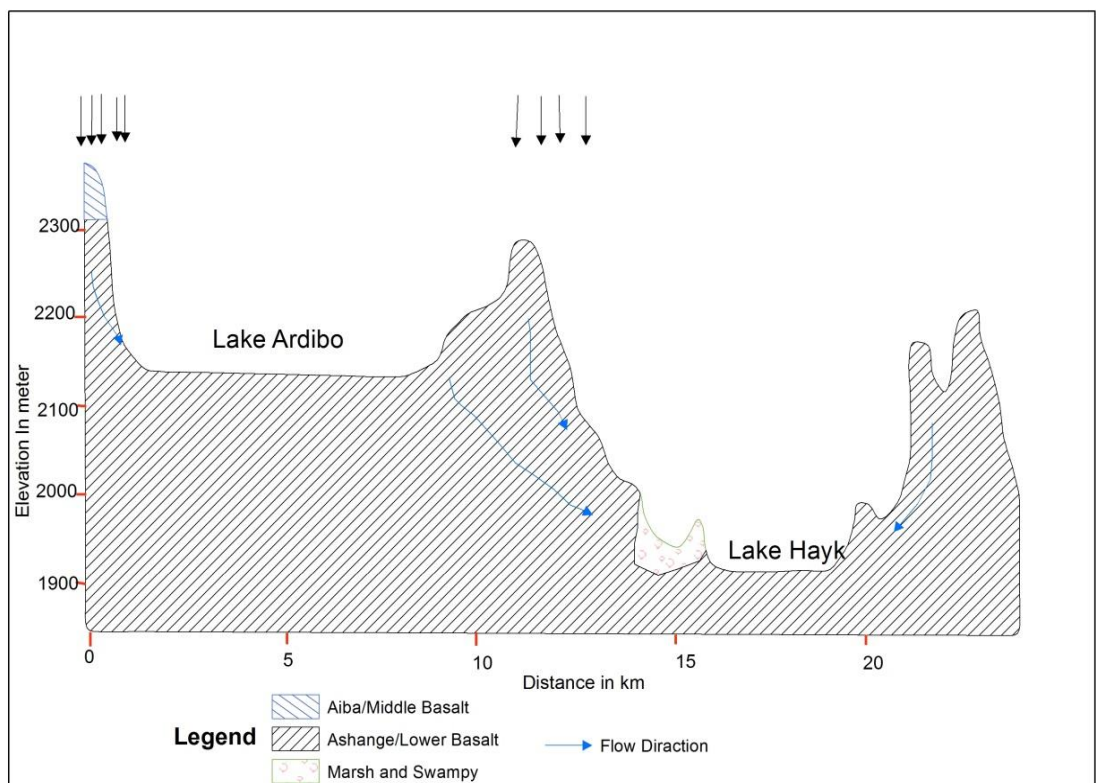


Figure 31 Simple hydrogeological cross-sections of Hayk and Ardibo lakes.

Furthermore Groundwater flow direction has been determined from the groundwater level contours. It is the direction of the groundwater flow perpendicular to the equipotential lines. Kriging with the help of ArcGIS 10.7 software were used to interpolate groundwater level data's in the study area figure (31).

According to the Groundwater flow contour map done from static water level data obtained from boreholes in the study area, Lake Ardibo and Lake Hayk have an

elevation difference more than 150m which is the hydraulic gradient is from Ardibo to Lake Hayk. The E-W trending faults are favourable for the groundwater flow from Ardibo to the Hayk.

In Addition to groundwater contour, field topographical, geomorphologic, structural and hydrogeological observations there are some Hydrochemical evidences that show there might be a groundwater flow between Lake Ardibo and Lake Hayk.

Hydrochemical data obtained from (Molla, 2000) shows samples from Lake Hayk show relatively higher magnesium and sodium than samples from Lake Ardibo. The high Mg content in the area is related to preferential leaching of host basalts, accordingly the concentration of Mg increases with the increasing flow time and distance.

On the other hand the silicate mineral weathering in volcanic rocks produces Na, HCO₃ and clay. Na will also increase with the increasing time and distance of the groundwater flow. An average total dissolved solids, two lakes are 665 mg/l and 498 mg/l for Lake Hayk and Ardibo. Since it is previously mentioned that the existence of N-S running faults allows the seepage of groundwater out of Lake Ardibo to Lake Hayk the increasing TDS to the Lake Hayk might suggest that there is an interaction between those two Lakes.

6.5 Hydraulic Characteristics of Aquifers

6.5.1 Types of Aquifer

Calculating hydraulic characteristics could be relatively easy if the aquifer system were precisely known (Kruseman and Ridder 1994). Understanding a pumping test is largely a matter of recognizing an unknown system. Identification of the aquifer system of the study area was done using three methodologies:

- carefully observing the lithological log of the wells,
- construction of plots (semi – log plot) of drawdown vs time, and
- Observing the static water level with respect to the position of water bearing formation.

A geologic log is assembled from sampling and analysis of well cuttings collected at regular intervals during drilling a well or test hole. Such logs furnish a description of

the geological character and thickness of each stratum encountered as a function of depth, thereby enabling aquifers to be delineated (Todd, 1980).

It is the furthestmost important way to understand the aquifer system. Type of aquifer and the inner and outer boundary conditions affect the drawdown behaviour of the system in their own individual ways during pumping test. So, to identify an aquifer system, it's necessary to compare drawdown behaviour by various theoretical models (Kruseman and Ridder 1994).

Construction of specialized (semi – log) as well as (log-log) models enables to identify the aquifer system of the area. The characteristic shapes of the curves can help in selecting the appropriate model figure 32 (Kruseman and Ridder 1994).

The other method is by observing the static water level/ pieziometric or potentiometric surface of the well. Even though it's not usually used method, but can provide a strong point for the above methods in confined aquifer, the parametric surface will lie above the top of the aquifer while in unconfined aquifer the static water level (SWL) doesn't lie above the top of the aquifer.

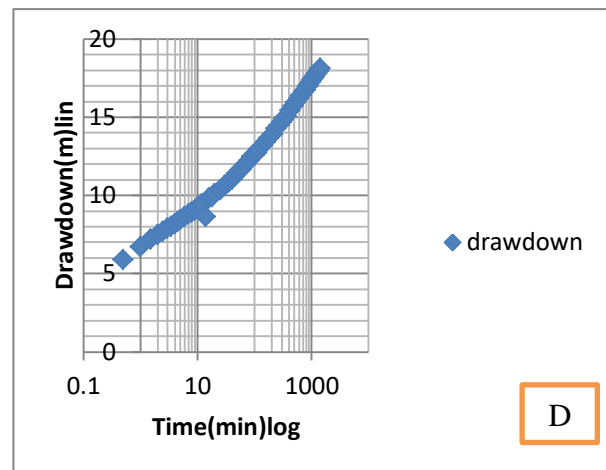
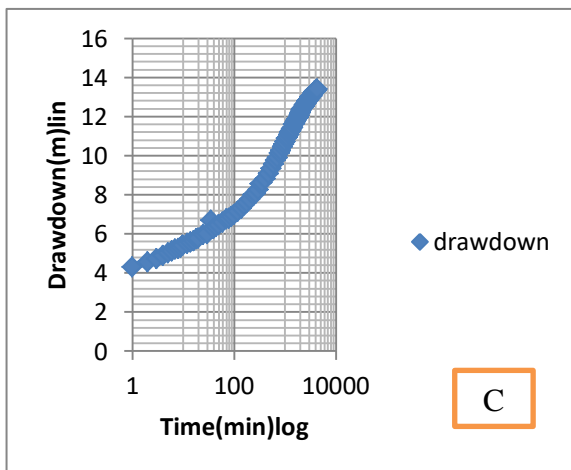
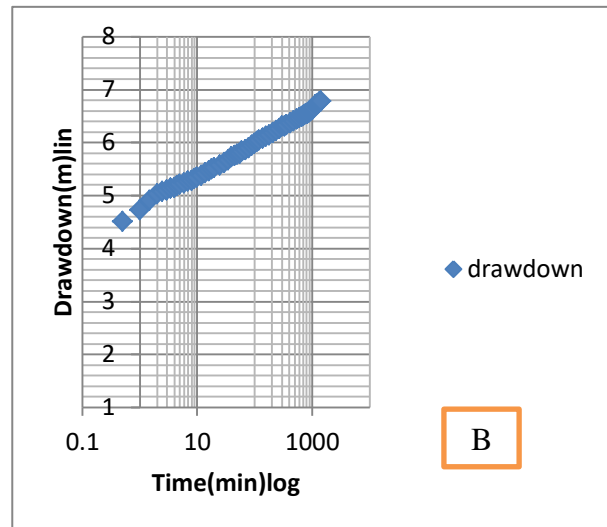
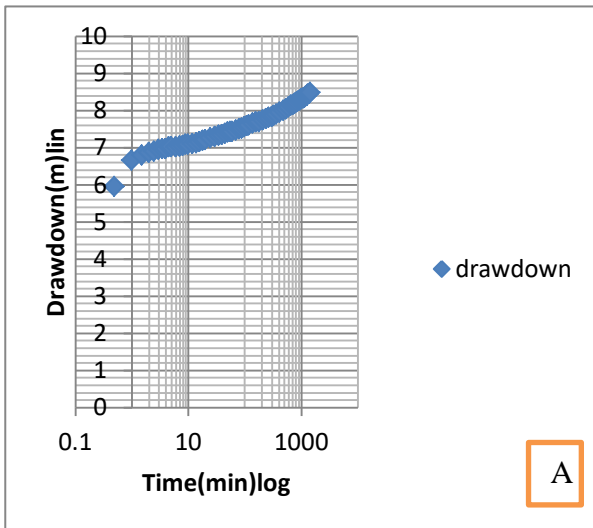


Figure 32 Specialized plots based on the analysis discussed above: C) Mehal Amba, D) Lipso Girana, treated to be confined aquifers because most of them have showed a best fit with Theis type curve and the lithological logs of these wells is dominated with gravel, boulder, sand, with small clay and silt, A) Robit Tisabalima and B) Seglen Hayk, are unconfined aquifer.

6.5.2 Transmissivity (TD or T)

It is the product of the average hydraulic conductivity K and the saturated thickness of the aquifer (D). Peat bogs, swamps and wetland deposits, have the lowest values for the transmissivity ($<50 \text{ m}^2/\text{d}$), whereas the wells tapping the colluvial and the alluvial deposits in the study area have high transmissivity value. Also at the foot of

the mountains high transmissivity values are observed. The values range from (2.41 m²/d -1580 m²/d).

This is clarified by the geological constitute of the rocks in these areas. In the west along the escarpment boundary, the geological material mainly consists of coarse sand, gravel, pebbles and boulders. This correlates with somehow high transmissivity in figure 33. For the purpose of qualitative analysis the transmissivity values of the wells can be categorized into five groups as follows.

- ❖ Very low: <50m²/d
- ❖ low : 50m²/d to 100 m²/d
- ❖ medium: 100 m²/d to250 m²/d
- ❖ high : 250 m²/d to 1000 m²/d
- ❖ very high: >1000 m²/d

Aquifers with transmissivity greater than 149.2m²/d can be sustain irrigation development (Johnson, 1966, as cited Sileshi Mamo, 2007).

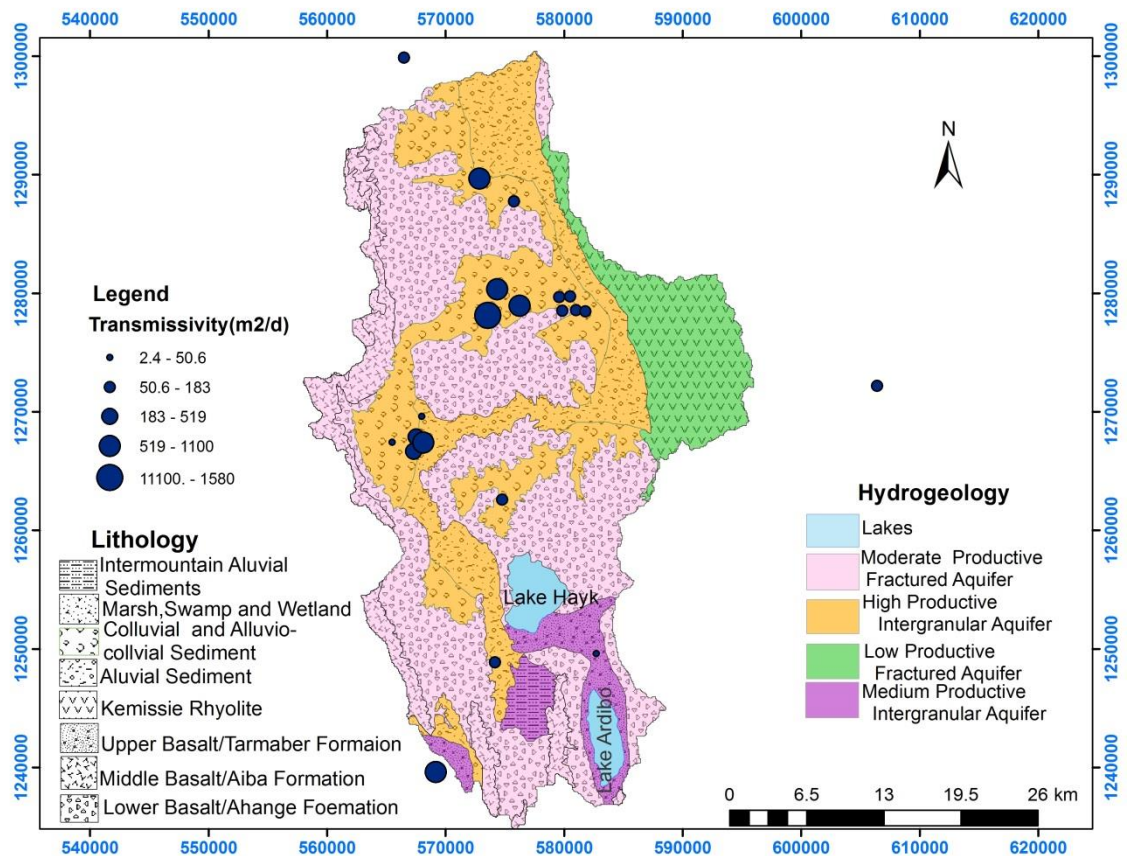


Figure 33 Spatial distribution of Transmissivity value map of the valley (in m²/d)

6.5.3 Hydraulic Conductivity (K)

Hydraulic conductivity is ruled by the size and shape of the pores, the effectiveness of the interconnection between pores, in addition to the physical properties of the fluid. If the interlocking tubes are small, the volume of water passing from pore to pore is constrained and it will result quite low hydraulic conductivity (Kruseman and Ridder 1994).

It determines the ease by which water can move through aquifers. It, therefore, determines the productivity of the aquifer. Hydraulic conductivity is higher in the western and eastern side of the graben than the southern part of the catchment. For the purpose of qualitative analysis the transmissivity values of the wells can be categorized into different groups as follows.

- ❖ Low: <3 m/d
- ❖ Medium: 5-3 m/d
- ❖ High: 10-5 m/d
- ❖ Very high: >10 m/d

There are few boreholes that tap the volcanic aquifer within the study area. The data obtained from borehole drilled their depth is relatively shallow to water level and discharge. For that reason, it was hard to calculate the hydraulic parameters for the volcanic aquifer figure 34 show the distribution of hydraulic conductivity.

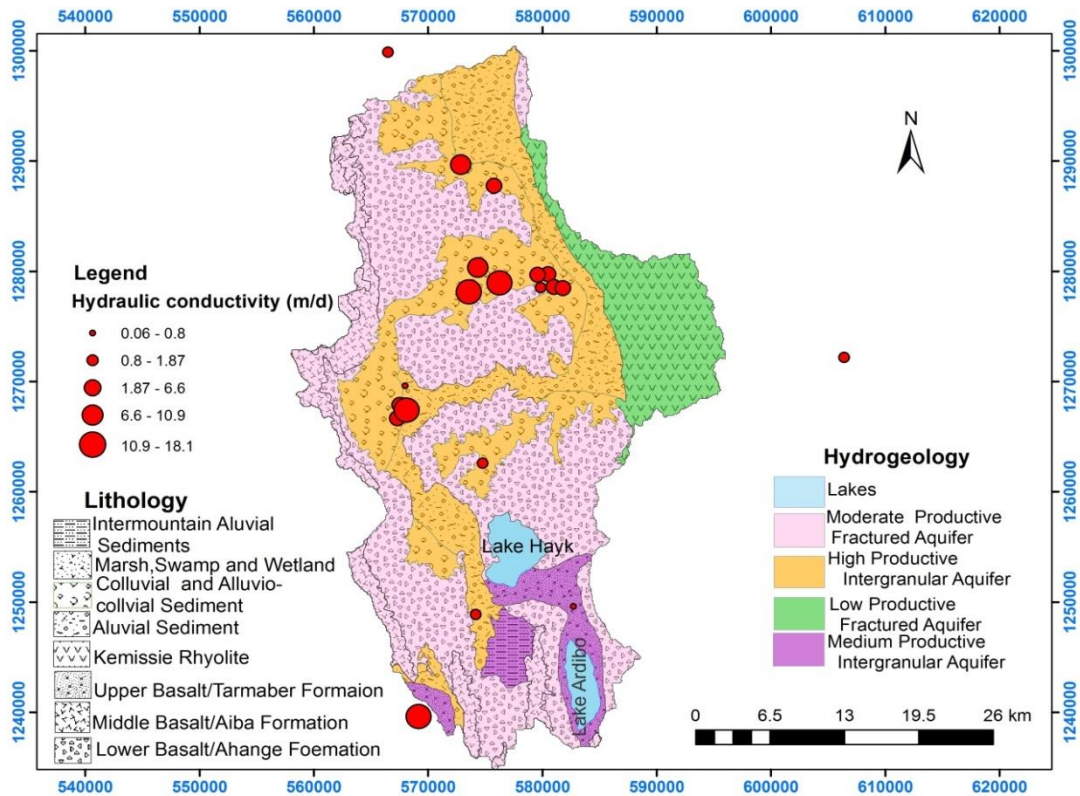


Figure 34 Spatial distribution of Hydraulic conductivity value map of the valley (in m/d)

6.5.4 Groundwater reserve estimation in study area

Calculation of ground water reserve is necessary for planning the optimum utilization for future development of the ground water resources of an area. The total subsurface water reserve is a function of saturated thickness and storage coefficient/specific yield. The aquifer system is generalized into water table aquifer of the sediment. The groundwater reserve in the study area can be estimated using the relation:

$$V = Sy * A * b$$

Where V: reserve (m³)

Sy: specific yield

A: surface area of the valley (m²)

b: saturated thickness (m)

The specific yield for the study area is 0.1, surface area of the graben estimated to be 452 km² and an average saturated thickness is 81.6m. Therefore, groundwater reserve of the graben is estimated as 3670.24 MC

CHAPTER SEVEN

7 HYDROGEOCHEMISTRY

Natural water comprises of dissolved minerals, dissolved oxygen, suspended particulate materials and etc. It is derived from different sources of solutes containing gases from the atmosphere, weathering and erosion of rock and soil, solution or precipitation, reactions occurring below the land surface and effect resulting from human activities (Hem, 1985).

Hydro geochemical studies are relevant in assessment of the groundwater potential of a given watershed providing an information on the interaction between water and the geological materials of the aquifer systems, understanding of the geochemical processes controlling the final make up of water chemistry, the hydrodynamic condition of groundwater and assessing the quality of water for sustainable use (Kassahun Beyene, 2005).

Within the study area, a total of 21 samples has been collected from boreholes, springs and Hand dug wells in the field by measuring their pH, EC and Temperature in the field. Samples that are believed to be a representative samples have been analysed for their major cation and anion (Na^+ , K^+ , Ca^{2+} , Mg^{2+} , Cl^- , F^- , NO_3^- and SO_4) Species in the Laboratory of Saba Engineering Company P.L.C.

Furthermore, before the usage of the water quality data, reliability check in (Figure 35) has been made of the groundwater samples of both primary and secondary data. According to the electron neutrality test the sum of cation should be nearly equal to the sum of Anions where by their concentration is expressed in mille equivalents per litre.

Only those data with percent error less 10 and two data's having percent error more than 10 ($\text{Ka_CSP6}=11.5$, $\text{Me_BH2}=-12.2$) but due to their significance in interpretation has been used. A total of 34 samples of secondary and primary data has been used for understanding of hydrogeochemical regime of the catchment in figure 36. Aquachem 4.0 software and Excel spread sheet has been used for preparation of data and interpretation.

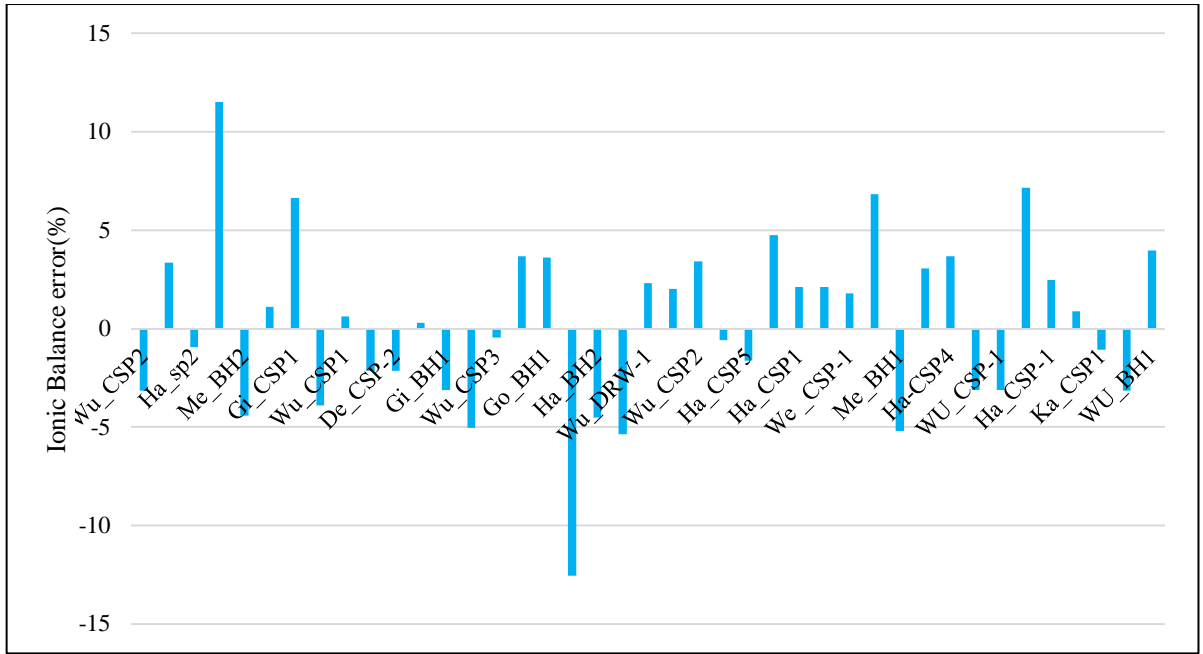


Figure 35 Error distributions Graph

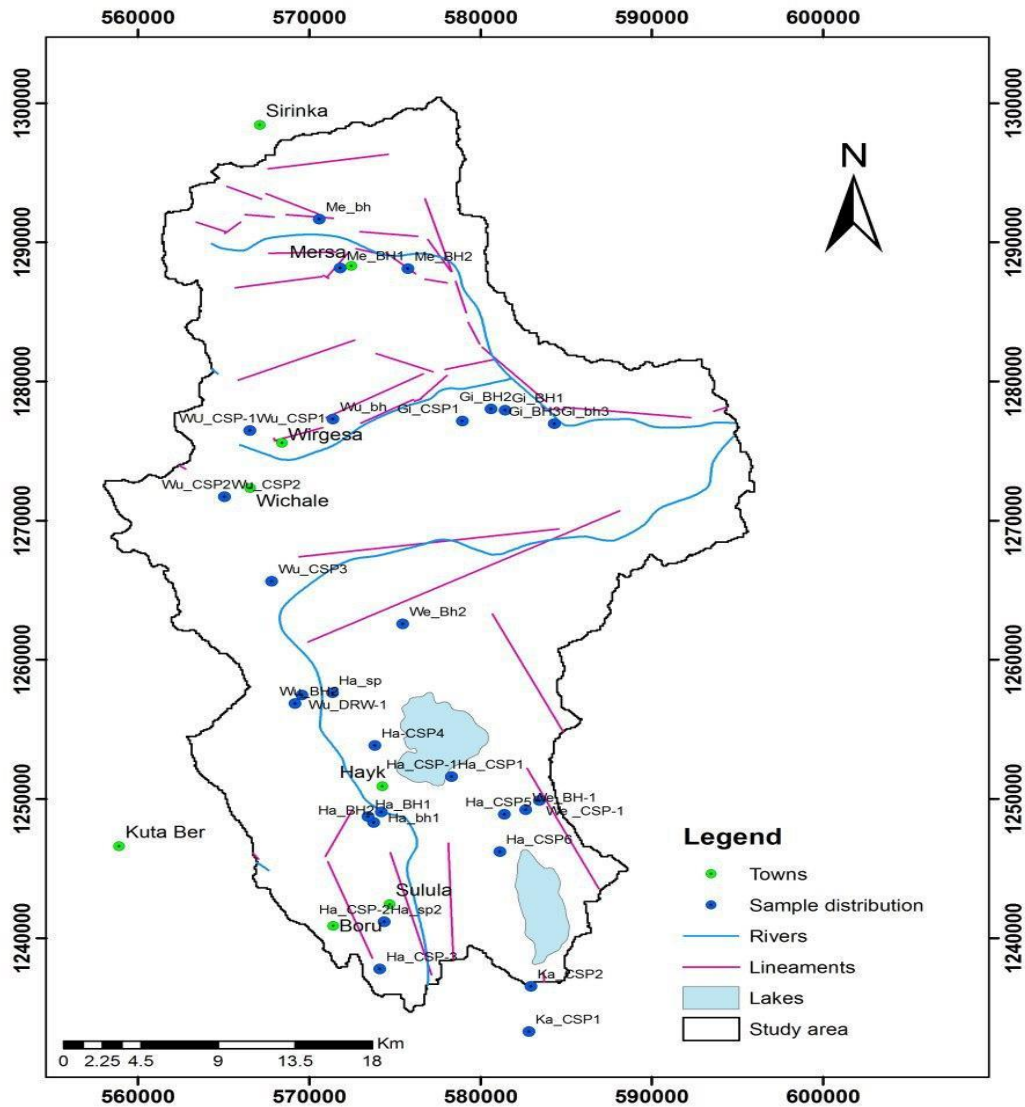


Figure 36 sample distribution of Hydrochemical data

7.2 Evaluation of Hydro chemical Parameters and Ions

7.2.1 Physiochemical Parameters

7.2.1.1 Electrical Conductivity

Electrical conductivity is a measure of the ability of the water to conduct electric current. Higher EC indicates the enrichment of salts/dissolved matter in the groundwater (Lawrence et al. 2000).

Dissolved ionic species presented within the groundwater give water property of electrolyte which leads the water to have capable of conducting an electric

current. Within the study area the value of EC ranges from 293 $\mu\text{s}/\text{cm}$ to 927 $\mu\text{s}/\text{cm}$ in boreholes and springs where the lowest value is observed in the southern and the highest being observed in the northern eastern and eastern part of the study area

Meanwhile increase in conductivity near the east of the study area might be related to the geology, the ground water flow direction and possible evaporation. Generally, dissolved solid concentrations in groundwater increase along flow paths, from the surface of the saturated zone and through the aquifer, due to the dissolution of minerals (Freeze and Cherry, 1979).

7.2.1.2 pH

pH is the measure of the concentration of hydrogen ion activity. According to Hem, 1959 the pH of natural water mainly depends upon the chemical reactions and the equilibrium among the ionic species in the solution.

The pH value ranges from 6.17 to 8.89 in the springs and borehole's with a mean 7.2. Samples tested in borehole shows low 6.67 Me_bh1 and high in 8.89 Me_bh2. Generally springs located in the recharge area are displayed relatively lower pH values closer to 7.

7.2.1.3 Total Dissolved Solids

Total Dissolved Solids is the concentration of all dissolved constituents within the groundwater and is directly related to electrical conductivity. Within the study area the concentration of TDS ranges from 253.52 mg/l to 835.08mg/l. The lowest concentration has been observed in the southern part of the study area (spring: HaSP2) and the Highest value is observed in bore hole drilled (i.e. GiBH2) in the eastern downstream part of the catchment.

Despite some anomalies of high TDS, concentration of TDS shows a definite trend where its concentration increases towards the downstream part (i.e. towards the east) of the study area in figure 37.

This implies shallow groundwater in recharge areas are lower dissolved solids than the water deeper in the same system and lower in dissolved solids than water in shallow zones in the discharge areas (Freez and Cherry 1979).

This suggests that as the water goes from the highland through fractured and unconsolidated sediments it acquires dissolved solids more and more depending on all the parameters that govern the evolution of groundwater chemistry. In which the generally the western and south western part of the area is the recharge zone, whereas the central and eastern part of the plain is discharge zone.

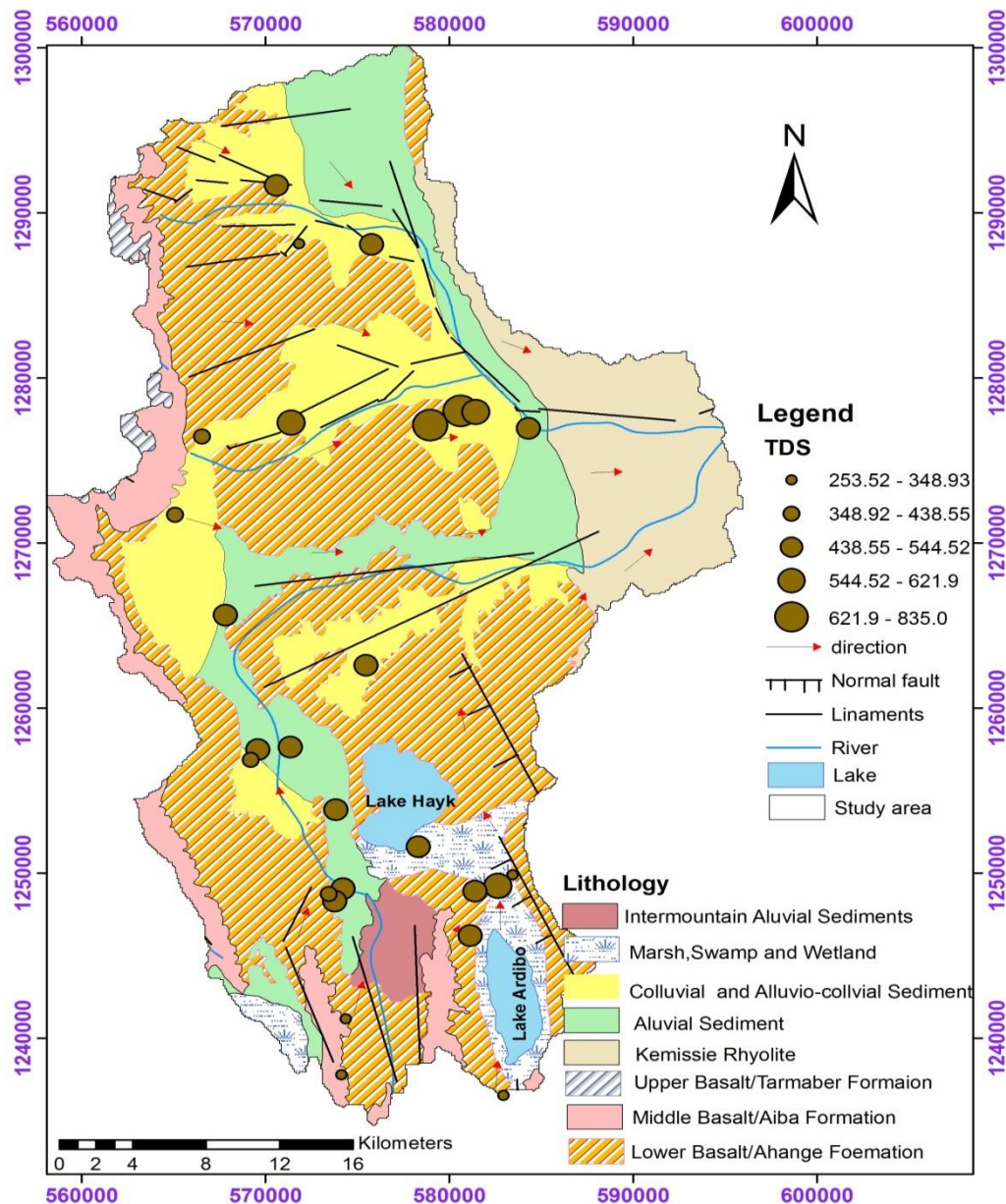


Figure 37 TDS distribution Map

7.2.1.4 Hardness

Hardness can be defined to the soap consuming property of water. The effect of this property is the result of calcium and magnesium. Other ions which precipitate soap

include H^+ and polyvalent metals but are insignificant. (Tenalem Ayenew and Tamiru Alemayehu, 2001). Hardness can be expressed in terms of the concentration of $CaCO_3$. According to Dufer and Becker (1964 as cited in Tenalem Ayenew and Tamiru Alemayehu, 2001) the range of hardness concentration in milligram per liter (mg/l) is given in the table below: The total hardness is defined as the sum of calcium and magnesium concentrations, both expressed as $CaCO_3$ in mg/l. It can be determined by substituting the concentration of Ca^{2+} and Mg^{2+} , expressed in milligrams per litre, in the expression

$$\text{Total Hardness} = 2.5 (Ca^{2+}) + 4.1 (Mg^{2+})$$

Table 12. range of hardness with its description

Hardness range, $CaCO_3$	Description
0-60	Soft
61-120	Moderately hard
121-180	Hard
Greater than 180	Very Hard

Within the study area, the hardness ranges from 124.896 mg/l to 447.76 mg/l where the majority of the water samples fall on within the range of Hard to Very Hard. As we can see in figure 38. High hardness is credited to the geological formations that characterize the area which are composed of Quaternary sediments which are derived from Tertiary basalt. The dominant cations of the basin are calcium and magnesium.

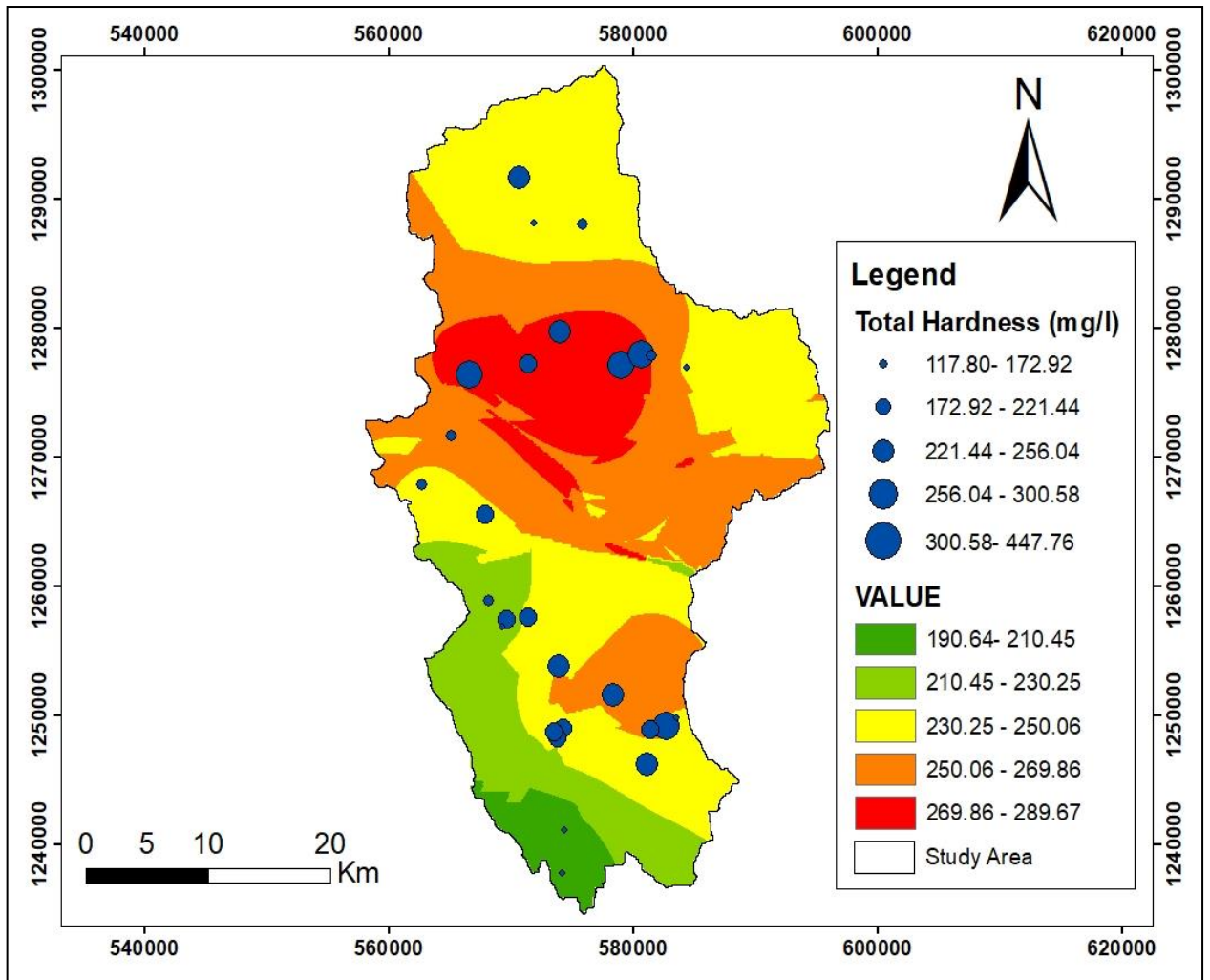


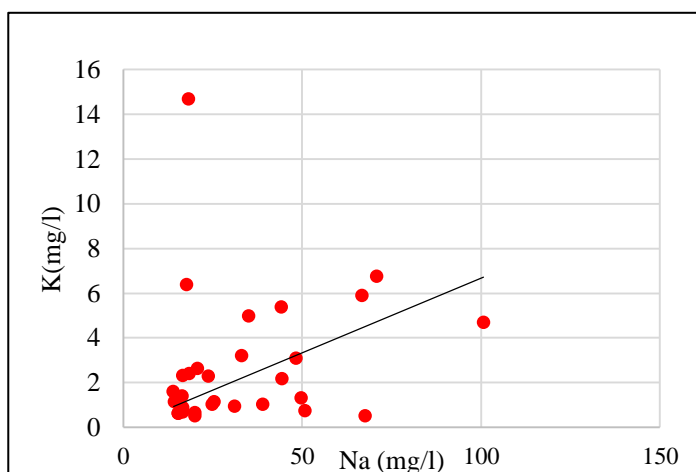
Figure 38 Hardness map of the area

7.3 Major ions

7.3.1 Sodium and Potassium

Sodium is the second most abundant cation following calcium in the study area (Table 12). In the samples examined it ranges from 14.3 in Wu_CSP2 to 100 mg/l in borehole Gi_bh. Na⁺ concentration shows in general an increasing trend along groundwater flow direction. This is due to the long-time water-rock interactions. The main source of sodium in the study area could be sodium plagioclase (albite) and to some extent sodium may be retained by adsorption on mineral surface of lacustrine deposits having high cation exchange capacities such as clay before directly recharge to groundwater.

Meanwhile the concentration of potassium is lower than sodium because of its resistant to weathering on the other hand sodium and calcium are more susceptible to weathering. The low concentration of potassium in general could be attributed to the lesser proportion of potassium feldspar (Afework, 2011).



7.3.2 Magnesium and Calcium

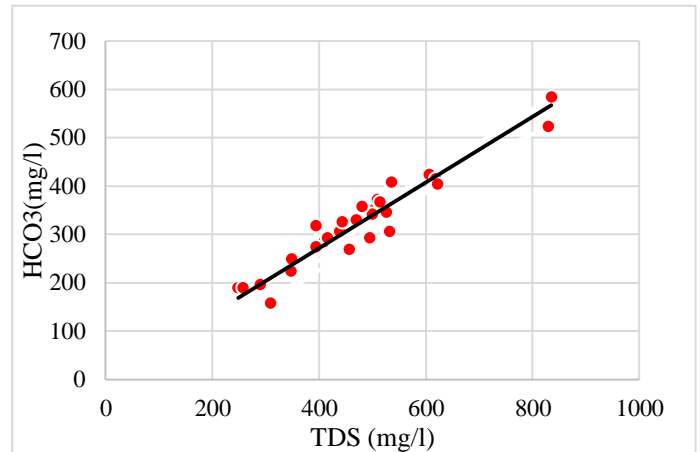
Calcium is the most abundant cations in the study area. Because of their similar geochemical behaviour calcium and magnesium are treated together. Most of the samples in the study area are calcium and magnesium bicarbonate water types. Calcium ranges from 18.8 mg/l in spring Ha_sp to 103 mg/l in We_BH-1. Higher concentrations are found in the southeast and southwest of the study area. Magnesium ranges from 9.6 mg/l in We_CSP-1 to 66.7 in Me_bh. The main source of Calcium in the study area could be derived from weathering of basaltic rocks. Though locally high and low values are found due to variation in depth of boreholes, geochemical reactions and presence of deep groundwater system.

7.3.3 Carbonates

Carbonates are found in a bicarbonate form in the area. It is mainly in the form of bicarbonate. It is the major ion in the groundwater and springs.

The concentration of bicarbonate in boreholes ranges from 157.38 mg/l in Ka_CSP2 to 583 mg/l in Gi_BH2. Higher concentrations of HCO_3^- are observed in wells located in the eastern part relatively shows a relatively decrease to Southern part of the area.

All samples shows higher TDS with high concentration of HCO_3^- and the lower TDS is the vice versa. The chemical weathering of Aluminium silicate like Albite or K-feldspar controls the CO_2 content of water Therefore its pH (Langmuir, 1997).



7.3.4 Major Ions and their relationship with TDS map

Relationship between Hydrochemical parameters is very helpful in understanding of the major processes that are responsible for the final make of groundwater chemistry. The composition of groundwater mainly depends upon the aquifer material with which in flows, ion exchanger reactions with clay minerals and the residence time along its flow path.

Major cations and their relationship with TDS have been used in order to understand the source of different solutes that that result the final make of groundwater.

As indicated from the Figure 6 below despite low correlation coefficient of the cross plot of Alkaline Metals with TDS, there is a general increment of TDS with rise in the cations (Na^+ and K^+). In the case of figure 39 cross plot of Alkaline Earth metals with TDS shows a good relation where the cations (Ca^{2+} and Mg^{2+}) increases with rise in TDS indicating no source of calcite precipitation indicating early stage of geochemical evolution.

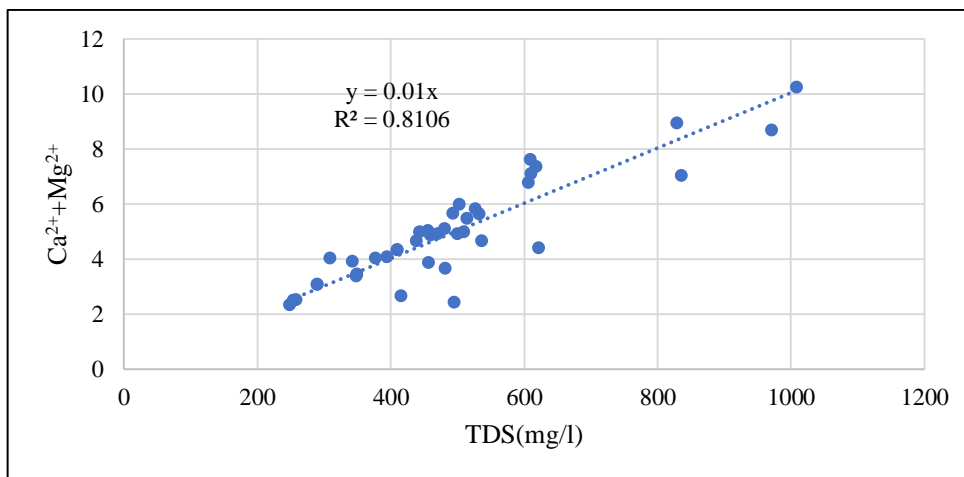
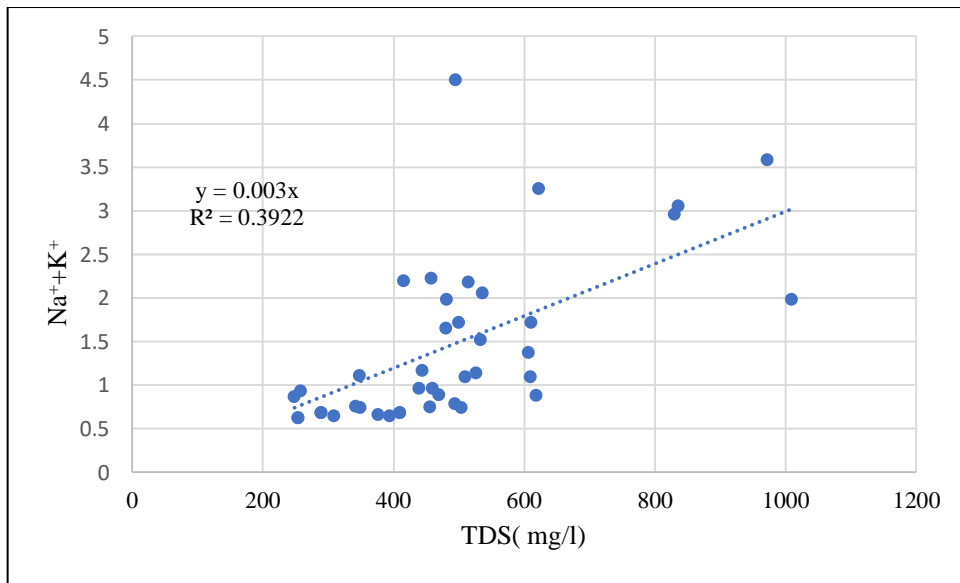


Figure 39 TDS vs. Na++ K+ and TDS vs. Ca+2 + Mg+2 relationships

7.3.5 Sulphates and Nitrates

Sulphate is the second most abundant anion next to bicarbonate in the area. Meanwhile bore holes samples ranges from 5 mg/l Ha_sp2 in to 49.42 mg/l in Gi_BH1. The mean is about 16.5 mg/l. Most of the samples are between 1.5 mg/l and 30 mg/l. Like other major ions, it relatively shows an increasing trend along the groundwater flow direction, but locally high and low values are found.

The mean concentration of nitrate is 13.9 mg/l in in the study area. That ranges in the boreholes from 0.1 mg/l in Gi_BH1 to 16.85 mg/l in Gi_BH3. In the meantime high nitrate concentrations were detected in springs which were more than 30mg/l and the source could be associated with agricultural chemicals.

On the other hand lower concentration of Nitrate relatively in boreholes might be related to the absence of deep aquifers affected by humans source related to agricultural fertilizers and animal manures.

7.3.6 Chloride

Chloride is a tracer that preserves in existing conditions; it is frequently used in flow path tracking and recharge estimation. Mostly, and igneous rocks couldn't produce very high concentrations of chloride in natural water. Significantly more essential sources are associated with sedimentary rocks, particularly the evaporites (Hem, 1985).

The mean concentration of chloride is 10.9 mg/l. In the boreholes it ranges from 7.2 mg/l in Wu_bh to 24.11mg/l in Gi_BH2. Most of the samples are between 1.4 mg/l and 30 mg/l.

The chloride concentration increases in the general ground flow direction which is from west to east.

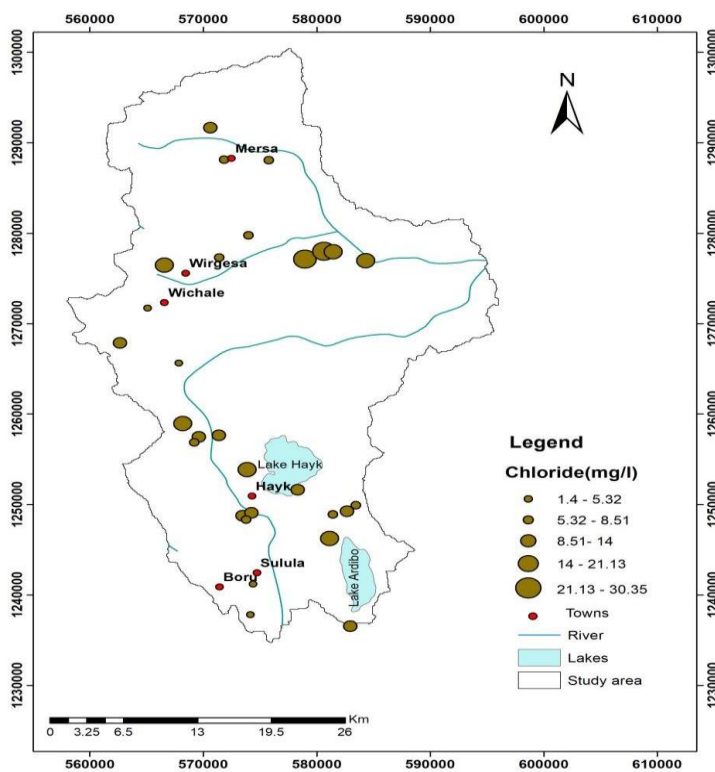


Figure 40 Chloride map

Table 13. Summary statistics of the groundwater sample result

Parameter	Unit	Min	Max	Average	St. Dev.	Dev. Coefficient	Sample Number
Ca	mg/l	18.8	103.6	55.09853	20.82605	37.79783	34
Mg	mg/l	9.6	66.7	26.74412	16.08134	60.1304	34
Na	mg/l	12.1	100.7	31.00294	20.98299	67.68063	34
Cl	mg/l	1.4	30.35	10.88294	6.47825	59.52664	34
HCO ₃	mg/l	157.38	583.16	313.2247	94.40898	30.14098	34
SO ₄	mg/l	5	49.42	16.55794	11.80211	71.27764	34
pH		7.03	8.25	7.64333	7.80014	102.0515	34
calc TDS	ug/l	257.26	835.08	455.0075	157.1576	34.53957	34
Total Hardness	meq/l	1.24896	4.47362	2.47514	0.79159	31.98147	34

7.4 Water Types

The piper plot has been used in order to identify water types within the study area. The three major cations (i.e. Sodium, Calcium and Magnesium) were found to be the dominant species and the bicarbonate ions being the dominant anion which makes up the water facies within the study area.

Ca-Mg-HCO₃/ Ca-Na-HCO₃ type

Ca-Mg-HCO₃ water types are the most dominant within the study area. This type of water facies exists in bore holes (e.g. We_BH1, Go_BH1, Ha_BH2, Wu_BH1) and springs (e.g. Ka_CSP1, Ha_CSP1, Wu_CSP2).

Within the study area this type of water types are mainly located at the upstream part of catchment associated with alluvial deposits and basaltic unit. Water types of this facies indicate early stage of geochemical evolution with short sub surface residence time whereby the groundwater doesn't undergo sufficient sub-surface interaction. TDS value ranges from 253.52 mg/l - 605.83 mg/l.

At the mean time Ca-Na- HCO₃ groups are chemically transitional type of water (mixture of Ca-HCO₃) more mineralized and evolved types of water with the TDS value ranging from 456 mg/l - 532 mg/l. This type water is found in relatively deep

7.5 Water Quality

The quality of water can be determined by the constituents of dissolved solute and gases. Different natural and anthropogenic factors are responsible for degradation of water quality. Assessment of groundwater quality is vital important for its usage for domestic consumption. Prescribed standards for drinking-water vary from country to country, depending upon economic conditions, climate, food habits and geographic location (Afework 2011).

There is also conflicting evidence with respect to safe limits for certain constituents different water quality standard has been established by different organization. Therefore, the suitability of groundwater for domestic purposes has been evaluated based on World health Organization (WHO, 2006) and Ethiopian Drinking guidelines for Drinking water (ES261, 2001). According to the guidelines listed below majority of the samples meets the standard guidelines.

Table 14 Comparison with water quality standards for drinking water

Parameters	Maximum Permissible level (ES261, 2001)	Maximum Permissible level (WHO, 2006)	Range of concentration	Number of samples in permissible level (ES261, 2001)	Number of samples in permissible level (WHO, 2006)
Na+(mg/l)	200	200	1-67	38	38
Ca ²⁺ (mg/l)	75	75	5-69	38	38
Mg ²⁺ (mg/l)	50	30	1-31	38	38
K+(mg/l)	1.5	-	0.15-17.1	16	-
Cl-(mg/l)	250	250	1-21.5	38	38
SO ₄ ²⁻ (mg/l)	250	200	1-35	38	38
NO ₃ (mg/l)	50	50	0.00-53.40	38	38
F-(mg/l)	1.5		0.08-2.48	37	
PH	6.5-8.5	7.0-8.5	6.04-8.25	29	16
EC(uS/cm)	1000	750	55-873	38	16
TDS(mg)	100	800	75.6-637.4	38	34
TH _{as} CaCO ₃ (mg/l)	300	800	20.11- 299.98	38	38

7.5.1 Water Quality for Irrigation Purposes

Quality of Water, Soil types and cropping practice play great role in irrigation. Good quality of water permits maximum yields consistent with proper soil and management (Ermias Hagos, 2005).

Sodium Adsorption Ratio

Salinity in the soil occurs when there is excessive accumulation of salt in the top soil. Excessive salt in soil can reduce water availability to the crop which could lead in reduction of Yield productivity.

The relative concentration of Na with respect to Ca and Mg is very important for the suitability of water for agricultural purposes. If the water used for irrigation is high in sodium and low in Ca and Mg the cation exchange complex may become saturated with sodium. This can destroy the soil structure owing to the dispersion of the clay particles and this in turn decreases permeability and aeration of the soil, which harm plant growth by limiting the uptake of water and air.

$$SAR = \frac{Na}{\sqrt{\frac{Ca + Mg}{2}}} \text{ (meq/lit)}$$

Table 15 General classification of water sodium hazard based on SAR values

SAR values	Sodium of hazard water	Comments
1-9	Low	Use on sodium sensitive crops must be cautioned.
10-17	Medium	Amendments (such as gypsum) and leaching needed.
18-25	High	Generally unsuitable for continuous use.
≥26	Very High	Generally unsuitable for use.

(Sources: Bauder et. al., 2003)

Combined SAR and salinity hazard (as measured by electrical conductivity) is the most widely used water quality for irrigation classification tool. These criteria which are called the Wilcox diagram. According to the Wilcox diagram of water is generally characterized by low sodium and majority of the samples are medium to rare high salinity hazards.

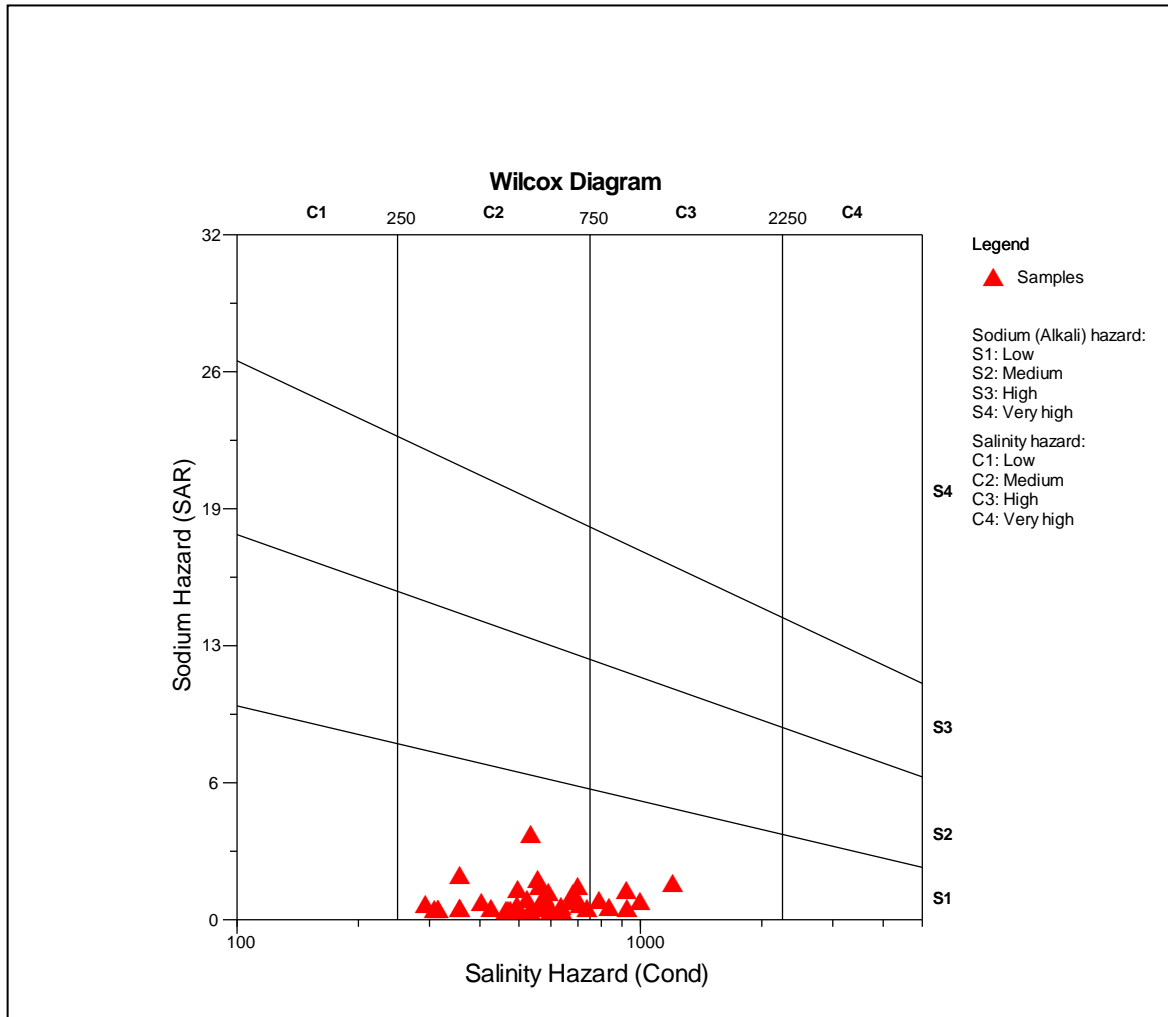


Figure 42 Irrigation water classification on samples collected from the study area

CHAPTER EIGHT

8 CONCLUSION AND RECOMMENDATION

8.1 Conclusion

The overall objective of this work is to assess the hydrogeology of the upper Mille River catchment and specific objectives were to estimate the groundwater recharge, Analyse and interpret water quality both in situ and in the laboratory, identify the recharge and discharge zones as well as to classify hydrogeological units based on its productivity.

The main outcomes of the study are described below:

- The precipitation component has been calculated using Thiessen polygon and SWAT model based estimation. The mean annual rainfall as calculated by Thiessen polygon method gives a value of 1157.6mm whereas after calibration and validation SWAT model, the results are found to be 1105.2 and 1102 mm respectively.
- The amount of recharge that is contributed to the subsurface as calculated by using Base flow separation, chloride mass balance and SWAT modelling gives a value of 135.9 mm/year mm, 115.66 mm and 140.48 mm(after calibration)and 138.5(after validation) respectively.
- To describe the aquifer system of the area pumping test data, well completion reports, well logs and geology of the area were analysed. The study area is characterized by deep groundwater systems on average 214 m (depth of the well) and groundwater reserve of the graben is estimated to be 3670.24 MCM.
- Hydraulic characteristics are spatially variable in the area. Transmissivity of the graben ranges from 2.4–1580 m²/d. High values are observed in the collovial and alluvial sediments low values are observed in the marsh, swamp and wetland deposits due to the existence of clay.
- Its hydraulic conductivity ranges from 0.06 – 18.2 m/d. High values are observed in the colluvial and alluvial sediments low values also are observed in the marsh, swamp and wetland deposits also due to existence of clay. The Quaternary unconsolidated sediments are the main aquifer units from the

other units in the area. These aquifers were found to be good groundwater potential zone.

- Groundwater flow direction is generally from west (from Ambasal Mountains) to east except that there are localized flow components observed in the vicinity of elevated hills, to the localized lakes and out of the lakes and along the river banks.
- The piper plot of the water, chemical analysis shows that shallow wells, bore holes and spring water samples are Ca-Mg-HCO₃ or Mg-Ca-HCO₃ type in the recharge area, intermediate water type Ca-Mg-Na-HCO₃ or Mg-Ca -Na-HCO₃ in northern and central part of the valley/graben to Na-Ca-HCO₃ type towards the east.
- In general, for most of the major constituents the samples show concentrations below the maximum allowable limits (WHO guideline) and Ethiopian guide lines i.e., the borehole waters could be used safely for drinking. From an agricultural point of view; the groundwater's in the area are low in the sodium adsorption ratio (SAR) values making them favourable for irrigation.

8.2 Recommendation

Evaluating the resource is very vital to bring attention to the importance of understanding and improving groundwater governance and management. Moreover, it is also useful to bring attention on this invisible water resource before pollution or depletion of the resource cause severe economic, environmental and social dislocations.

The following significant points, if dealt, will support in alleviating the difficult condition that happen in future groundwater investigation.

- Groundwater monitoring has been given a very little consideration in the country. However, it is a very fundamental step towards evaluating groundwater resources. That is why it is essential to do more work on the groundwater monitoring.
- Observation pipes should be installed in the existing and newly constructed boreholes especially for the wells that could be significant for scientific purpose.
- Data have to be collected properly in order to be used for research and/or scientific intention.

References

- A. Marei, S. Khayat, S. Weise, S. Ghannam, M. Sbaih and S. Geyer. (2010). Estimating groundwater recharge using the chloride mass-balance method in the West Bank. *Hydrogeology, Science* , 55 (5):780-791.
- Abel Beruk. (2010). Ground Water Resource Evaluation and Management Practices in Gilgel Abay Catchment, Tana Basin. Unpublished MSc Thesis: Addis Ababa University, Addis Ababa, Ethiopia, pp 128.
- Afewerk Dessalegn.(2011). Groundwater Potential Evaluation and Flow Dynamics of Hormat-Golina River Catchment, Kobo Valley, North Ethiopia. Unpublished MSc Thesis: Addis Ababa University, Addis Ababa, Ethiopia, pp 139.
- Arnold J.G, Srinivasan R., Williams and R. R. S. (1998). Large area hydrologic modeling and assessment part I: model development. *American Water Resources*,34(1):73-89.
- Arnold R, J.G, Muttaih S., Allen and P.M., R. S. (2000). Regional Estimating of Base Flow and Ground Water Recharge in the Mississippi River Basin. *American Water Resources*, 227:21-40.
- Ayeneu A., Gebreegziabher Y. (2006). Application of a spread sheet Hydrological Model for Computing the Long-Term Water Balance of Lake Awassa. *Ethiopia Hydrological Sciences*, 51: 418-431.
- Ayeneu T. (2004). Environmental Implications of Changes in the Levels of Lakes in the Ethiopian Rift since 1979. *Regional Environmental Change*, 4: 192-204.
- Bayabil H.K. (2009). Modeling rainfall runoff relationships at Maybar watershed, Wollo, Ethiopia, Unpublished MSc Thesis: Cornell University, Bahr Dar, Ethiopia, Ithaca, New York, USA.
- Beven K. (1989). Changing Ideas in Hydrology the case of Physically-Based Models. *Hydrogeology*, 105 (1-2): 157-172.
- Block P., and Balaji Rajagopalan (2007). Interannual Variability and Ensemble Forecast of Upper Blue Nile Basin Kiremt Season Precipitation. *Hydrogeology* ,8(10): pp 1175.

- Brehe S, Desta B., Nicoletti M., and Tefera M. (1987). Geology, Geochronology and Geodynamic Implications of the Cenozoic Magmatic Province in West and Southeast. Geological Society London, 144: 213-226.
- Dagnachew. D. (2018). Evaluation of Surface and Groundwater Availability. Unpublished Phd Thesis, Addis Ababa University, Addis Ababa , pp 256.
- Davis N. and Dewiest J. (1966). Hydrogeology. John Wiley Sons, New York.
- Dereji Gidafie. (2012). Potential groundwater and investigation of the Gerado River catchment water quality. Unpublished MSc Thesis, pp 160.
- Duffer C. N. & Becker E. (1964). Public water supplies for the 100 largest cities in the United States. Geological Survey of Water Supply, 18 (12): pp 364.
- EGS.(1996). Explanation of the Geological Map of Ethiopia. 2nd ed., Ministry of Mines and Energy, Addis Ababa, Ethiopia.
- Endalew Gebru. (2007). Changes in the frequency and intensity of extremes over Northeast Africa. De Bilt, Netherland.
- Ermias Hagos. (2005). Hydrogeology of Mehoni Sub-Basin and Lake Ashange Catchment in the Raya Valley, Northern Ethiopia, Unpublished MSc Thesis, 112 pp.
- Eskinder Zinabu. (2019). Estimating combined loads of diffuse and point-source pollutants into the Borkena River, Ethiopia. Unpublished PhD Thesis, 166 pp.
- Fetter C. (2001). Applied Hydrology Upper Saddle River. Prentic-Hall, Newjersey.
- Freeze R. and Cherry J. (1979). Groundwater Englewood Cliffs, New Jersey.
- Gadgil S., and M. Rajeevan. (2007). Monsoon variability links to major oscillations over the equatorial Pacific and Indian oceans. Current Science, 93(2):182-194.
- GSE &Cherenet T. (1993). Hydrogeological Map of Ethiopia. Addis Ababa, Ethiopia.
- GSE. (1974). Report on Geological and Petrological Researches on the Volcanics of Central Ethiopia. Addis Ababa, Ethiopia.
- Haile A. Shishaye and Ararso Nagari. (2016). Analysis and evaluation of the groundwater in the Haramaya well field, Eastern Hararghe Zone, Ethiopia. International Journal of Science, 5:4.

- Haile T. (1990). Drought in Ethiopia. In: 3rd WMO Symposium on Meteorological Aspects of Tropical Drought. WMO TMRP Series 36, 273-278.
- Hem J. D. (1985). Research and Interpretation of the Chemical Characteristics of Natural Water (3rd Ed.). United States Geological Survey Water Supply, Alexandria, pp 263.
- Hobbs NB. (1986) .Mire morphology and the properties and behavior of some British and foreign peats. Quarterly Journal of Engineering Geology, 19(1): 7-80.
- Hofmann C., Courtillot V., Feraud G., Rochette P., Yirgu G., and Ketefo E. A. (1997). Timing of the Ethiopian Flood Basalt Event and Implications for the Plume Birth and Global Change. Nature, 389: 338-341.
- Holvoet VanGriensven K., A. P., Seuntjens Vanrolleghem and P. A. (2004). Hydrodynamic modeling with SWAT for predicting dynamic behavior of pesticides. USA: Water and Environment Management Series, Young Scientist, 211-213.
- Kassahun Beyene. (2005). Groundwater resource evaluation of Walga river basin, Central Ethiopia, South West Shoa. Unpublished MSc Thesis, Addis Ababa, Ethiopia, pp115
- Seifu Kebede., Travi Y. Tenalem Ayenew and Tamiru Alemayehu. (2006). Groundwater recharge, circulation and geochemical evolution in the source region of the Blue Nile River. Applied Geochemistry, Ethiopia,20: 1658-1676.
- Kelly L., Kalin R. M., Bertra D., Kanjaye M., Nkhata M., and Sibande H. (2019). Quantification of Temporal Variations in Base Flow Index Using Sporadic River Data: Application to the Bua Catchment, Malawi. Water,1-17.
- Kidest Ayalew. (2018). Numerical groundwater flow modelling of the Gerado river catchment. Unpublished MSc Thesis, 120 pp.
- Kieffer B., Arndt N., Lapierre H., Bastien F., Bosch D. and Pecher A. (2004). Flood and Shield Basalt from Ethiopia, Magmas from the African super swell. Petrography, 45(4): 793-834.
- Kruseman G. and Ridder N. (1994). Analysis and Evaluation of Pumping Test Data (2nd ed.). International Institute for Land Reclamation and Improvement, Wageningen, Netherlands.

- Langmuir D. (1997). *Aqueous Environmental Geochemistry*. Prentice-Hall, Englewood Cliffs, 601 pp.
- Lenhart K. T., Eckhardt Fohrer N., H.G. and Frede. (2002). Comparison of two different approaches of sensitivity analysis *Physics and Chemistry of the Earth. Els. Sci*, 645–654.
- Mesifn Sahele. (2001). Groundwater resource potential evaluation in Borkena River catchment, South Wollo, Ethiopia. Unpublished MSc Thesis, pp 156.
- Molla Demile. (2000). *Hydrology, Hydrogeology and Hydrochemistry of the lake system in Hiq-Ardibo, Northern Ethiopia*. Addis Ababa University, Addis Ababa, 140 pp.
- Molla Demlle, Tenalem Ayenew and Stefan Wohnlich. (2007). Comprehensive Hydrological and Hydrogeological Study of Topographically closed lakes in Highland Ethiopia: The Case of Hayk and Ardibo. *Hydrogeology*, 339: 145-158.
- Moore, J.E. (1995). *Groundwater. A Primer*, American Geological Institute, united states of America. 52 pp.
- Muluken Tilahun. (2015). Assessment of groundwater potential and its quality for irrigation purpose in sub catchment of Borkena River. Unpublished MSc Thesis, Kombolcha, Northern Ethiopia, 113 pp.
- Neitsch S.L., J. G., Arnold Williams and J. R., J. K. (2005). *Soil and Water Assessment*. Agriculture Ressource, United States, 52 pp.
- O'Kelly BC. (2013) Undrained shear strength-water content relationship for sewage sludge. *Proceedings of the Institution of Civil Engineers - Geotechnical Engineering*, 166(6): 576-588.
- Orkodjo, T. P. (2014). Impact of land use land cover change on catchment hydrology a case study of Awassa catchment. Unpublished MSc Thesis, Arbaminich University, Ethiopia, 7-8.
- Otterbach L. (1995). Report on water resources quality and potential assessment for irrigation agriculture in the Abaya-Chamo Basin, South Ethiopia. The University of Siegen, Germany.
- Panhalkar S. S. (2014). Hydrological modeling using SWAT model. *The Egyptian Journal, Egypt*, 8.

- Setegn S. (2010). Modeling, hydrological and hydro dynamic processes in Lake Tana. unpublished PhD Thesis, Addis Ababa, 10(57): 10-15.
- Sileshi Mamo. (2015). Integrated Hydrological and Hydrogeological system Analysis of the Lake Tana Basin, North Western Ethiopia. Unpublished PhD Thesis, Addis Ababa, Ethiopia, 280 pp.
- Smakhtin V. U. (2001). Low flow hydrology: a review. *Hydrogeology*, 240(3-4): 147-186.
- Tenalem Ayenew, Molla Demlle and Wohnlich S. (2008). Hydrogeological framework and occurrence of groundwater in the Ethiopian aquifers. *Afr. Ear. Sci.*, 52: 97-113.
- Tenalem Ayenew and Tamiru Alemayehu. (2001). Principle of Hydrogeology. Addis Ababa University Press, 125 pp.
- Tesfa Yimer. (2015). Hydrological modelling of Mayaber watershed using Arc SWAT Awash basin Amhara Region. Arba Minch University Arba Minch, 109 pp.
- Tesfaye Tessema. (2015). Groundwater Potential Evaluation Based on Integrated GIS and Remote Sensing Techniques, in Bilate River Catchment, South Rift Valley of Ethiopia. Unpublished MSc Thesis, Addis Ababa University, Addis Ababa, Ethiopia, 130 pp.
- Todd D.K. (1980). *Groundwater Hydrology*. 2nd ed., John Wiley and Sons, New York, 535 pp.
- USDA-SCS. (1972). National Engineering Handbook .Hydrology, Chapter: 4-10. WB Theortical Documentation. Cornell university, Ithaka, New York,3-4.
- White Zarch M. Easto Dan R.Fuka, Tammos and Steenhuis. (2009). SWAT-WB Theortical Documentation. In White, Zarch, M.Easto, Dan, R.Fuka, Tammos, and Steenhuis, SWAT-modeling.
- Williams, J.R. (1995). The EPIC model. In: V.P. Singh (eds.), *Computer models of Watershed hydrology*. Water Resources Publications, Highlands Ranch, 909-1000.

Annex 1 hydro geological data

X	Y	Depth m	SWL m	DWL m	DD m	Q LPS	Specific capacity m3d m	T m2 d	K m d	Aquifer type
606413	1272191	243	35.59	58.21	22.62	19	72.57	114	1.52	weathered and fractured rhyolite and basalt
567514	1267867	253	7.92	22.16	14.24	56.9	345.24	519	6.02	sand, gravel and boalder
567307	1266660	248	14.58	35.76	21.18	62	252.92	343	3.61	sand, gravel and boalder
574345	1280320	251	23.15	34.38	11.23	62	477.01	867	8.57	sand, gravel and boalder
576148	1288640	282	0	36.47	36.47	57	135.04	135.04	1.34	sand & gravel with intercaltion of clay and silt
598022	1230466	208.5	36.99	46.01	9.02	28	268.2	696	11	alluvial deposits (sand and gravel), wetherd and fractured basalt
580516	1279739	164	2.63	41.9	39.27	52	114.41	155	3.24	sand & gravel with intercaltion of clay and silt
581014	1278563	143	0.75	37.57	36.82	55	129.06	174	4.3	sand & gravel with intercaltion of clay and silt
579579	1279670	126	11.04	37.47	26.43	30	98.07	132	3.81	sand & gravel with intercaltion of clay and silt
579838	1278511	120	11.7	47.52	35.82	20	48.24	75.6	1.87	sand & gravel with intercaltion of clay and silt
581793	1278463	173	0	29.41	29.41	43	126.32	183	3.53	sand & gravel with intercaltion of clay and silt
567983	1269605	183	20.33	42.68	22.35	20	77.32	50.6	0.8	gravel, weatherd and fractured basalt
582705	1249598	126	3.26	77.98	74.72	4	4.63	2.41	0.06	moderaty weatherd basalt
574158	1248856	105	5.78	37	31.22	24	66.42	77.1	1.68	Proclastic material
575773	1287753	290	7.36	54.55	47.19	78	142.56	152	6.6	Alluvial
576255	1278949	250	7.9	21.3	13.4	84.3	342.14	868.5	15.7	Alluvial
565492	1267426	280	67.19	75.67	8.48	58	597.98	7.92		Alluvial
573560	1278119	300	58.4	34.57	38.84	69	152.93	1580	14.7	Alluvial
572853	1289659	282	14.78	90.43	75.65	46	525.31	1030	10.9	Alluvial
568109	1267394	276.63	9.18	43.75	34.57	78	194.92	1100	14.4	Alluvial
574774	1262582	208	32.03	38.81	6.78	60	367.785	151	1.72	Alluvial

Annexes 2 hydrochemistry data

Sample Code	x	y	Na	K	Ca	Mg	Cl	SO4	HCO3	calc TDS
			mg/l	mg/l	mg/l	mg/l	mg/l	mg/l	mg/l	mg/l
Ha_sp2	574382	1241174	18.5	2.4	26.4	28.6	1.4	5	189.1	274.29
Me_BH2	575782	1288089	44.4	2.19	46.9	16.3	6.45	5.67	358.68	480.94
Wu_CSP2	565082	1271718	14.3	1.16	56	15.7	5.32	5.8	273.28	393.96
Ha_CSP1	578323	1251602	15.1	1.13	42.6	11.7	4.18	5.9	195.26	289.26
Ha_CSP-3	574139	1237780	15.1	1.13	42.6	11.7	4.18	5.9	195.26	289.26
De_CSP-1	560001	1215214	12.1	4.05	27.3	13.8	3.62	6.7	176.9	253.52
Ha_bh1	574236	1249058	35.1	5	38.4	62.16	10	7	357.5	518.49
Ha_sp3	567735	12668025	17.8	6.4	35.6	30.64	4.1	7	189.1	293.35
Ha_sp	571374	1257637	18.3	14.7	18.8	60.7	14	8	325.7	462.13
Ka_CSP1	582840	1233294	14.5	1.35	52.1	17.5	5.96	8.2	256.2	376.34
Gi_BH3	584325	1276956	16.7	0.69	74.85	27.6	6.7	9.1	350.14	502.96
Ha_CSP5	581413	1248894	20.1	0.65	69.2	18	7.44	10.12	329.4	469.4099
We_BH-1	582655	1249229	31.1	0.94	103.6	19.7	12.55	12.1	423.34	605.83
We_CSP-1	583463	1249891	24.9	1.05	52.2	9.6	6.81	12.5	223.26	347.83
Me_BH1	571830	1288141	16.6	0.9	36.1	20.1	8.51	13.04	249	348.92
Ha_CSP-2	574382	1241174	15.4	0.63	55.1	19.5	9.78	13.3	284.26	409.61
WU_CSP-1	566550	1276454	15.4	0.63	55.1	19.5	9.78	13.3	284.26	409.61
Wu_bh	571405	1277293	44.2	5.4	61.2	56.9	7.2	14	407.5	597.02
Ha_BH2	573788	1248305	23.8	2.31	64.8	21.4	8.15	14.15	372.1	509.2
Me_bh	570610	1291661	48.4	3.1	30.8	66.7	12.6	15	366	544.52
Ha_BH1	573461	1248733	20.7	2.64	55.5	23.2	11.2	15.6	305	438.55
Wu_BH2	569202	1256859	49.8	1.32	33.9	11.8	8.51	16.79	292.8	415.5
Wu_CSP3	567822	1265637	16.5	1.41	63.2	23	4.96	16.8	317.2	455.24
Ha_CSP6	581141	1246219	16.7	2.33	79.8	20.5	21.13	17.7	292.8	493.24
Ka_CSP2	582960	1236526	14	1.61	55.9	15.3	10.99	17.9	157.38	308.76
Ha_CSP-1	578323	1251602	25.5	1.14	86	18.8	11.77	19.1	345.26	526.06
Wu_CSP2	565082	1271718	50.8	0.75	51.5	15.9	15.46	20.4	268.4	456.79
Wu_DRW-1	569592	1257474	39	1.04	66.9	19.3	10.64	20.7	341.6	499.64
Ha-CSP4	573848	1253840	33.2	3.2	84.8	17.2	21.13	23	305	532.24
Gi_CSP1	578964	1277139	67.7	0.53	98	49.3	30.35	26.2	523.38	829.01
Wu_CSP1	566550	1276454	20.1	0.53	73.3	45.1	16.31	34.1	414.8	617.8399
Gi_BH2	580640	1278013	66.8	5.91	61.9	48.2	24.11	44.48	583.16	835.08
Gi_bh3	584325	1276956	100.7	4.7	24.4	29.6	17	49	292.8	518.963
Gi_BH1	581461	1277934	70.8	6.75	48.6	24.3	17.73	49.42	403.82	621.9

Annexes 3 Laboratory chemistry

x	y	stationId	Ca	Mg	Na	K	HCO3	So4	cl	NO3
571405	1277293	Wu_bh	61.2	56.9	44.2	5.4	407.5	14	7.2	0.55
574236	1249058	Ha_bh1	38.4	62.16	35.1	5	357.5	7	10	3.3
570610	1291661	Me_bh	30.8	66.7	48.4	3.1	366	15	12.6	1.89
584325	1276956	ma_bh	24.4	29.6	100.7	4.7	292.8	49	17	0.75
571374	1257637	Ha_sp	18.8	60.7	18.3	14.7	325.7	8	14	1.89
574382	1241174	Ha_sp2	26.4	28.6	18.5	2.4	189.1	5	1.4	2.86
567735	12668025	Ha_sp3	35.6	30.64	17.8	6.4	189.1	7	4.1	2.64

Annexes 4 Monthly and mean temperature of 6 stations (in °C).

			Jan	Feb	Mar	Apr	May	Jun	Jul	Aug	Sep	Oct	Nov	Dec	mean
Combolch	TMPMIN	1987-2018	10.48	11.25	12.87	13.99	14.38	15.34	15.36	14.97	13.89	10.96	9.07	8.91	annual
	TMPMAX	1987-2018	24.66	26.17	27.12	27.52	28.89	30.32	28.26	26.96	26.61	25.93	25.29	24.67	
	Average		17.57	18.71	20.00	20.76	21.63	22.83	21.81	20.96	20.25	18.44	17.18	16.79	
Bati	TMPMIN	1988-2018	10.98	12.36	13.71	14.86	15.69	17.00	16.77	15.79	14.89	11.57	9.88	9.72	
	TMPMAX	1988-2018	24.32	25.09	27.43	28.75	30.97	32.86	30.61	28.59	28.99	28.27	26.70	25.14	
	Average		17.65	18.72	20.57	21.81	23.33	24.93	23.69	22.19	21.94	19.92	18.29	17.43	
Sirinka	TMPMIN	1987-2018	11.44	11.90	13.62	14.68	15.55	16.50	16.04	15.37	14.51	12.45	11.01	10.58	
	TMPMAX	1987-2018	23.04	24.64	26.01	27.13	28.92	30.78	28.87	27.28	27.09	25.91	24.86	23.87	
	Average		17.24	18.27	19.81	20.90	22.24	23.64	22.46	21.33	20.80	19.18	17.93	17.22	
Werebabc	TMPMIN	2000-2018	10.07	10.85	11.91	12.53	13.55	13.99	12.69	12.33	12.51	11.21	10.25	9.54	
	TMPMAX	2000-2018	20.58	21.93	23.22	24.09	25.23	26.31	24.78	23.47	23.41	22.19	21.34	20.34	
	Average		15.33	16.39	17.56	18.31	19.39	20.15	18.74	17.90	17.96	16.70	15.79	14.94	
Merssa	TMPMIN	1987-2018	11.22	11.56	12.58	14.16	14.67	15.01	14.82	14.20	13.50	11.54	10.31	10.04	
	TMPMAX	1987-2018	26.30	27.22	28.40	29.60	31.36	32.77	30.65	29.21	29.62	28.24	27.35	26.45	
	Average		18.76	19.39	20.49	21.88	23.01	23.89	22.73	21.70	21.56	19.89	18.83	18.24	
Haik	TMPMAX	1987-2018	23.7	25.1	26.0	26.6	28.0	29.7	27.5	26.0	26.0	25.5	24.9	23.7	
	TMPMIN	1987-2018	8.1	8.8	10.9	12.0	12.0	12.4	13.7	13.5	12.4	9.0	7.0	6.8	
	Average		15.9	17.0	18.4	19.3	20.0	21.1	20.6	19.8	19.2	17.3	15.9	15.2	

Annex 4 Relative humidity, sunshine hours and wind speed for selected stations

Stations	Type of data's	Jan	Feb	Mar	Apr	May	Jun	Jul	Aug	Sep	Oct	Nov	Dec
Bati	SUNHRS	7.1	8.1	7.3	7.7	8.5	7.0	5.9	6.4	6.7	8.2	9.0	8.1
Sirinka	SUNHRS	7.1	8.0	7.8	8.0	8.5	6.9	5.1	6.1	6.9	8.2	8.3	7.8
Kombolcha	SUNHRS	8.1	9.1	8.3	8.3	8.7	7.5	6.4	6.5	7.0	8.3	8.8	8.5
Kombolcha	WINDLY	57.3	62.1	60.5	58.4	58.1	68.3	62.1	49.5	37.7	33.8	36.9	44.0
Sirinka	WINDLY	114.0	123.9	119.2	109.6	113.5	131.0	115.6	103.0	86.4	79.8	94.9	121.3
Bati	WINDLY	66.4	75.5	80.0	79.1	78.2	95.5	104.4	90.0	60.9	52.3	59.9	62.3
Sirinka	RELHUM	74.5	65.8	64.9	63.7	55.7	47.9	62.4	71.3	66.6	65.6	64.5	65.3
Bati	RELHUM	73.9	67.1	66.8	64.5	58.3	50.6	63.1	73.1	70.6	64.9	65.4	58.4
Kombolcha	RELHUM	64.4	58.1	58.9	58.5	51.6	42.8	59.4	66.7	64.5	60.3	60.3	60.3